

# **OPTIMAL APPLICATIONS OF HIGH-STRENGTH CONCRETE IN STRUCTURAL WALLS OF TALL BUILDINGS**

by

**Budi Galiano Bong**

Supervised by

Associate Professor Mike Xie and Dr. P. Mendis

A thesis submitted in fulfilment of the requirement for the degree of Master of  
Engineering at the Victoria University of Technology



School of the Built Environment  
Victoria University of Technology  
Victoria, Australia

February, 1998

FTS THESIS

693.54 BDN

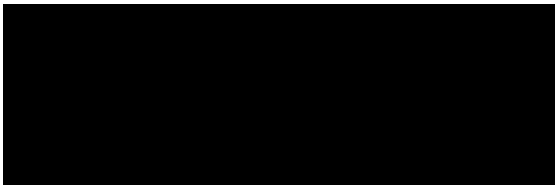
30001006465738

Bong, Budi Galianto

Optimal applications of  
high-strength concrete in  
structural walls of tall

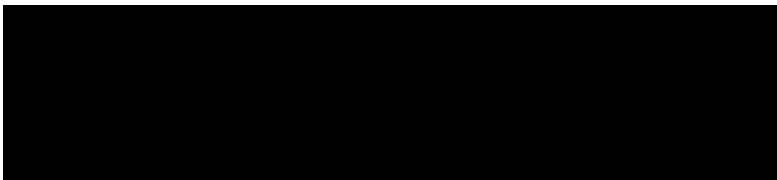
**DECLARATION**

*This thesis contains no material that has been submitted at another university for the award of a degree, and to the best of the writer's knowledge and belief, the thesis contains no material previously published by others, except where specific reference is made.*



*BUDI GALIANTO BONG  
MELBOURNE  
FEBRUARY, 1998*

***SUPERVISORS:***



*ASSOCIATE PROFESSOR MIKE XIE*

*DR. PRIYAN MENDIS*

## **SUMMARY**

*This study examines the application of high-strength concrete (HSC) in structural walls of tall buildings. Emphasis is put on the cost-benefits corresponding to the use of higher concrete strengths. The parameters included in the cost analysis are: the material cost of concrete and reinforcing steel; the construction costs including the placement costs of the steel reinforcement and wet concrete, and the formwork cost; and the cost-benefit of additional floor area gains, corresponding to thinner walls resulted from HSC applications.*

*In lateral load resisting buildings, HSC are more likely to be used in the structural columns and walls. It is shown in the review of literature (Chapter 2) that the utilisations of HSC in building applications are economical. The work done so far was mostly involving the use of HSC columns in the medium-rise buildings. The cost analyses carried out in this thesis reveals that significant cost-benefits can also be achieved in the HSC walls. Comparing to the 40 MPa concrete, a 120 MPa concrete wall building capitalising at \$8,000 per square meter results in a cost-benefit more than 2.5 times the construction costs of the 40 MPa wall, a significant amount.*

*The structural walls investigated are two-dimensional cantilever and coupled walls, and a three-dimensional core wall comprising two 'C' shape walls and header beams coupling the two walls. The results of the investigations are presented in Chapters 6 and 7. A case study of a model 30-storey building is also given in Chapter 8. This study concluded that the use of HSC in structural wall buildings is recommended.*

## **ACKNOWLEDGMENTS**

*There are many people that I wish to thank, who have assisted and supported me throughout my research study. Not only have I learned about the research but also a lot about myself. There were many obstacles and hurdles I faced along the way; without the people close to me, this thesis would not have been possible.*

*Special thanks are due to my thesis supervisor Associate Professor Mike Xie for being the first person who introduced me to this Department, guiding me throughout the entire duration of my research study, and being the last person who got everything organised and letting my dream come true. Sincere thanks for his understanding, caring, his valuable advice at all times and comments on the final drafts etc. etc. And you know that you are the best.*

*I would like to sincerely thank my thesis co-supervisor Dr Priyan Mendis, at The University of Melbourne, for his constant help and support particularly during the initial stages of this project and reading the final draft of the thesis, and more importantly for being there whenever I needed his valuable advice.*

*I would like to express my gratitude to Mr Ian Campbell, the Head of Department of Civil and Building Engineering, for the support he gave me in all the administrative and technical matters I have approached him about, for being the right person at the right time and place.*

*I wish to express my sincere thanks to Mr Anil Hira, whose invaluable encouragement, advice and guidance throughout the entire duration of my research study, has enabled me to bring this thesis into fruition, for the enthusiasm he has shown towards the research topic and great support during writing this thesis, without his scrutiny of so many revised versions, my dream of completing this thesis would never become true.*

*I am indebted to the Department of Civil and Building Engineering for the multiple financial supports. I acknowledge and express my gratitude for receiving the South East Asia Postgraduate Scholarships. I am also grateful to the staff of the Department, particularly Ms Glenda Geyer and Lyn Allis, for their help in multiple administrative and English language matters. My colleagues in this Department, in particular Gino Catania, Scott Young, and Francisco Jong, who have, in one way or another, rendered their kind assistance. Thanks guys, I could not have done this without your support.*

*I am also indebted to the Office of Student Affairs, who granted me a waiver of fees for semester one 1997. I especially thank Ms Jenny Butler, Senior International Students Adviser, for her multiple supports and helps during my last year at the University. Her initiation and continuous effort making the*

*waiver of fees be granted are greatly appreciated. Without it, the degree of Masters of Engineering would still be my dream.*

*My acknowledgment and gratitude go to Carmel and Holy Wall for their warm hospitality, help, and encouragement, and having had to put up with me through the good and bad times. My gratitude also goes to Peter Surna, who had tirelessly taught me computer and human language, English. My friends: Tn and Vu, your supports, helps, and friendship are never forgotten.*

*I wish to express my most sincere gratitude to my brother and sisters and my brother-in-law, Budi Darmawan, for their unfailing encouragement during all these years, for all they taught me and for all they did for me. Most of all I shall forever love my Mum and Dad. They have been the ones to encourage and inspire me whenever my spirit flagged. I love you both very much. To them I dedicate this thesis.*

**BUDI GALIAN TO BONG  
FEBRUARY, 1998**

## CONTENTS

<i>Declaration</i> .....	ii
<i>Summary</i> .....	iii
<i>Acknowledgments</i> .....	iv
<i>Contents</i> .....	vi
<i>Definitions</i> .....	ix
<i>Notations</i> .....	x
CHAPTER 1. INTRODUCTION .....	
1.1 Introductory review .....	1-1
1.2 Aims of research .....	1-3
1.3 Significance of thesis .....	1-4
1.4 Outline of thesis .....	1-4
CHAPTER 2. BACKGROUND AND LITERATURE REVIEW	
2.1 Current research and developments of high-strength concrete (HSC).....	2-1
2.2 Economic considerations .....	2-4
2.3 A close look at the cost-benefits .....	2-7
2.4 Major concerns.....	2-10
2.5 Comments on current research and applications.....	2-11
CHAPTER 3. STRUCTURAL MODELS AND DESIGN CRITERIA	
3.1 Structural wall systems.....	3-1
3.2 Design criteria .....	3-3
3.2.1 Loading.....	3-5
3.2.2 Serviceability criteria.....	3-9
3.2.3 Strength design .....	3-11
3.2.4 Ductility .....	3-14
3.3 Concluding remarks .....	3-16
CHAPTER 4. STRUCTURAL OPTIMISATION	
4.1 Principle of virtual work: Unit load method .....	4-2
4.2 Structural optimisation techniques .....	4-4
4.3 Illustrative examples .....	4-9
4.3.1 18-bar truss.....	4-9
4.3.2 30-storey cantilever wall .....	4-11
4.3.3 30-storey coupled wall .....	4-13
4.4 Concluding remarks .....	4-15
CHAPTER 5. RESEARCH METHODOLOGIES AND PARAMETERS	
5.1 Methodology of member-linking technique.....	5-1
5.2 ETABS™ and DISPAR™ .....	5-6
5.3 Variable-linking technique.....	5-7

5.4	Illustrative examples .....	5-10
5.4.1	18-bar truss .....	5-10
5.4.2	30-storey cantilever wall.....	5-12
5.4.3	30-storey coupled wall.....	5-13
5.5	Approximate method.....	5-13
5.6	Example of approximate method .....	5-17
5.7	Variable concrete strengths .....	5-21
5.8	Parameters in cost analysis.....	5-23

## CHAPTER 6. USE OF HIGH-STRENGTH CONCRETE IN RECTANGULAR WALLS

6.1	Cantilever wall .....	6-2
6.1.1	Structural model and loading.....	6-2
6.1.2	Uniform concrete strengths .....	6-3
6.1.2.1	Volume v. number of thickness transitions .....	6-3
6.1.2.2	Cost analysis .....	6-5
6.1.3	Variable concrete strengths.....	6-6
6.1.3.1	Volume v. number of lower storeys utilising HSC.....	6-6
6.1.3.2	Cost analysis .....	6-8
6.1.4	Implication of wall thickness optimisation to seismic design load .....	6-10
6.2	Coupled wall .....	6-14
6.2.1	Structural model and loading.....	6-14
6.2.2	Uniform concrete strengths .....	6-15
6.2.3	Variable concrete strengths.....	6-17
6.2.4	Implication of wall thickness optimisation to seismic design load .....	6-20
6.3	Strength and ductility .....	6-21
6.3.1	Cantilever wall.....	6-22
6.3.2	Coupled wall.....	6-26
6.3	Concluding remarks .....	6-27

## CHAPTER 7. USE OF HIGH-STRENGTH CONCRETE IN COUPLED 'C' SHAPE CORE WALLS

7.1	Multiple-direction displacement constraint problem .....	7-1
7.2	Structural model and loading .....	7-2
7.3	Uniform concrete strengths .....	7-2
7.4	Variable concrete strengths .....	7-6
7.5	Implication of wall thickness optimisation to design seismic load.....	7-9
7.6	Strength and ductility .....	7-10
7.7	Concluding remarks .....	7-13

## CHAPTER 8. A CASE STUDY

8.1	Model building.....	8-1
8.2	Cost analysis.....	8-3
8.2.1	Concrete volumes at various concrete strengths.....	8-3
8.2.2	Cost-benefits from using various concrete strengths.....	8-4
8.3	Design for strength.....	8-5
8.4	Concluding remarks .....	8-12

CHAPTER 9. CONCLUSIONS AND RECOMMENDATIONS

9.1 Conclusions ..... 9-1  
9.2 Limitations of this research ..... 9-5  
9.3 Recommendations for further research ..... 9-6

REFERENCES

APPENDICES

Appendix A. Results of cost analysis for Chapters 6 .....  
Appendix B. Results of cost analysis for Chapters 7 .....  
Appendix C. RCDESIGN© computer program.....  
Appendix D. Conference papers .....

## **DEFINITIONS**

ACI	= American Concrete Institute
DPF	= Displacement Participation Factor
HSC	= High-Strength Concrete
HS/HPC	= High-Strength / High Performance Concrete
NSC	= Normal Strength Concrete

## NOTATIONS

A	= cross sectional area
$A_g$	= gross area of concrete section
$A_s$	= area of tension reinforcement
$b_w$	= web width
c	= distance from max. compression edge to neutral axis
$c_c$	= critical depth of neutral axis distance
C	= seismic coefficient
d	= effective depth of section; deformation due to unit virtual load
$d_M$	= flexural deformation
$d_N$	= axial deformation
$d_V$	= shear deformation
D	= dead loads; displacement in the direction of virtual load
E	= load effects of earthquake
$E_c$	= modulus of elasticity of concrete
$f_y$	= specified yield strength of reinforcing steel
$f'_c$	= specified compressive strength of concrete
F	= horizontal seismic load
G	= shear elastic material modulus
h	= overall thickness of member
H	= horizontal loads
$H_s$	= storey height
$H_w$	= height of entire wall
I	= importance factor; flexural moment of inertia
$I_e$	= effective moment of inertia for computation of deflection
$I_g$	= moment of inertia of gross concrete section, neglecting reinforcement
k	= square of the ratio of calculated displacement to desired displacement
K	= structural factor
l	= lever arm of coupled wall system
$l_n$	= length of clear span

L	= live loads due to intend use or occupancy
$L_p$	= plastic hinge length
$L_r$	= reduced live load
$L_w$	= horizontal length of wall section
m	= number of elements; moment due to virtual unit load
M	= moments; moment due to actual load
$M_{o,w}$	= flexural overstrength
$M_u$	= factored moment
n	= number of storeys
N	= axial forces
$N_u$	= factored axial load occurring simultaneously with other loads
$P_u$	= factored axial load
R	= force reduction factor
s	= spacing of shear reinforcement
u	= internal forces due to unit virtual load
U	= required strength to resist factored loads
$U_M$	= flexural moment due to actual load
$U_N$	= axial force due to actual load
$U_V$	= shear force due to actual load
$v_c$	= shear stress = $V_c/bwlw$
$v_i$	= average shear stress at ideal strength
v	= volume of structural member
V	= base shear due to seismic loading; vertical loads; structural volume
$V_c$	= nominal shear strength provided by concrete
$V_i$	= ideal shear strength
$V_s$	= nominal shear strength provided by shear reinforcement
$V_u$	= factored shear force
$V_w$	= shear demand at the base section of wall
W	= total weight of structure
$W_f$	= floor weight
$W_w$	= self weight of wall
x	= locations of thickness transition

## GREEK SYMBOLS

$\alpha$	= ratio of optimum to initial values
$\delta$	= displacement participation factor
$\phi$	= strength reduction factor
$\phi_{o,w}$	= flexural overstrength factor
$\lambda$	= Lagrange multiplier
$\lambda_o$	= overstrength factor
$\mu$	= ductility factor
$\mu_{\Delta}$	= displacement ductility factor
$\rho_v$	= ratio of longitudinal reinforcement to cross sectional area
$\rho_h$	= ratio of shear reinforcement
$\omega_v$	= dynamic magnification factor for shear
$\psi$	= live load reduction coefficient

**UNITS**, unless specified otherwise, all dimensional units in expressions for length, force and stress shall be taken as millimetres (mm), Newton (N) and MegaPascal (MPa)

# CHAPTER ONE

---

## INTRODUCTION

### 1.1 INTRODUCTORY REVIEW

Concrete as a structural material has been used since ancient times. However, the practical application of reinforced concrete was only demonstrated in 1867 by Joseph Monier in Paris (Straub, 1964), when a logical union of two materials, steel and concrete was utilised. Unlike steel, which was dominating the high-rise construction scene at that time, concrete had the unique property of moldability, which allowed architects and engineers to shape the building and its elements in differing elegant forms. However, it was still no match for structural steel in term of strength.

The use of reinforced concrete as the primary material for the structural system of tall buildings is a recent development. It is only made possible by a number of factors including: improved and sophisticated construction techniques, innovative structural systems, availability of advanced computer technology in terms of hardware and analytical software and the development of high strength and high performance concrete.

Prior to the construction of the 76-storey Water Tower Place in Chicago in 1975, until recently the tallest concrete building in the world, the tallest concrete buildings were limited to the 20 storeys range. Over the last decade, numerous very tall buildings have sprouted out worldwide, primarily resulting from the tremendous building boom that has taken place throughout many urban centers, particularly in South East Asia.

Concrete typically has been the more competitive option over steel in these rapidly developing countries. For example a core and cylindrical perimeter frame system constructed entirely of cast-in-place high-strength concrete (HSC) provides the main structural framing for the world's current tallest building: the Kuala Lumpur City Centre Petronas Twin Towers in Malaysia. Five alternatives were reviewed for the main structural framing system of the towers. Concrete core/concrete cylindrical tube system was chosen due to the local availability of concrete at a relatively low cost. HSC was found to provide more strength per unit cost and participate more efficiently in resisting the wind load than steel. (Mohamad *et al.*, 1995)

HSC research began in the 1970s and has progressed ever since. The objectives were to study the fundamental properties of the material and to validate the existing code requirements to HSC. Substantial work has also been reported in the area of materials development for producing higher strength concrete, production methods, material properties, and their implication on structural design and performance. In recent years, the applications of HSC have increased, and HSC has now been used in many parts of the world.

The use of HSC in building applications has been shown to be beneficial in terms of cost and structural efficiency. However, the current research findings are considered to be insufficient to draw a significant conclusion, particularly for buildings subjected to high lateral loads due to wind and/or earthquake. For these buildings, HSC will more likely be used in the vertical elements. A review of the current literature has indicated the lack of information for HSC walls subjected to lateral loads. This has been investigated as part of this study.

Two distinct wall systems, cantilever walls and coupled walls, are investigated. From results of the analysis, the structure is initially optimised for minimum volume and then subsequently designed for strength and ductility. Concrete strengths ranging from 40 MPa to 120 MPa are used for the cost benefit analysis. Two conditions are considered: (1) uniform concrete strength at all levels; (2) HSC in the lower levels and

normal strength concrete (NSC) in the upper levels. The results of the investigation and the subsequent appraisal of the design recommendations form the basis of this thesis.

## 1.2 AIMS OF RESEARCH

The main stimulus of this study is the realisation that over the last decade there has been significant progress in the HSC applications. However, its application to the tall buildings in seismic regions has been minimal. This is particularly important when one considers that seismic loads significantly govern the structural system of a typical tall building.

The thesis aims to examine and develop recommendations for optimal use of HSC in tall buildings subjected to seismic loads. The principle lateral load resisting system considered will be cantilever structural walls and coupled structural walls. The objective is to formulate a general design methodology with the aim of achieving the most cost benefit solution.

In order to fulfil this objective, several specific aims are established:

- ◆ To understand the behaviour of the lateral load resisting systems of tall buildings comprising of cantilever walls or coupled walls, when subjected to seismic loads.
- ◆ To review the existing traditional design philosophy for structural analysis and subsequently design of wall elements with particular emphasis on the parameter governing the thickness of the structural walls.
- ◆ To apply suitable structural analysis techniques, in particular the optimisation program DISPAR™, which is a post-processor of ETABS™, to investigate the distribution of concrete volume and concrete strengths of the wall elements to achieve optimal cost solutions whilst satisfying specific displacement criteria.
- ◆ To ensure that strength and ductility criteria are satisfied

- ◆ To develop a systematic procedure for the design of the cantilever and coupled wall utilising the HSC beneficially and to demonstrate the procedure on a case study.

### **1.3 SIGNIFICANCE OF THESIS**

The application of optimisation techniques to structural sizing and the subsequent design of reinforced concrete structural wall elements for high-rise buildings utilising high strength concrete have an attractive objective of producing the most economical structure whilst satisfying structural constraints.

Due to overall planning requirements for various disciplines, the sizing of the wall elements is required during the early conceptual phases of the design process. Due to the multi-disciplinary implications, further modifications are discouraged and in many cases not possible. Therefore it is imperative that the design effort to optimise the walls should take place during this early phase. It is common that conservatism adopted in sizing the wall thickness at this early phase leads to uneconomical design.

The benefits of optimising the wall area by introducing HSC are immense in terms of cost savings. In addition to the obvious savings associated with construction cost, the savings associated with the corresponding increase in lettable areas are large. Areas of the community that will benefit from this work are building owners and construction industry, the concrete producers and building consultants.

### **1.4 OUTLINE OF THESIS**

The thesis is divided into nine chapters and four appendices:

Chapter 2: Literature review. A review of literature relating to the research of HSC, economic considerations, and concerns regarding to the use of HSC in tall building applications are presented.

Chapter 3: Structural models and design parameters. The behaviour of structural walls as the chosen structural systems in this study is discussed. Parameters governing the design, the criteria and requirements for limit state are also described, including the loading parameters.

Chapter 4: Structural optimisation. The classical method of structural optimisation for a single displacement constraint problem is discussed. This technique forms the basis of a more practical optimisation technique for use in high-rise building designs.

Chapter 5: Research methodologies and parameters. This chapter describes the methodologies adopted to carry through the thesis' aims. The development of two techniques, the member-linking technique and the approximate numerical method, used to compute the optimum structure is presented. Examples are given to demonstrate the use of these techniques. The method of cost analysis is also described.

Chapter 6: Use of high-strength concrete in rectangular walls. The results from structural and cost analyses for a range of concrete strengths and capitalised values are presented. The implications of the optimum design wall sections to the structure mass and subsequently the seismic loads are discussed. The design for strength and ductility is also performed in this chapter and the problems that may arise are addressed. The chapter concludes with recommendations and guidelines on the use of HSC in the most economical way.

Chapter 7: Use of high-strength concrete in coupled "C" shape core walls. The results for coupled "C" shape core walls are presented in this chapter following the design method discussed in the previous chapter.

Chapter 8: A case study. Finally, a case study is presented to illustrate the design method and procedure for the design of a building structure utilising structural walls using HSC. This case study also demonstrates the substantial savings gained by application of optimisation techniques developed in this research.

Chapter 9: Conclusions and recommendations. The results of the thesis are reviewed and further research needs are suggested.

## **CHAPTER TWO**

---

### **LITERATURE REVIEW**

The rapid development of concrete technology, advances in design methodology and use of innovative structural systems, augmented by the significant advances in construction techniques during the past decade, has facilitated the evolution of concrete into a viable structural material for tall buildings. This chapter reviews the studies that were done on high-strength concrete (HSC), primarily focusing on its unique characteristics and the economic benefits resulting from its application in tall buildings. The limitations associated with HSC, in particular with its application in high seismic areas is also discussed. In addition, comments on the current research on HSC are presented.

#### **2.1 CURRENT RESEARCH AND DEVELOPMENT OF HSC**

Although HSC is often considered a relatively new material, it has evolved over many years via a gradual increase. As the development and applications of HSC advanced, the bounds defining HSC has continually changed. In the 1950s, concrete with a compressive strength of 34 MPa was considered high strength. In the 1960s, commercial usage of concrete with 41 and 52 MPa compressive strength was achieved, increasing to 62 MPa a decade later. More recently, compressive strengths of 100 MPa have been commonly applied and strengths as high as 138 MPa have been used in cast-in-place buildings (ACI Committee, 1984).

For many years, concrete with compressive strength in excess of 41 MPa was commercially available at only a few geographic locations. However, in recent years, the applications of HSC have increased significantly and are widespread throughout

the world. The growth of its applications has been possible as a result of recent developments in material technology and a strong demand for higher strength concrete.

HSC research began in the 1970s and has progressed exponentially ever since. Research at Cornell University started in 1976 (Nilson, 1987). The objectives of the research were: (1) to study the fundamental nature of the material, as indicated by changes in internal structure and micro-cracking when subjected to short-term and sustained loads; (2) to establish the engineering properties needed for practical design, and; (3) to study the behaviour of both reinforced and prestressed concrete members made of HSC to check the validity of existing design equations and methodology.

In 1979, the American Concrete Institute (ACI) Committee 363 was formed with its mission to study and report on HSC (ACI Committee, 1984). In the same year, a National Science Foundation sponsored workshop was organised to define the scope of existing knowledge, and to recommend future research in the field of HSC, by means of generating dialogue among material scientists, material engineers, researchers with interest in theoretical mechanics, and structural engineers (Shah, 1981). An excellent state-of-the-art report on HSC, and a subsequent discussion on the report was published in 1984. In 1985, a special ACI publication SP-87 on HSC was published (Russell, 1985).

A major research on HSC was carried out by SINTEF in Norway (Holand, 1987). During the pre-project stage a state-of-the-art report and a research work plan were produced in close collaboration with the industry participants, suggesting four sub-projects: SP.1-Beams and columns, SP.2-Plates and shells, SP.3-Fatigue, and SP.4-Materials design. The main emphasis was placed on concrete with cube strengths of 95 MPa for normal density and 75 MPa for light-weight aggregates. The general aim of the research program was to study material parameters for HSC mixes, suitable for large-scale production in construction plants. The principle emphasis was directed to

structural properties and design parameters, and to extend the existing knowledge on HSC for possible adoption in the revision of NS3473. (Holand, 1992)

In the last decade, several national-scale research programs have been established to study various aspects of high strength/high performance concrete (HS/HPC). These include two in the US: Center for Science and Technology for Advanced Cement-Based Materials, Strategic Highway Research Program; the Canadian Network of Centers of Excellent Program on High Performance Concrete; the Royal Norwegian Council for Scientific and Industrial Research Program; the Swedish National Program on High Performance Concrete; the French National Program 'New Ways for Concrete' and the Japanese 'New Reinforced Concrete' Project. (Shah & Ahmad, 1994)

A substantial amount of research work was reported from the results of the above programs and experts in HSC. In June 1987, the first international symposium on utilisation of HSC was held in Stavanger, Norway. The meeting discussed the engineering development, including materials technology, mechanical properties, fatigue of HSC, and various aspects within design and construction utilising HSC. The ideas and applications discussed during this symposium served the basis for even greater utilisation of HSC in the future (Holand *et al.*, 1987).

The second symposium was held in Berkeley, California, USA, in May 1990. Substantial research work and project constructions with HSC were completed in the period between the two symposiums. The findings presented ranged from structural design issues to materials selection, development of high strength light weight concrete, construction methods, and repair techniques. A survey made amongst the participants concluded that HSC was also very durable and commercially obtainable. Furthermore, additional research needed in the area of testing methods was also identified. (Hester, 1990)

The third symposium was held in Lillehammer, Norway, in June 1993. Apart from the similar materials presented in previous symposia, the experience from construction utilising HSC described by case records was also included. The developments of HSC with light weight aggregates were notably reported. (Holand & Sellevold, 1993)

A large number of findings were presented in the following symposium, the fourth international symposium on the utilisation of high strength/performance concrete, also known BHP96, in May 1996, in Paris, France. Among the materials discussed in the meeting are the production of HS/HPC, the material properties including mechanical strength, shrinkage, creep, and durability, the structural behaviour of HS/HPC, bond characteristic, utilisation of light weight aggregate HS/HPC, and the applications in structures and bridges. (de Larrard & Lacroix, 1996)

HSC is a state-of-the-art material, and like most state-of-the-art materials, it commands a premium price. In some cases, the benefits are well worth the additional effort and expense; in others they may not be justifiable. Before the cost-benefits in specific applications are discussed, the economic considerations regarding the use of HSC will be examined.

## **2.2 ECONOMIC CONSIDERATIONS**

For many applications, the cost-benefits of using HSC more than compensate the additional costs of the raw materials and increased quality control. Studies have shown that the benefits associated with the higher load carrying capacities of columns utilising HSC more than offset the additional costs associated with materials and quality control.

The three biggest advantages of HSC that make its use attractive in high-rise buildings are that it provides (1) greater strength per unit cost; (2) greater strength per unit weight; and (3) greater stiffness per unit weight; than most other building materials

(Ghosh & Saatcioglu, 1994). Fig. 2.1 clearly illustrates these trends based on typical unit costs in Australia.

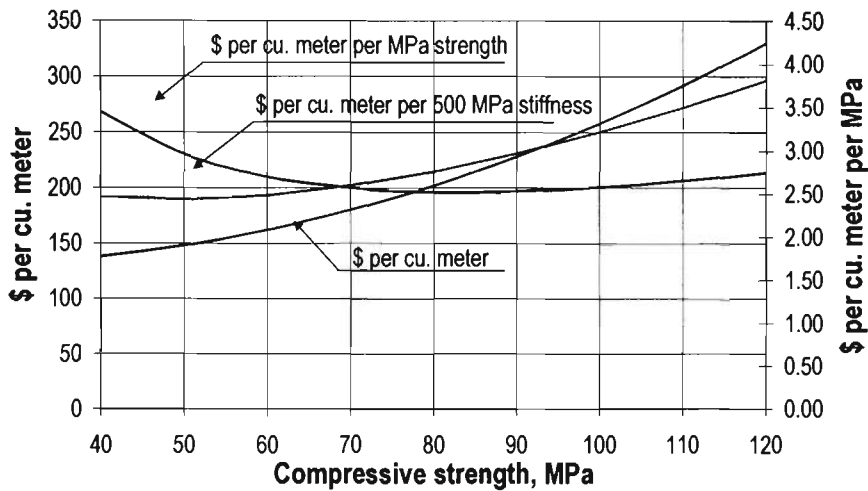


**Fig. 2.1** Concrete cost per unit strength and stiffness. (“Current construction”, 1997)

The unit weight of concrete increases insignificantly as concrete strength increases from moderate to very high levels. Thus, more strength per unit weight is obtained, which can be a significant advantage for construction in high seismic regions, where earthquake induced forces are directly proportional to mass.

The modulus of elasticity of HSC remains to be proportional to the square root of its compressive strength, as found for normal-strength concrete (NSC). Thus, higher stiffness per unit weight is obtained. Indeed, it is quite common for a structural engineer to consider and specify HSC for its stiffness rather than for its strength. The highest concrete strength ever used in a building application has been 131 MPa, which was utilised in the composite columns of 62-storey, 231 m high Two Union Square in Seattle. The 131 MPa was the by-product of the design requirement for an extremely high modulus of elasticity of 49,650 MPa in order to meet the occupant-comfort criterion for the completed building. (Ghosh & Saatcioglu, 1994)

The specific creep of concrete decreases significantly as the concrete strength increases. Due to this lower specific creep, the differential shortening between HSC columns with high stress levels and HSC walls with lower stress levels is minimised.

Reinforced concrete has a positive aspect in regard to its adaptability to fast-track construction of high-rise buildings. In developed countries with a high construction cost environment, reducing the construction time not only reduces labour costs but also the financial cost in terms of interest component. The use of HSC provides further cost benefit as it allows for the construction forms to be stripped sooner due to the early high concrete strength, reducing the overall construction time.

The most tenable advantage of HSC is the reduction in member size, which mean more floor area available for rental, a significant factor in commercial buildings. In the case of a major city such HongKong, where office space costs over US\$12,000 per m<sup>2</sup> (Chan & Anson, 1994), the extra revenue generated by the additional floor space can be very large indeed.

ACI Committee 363 (1984) presented two case histories translating the savings into actual dollars. In 1968, Philadelphia's first high-rise office building was designed using 41 MPa concrete. Columns of the first three floors were built of structural steel to avoid unacceptable oversized columns on the lower floors. However, a comparison study made by the design engineers for 55 MPa concrete showed that (1) with the same column size as the original 41 MPa concrete size, a 60% reduction in reinforcing steel would have been made by using 55 MPa concrete or (2) with the same amount of reinforcing steel used as in the original column, the column size could have been reduced from 915x1170 mm to 760x760 mm. This size would have been accepted by the architect and owner and would have eliminated the need for an additional trade, structural steel, on the job. Approximate calculations showed that by using 55 MPa concrete, the savings would amount to US\$530,000.

The second case history was demonstrated in the construction of New York City's first building using 55 MPa concrete, The Palace Hotel built in 1979. The building was originally conceived using structural steel for the lower floors with a reinforced concrete superstructure. However, the engineers were able to convert the entire

design, except for the two columns on the lowest four levels, to reinforced concrete by the use of 55 MPa concrete. Increasing the common limitation of 41 MPa concrete to 55 MPa reduced the column size by approximately 25 percent, resulted in a 10% reduction in reinforcing steel.

### 2.3 A CLOSE LOOK AT THE COST-BENEFITS

Schmidt and Hoffman (1975) were the first to publish data indicating that the most economical way to design columns was to use the highest available strength concrete resulting in the least amount of reinforcing steel. They compiled a table indicating the cost of supporting 444.8 kN (100 kips) of service load. The cost per storey was US\$5.02 with 41.4 MPa (6,000 psi) concrete, \$4.21 with 51.7 MPa (7,500 psi) and \$3.65 with 62 MPa (9000 psi) concrete. While the figures reflect 1975 costs, the relative cost are relevant to present day.

Material Service Corporation of Chicago conducted a pricing study in 1983 that demonstrated the definite cost advantages resulting from reduced reinforcing steel percentages by use of HSC in short tied columns. The study was made for a column supporting a design ultimate load (1.4D+1.7L) of 4,448 kN (1,000 kips).

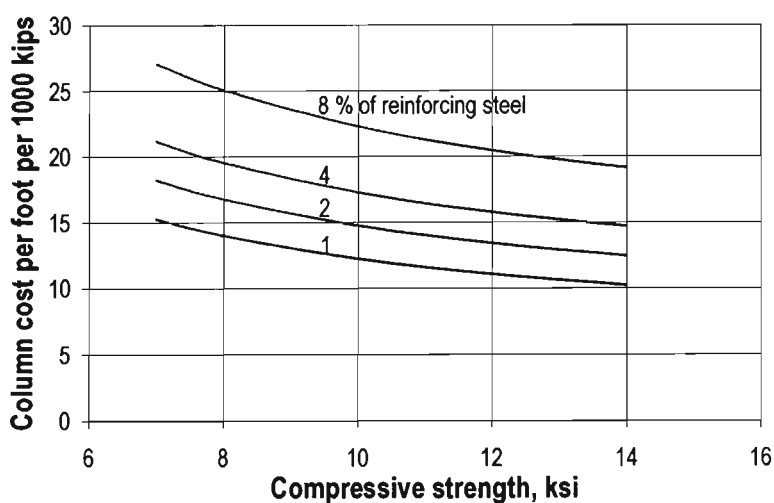


Fig. 2.2 Concrete column cost (ACI committee, 1984).

Fig. 2.2 shows, the most economical design was using HSC with a minimum percentage of reinforcing steel. (ACI Committee, 1984)

In 1984, a study was conducted to investigate possible cost savings in the design of over 1700 columns in a 45-storeys high-rise building that were already under construction in Chicago. A computer program was developed that examined several variables and their effect on the column cost. All of the columns were designed to carry the same load, but with differing amounts of reinforcement and cross sectional areas with variable concrete strengths. The study concluded that the most economical column design used about 1 percent longitudinal reinforcing steel in conjunction with higher strength concrete. ("Computer cuts," 1989)

In 1985, Moreno and Zils (1985) examined several factors associated with the optimum design of high-rise buildings. Among these factors were lateral forces, building drift, foundation systems and cost of concrete material and placement, reinforcement and column formwork. Three column sizes, 51, 76 and 102 cm (20, 30 and 40 in.), were selected and construction cost were computed per unit of axial load. Cost-load evaluation indicated that cost per unit of axial load decreased as the concrete strength increased.

Smith and Rad (1989) investigated the economic advantages of using HSC in columns in low-rise and medium-rise buildings using ACI 318-83 provisions. Two-dimensional frame model consisting of 4 bays (5 columns) without structural walls was selected for the analysis. 5-storeys were chosen to represent a low-rise building and 15 for a medium-rise building. The parameters, which were varied in the study, included loading, geometry of the structure and concrete strength. Cost related to formwork, reinforcing steel, concrete and form rental were considered. For the design and cost analysis, three concrete strengths, 28, 55 and 83 MPa (4,000, 8,000 and 12,000 psi), were used. Based on the initial gross column sizes using the 8% maximum reinforcement with an initial concrete strength of 4,000 psi, they concluded that (1) relative reduction in percentage of reinforcement is in the order of 40% for

8,000 psi concrete and 67% for 12,000 psi concrete; (2) relative reduction in the column construction cost is in the order of 26% for 55 MPa concrete and 42% for 83 MPa concrete. See Fig. 2.3.

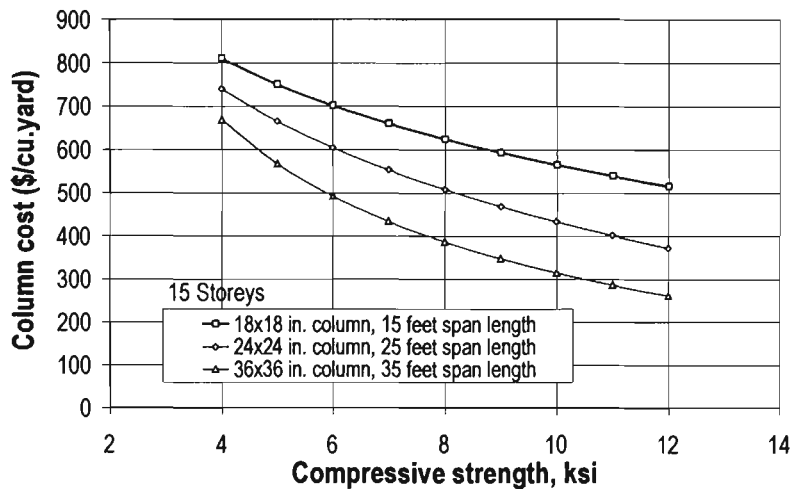


Fig. 2.3 Concrete column cost (Rad and Smith, 1989)

Martin (1989) and Burnett (1989) presented the economic evaluations for core walls of 55-storey Bourke Place building in Melbourne. Increasing the concrete strength from 40 MPa to 60 MPa gave approximately 27 m<sup>2</sup> of additional lettable area per floor. By taking the capitalised value of \$3,500/m<sup>2</sup>, it resulted in an effective benefit of about \$99,000 per floor for the client.

Paks and Hira (1994) demonstrated the cost benefits of minimising the core area for a typical 50-storey prestigious CBD building in Australia. Based on the 1994 prevailing yield rate of 7% and rental income of \$500 per m<sup>2</sup>, the capitalised value was \$10,000 per m<sup>2</sup>. A modest 50 mm reduction in the thickness of all walls of a typical 6-cell core element represented a capitalised value of over \$5 million (approximately 30% to 40% of the total structural cost of the core)

Fragomeni *et al.* (1994) performed a cost analysis of a typical concrete building in Melbourne. A spreadsheet program was developed that examined the cost saving of each wall. The analysis considered the effect of using HSC and resulted in an increase in net lettable area. A 47-storey 8-cell core was taken as an example to illustrate the

use of the spreadsheet and the significance of a proposed modified wall design formula for the Australian concrete code AS3600. Based on capitalised value of \$3,500 per m<sup>2</sup> and concrete cost \$250 per m<sup>3</sup> for 40 MPa increasing proportionally to \$306 per m<sup>3</sup> for 80 MPa, they concluded that a total saving per core per storey of \$7,400 could be achieved with 50 MPa concrete and \$15,000 with 80 MPa concrete, compared to the 40 MPa concrete option.

## 2.4 MAJOR CONCERNS

Despite the numerous studies that have demonstrated the significant economy achieved by using HSC in columns and core walls of buildings, some concerns have been expressed. Two principle areas of concern exist: (1) applicability of current code requirements to HSC; (2) inelastic deformability of HSC structural members under cyclic loading of the type induced by earthquake excitation. These concerns stem from the fact that the requirements for design and detailing of reinforced concrete elements in different model codes are primarily empirical and are developed based on experimental data obtained from testing specimens having compressive strength below 40 MPa.

Azizinamini *et al.* (1994) concluded that when axial load levels are below 20% of the column's concentric axial load capacity, test results indicate that high-strength concrete columns (compressive strength in the range of 70 to 100 MPa) designed based on seismic provisions of ACI 318-89 building code achieve a 4% drift index without failure. When the level of axial load is above 40% of the column's axial load capacity a higher amount of transverse reinforcement than that specified in seismic provisions of ACI 318-89 building code is needed. Test results indicate that this higher amount of transverse reinforcement should be provided in part in the form of higher yield strength transverse reinforcement. Similar results have been reported by several researchers (Watanabe *et al.*, 1987; Muruguma *et al.*, 1992; Pendyala *et al.*, 1995)

In general, the major focus of the reported investigations has been to study the validity of extending the current building code requirements to HSC and to evaluate the similarities and differences between HSC and NSC. Subsequently, modifications for the current codes allowing the use of higher strength concrete were proposed and many of them have been incorporated in the new revised codes. (FIP-CEB, 1990; CEB-FIP, 1995)

## 2.5 COMMENTS ON CURRENT RESEARCH AND APPLICATIONS

Despite the significant effort directed towards the study of HSC over the last decade, most research has been restricted to the area of material development for producing higher strength concrete, production methods, material properties evaluations, and the implication of the material properties on the structural design and performance.

Cost-benefit analysis carried out showed the use of HSC in low and high rise constructions was of financial benefit. Apart from the obvious higher compressive strength, HSC offers greater elastic modulus, improved durability, early stripping, increased tensile strength, and lower creep characteristics. A review of literature has indicated the lack of work directed to the economy study of structural wall utilising HSC.

Fig. 2.4 shows a series of nine concrete buildings, each of which, with the exception of Two Prudential Plaza, was the tallest concrete building in the world at the time of its completion. It is clear the growth in the height of concrete buildings has gone hand-in-hand with the availability of higher and higher strength concretes.

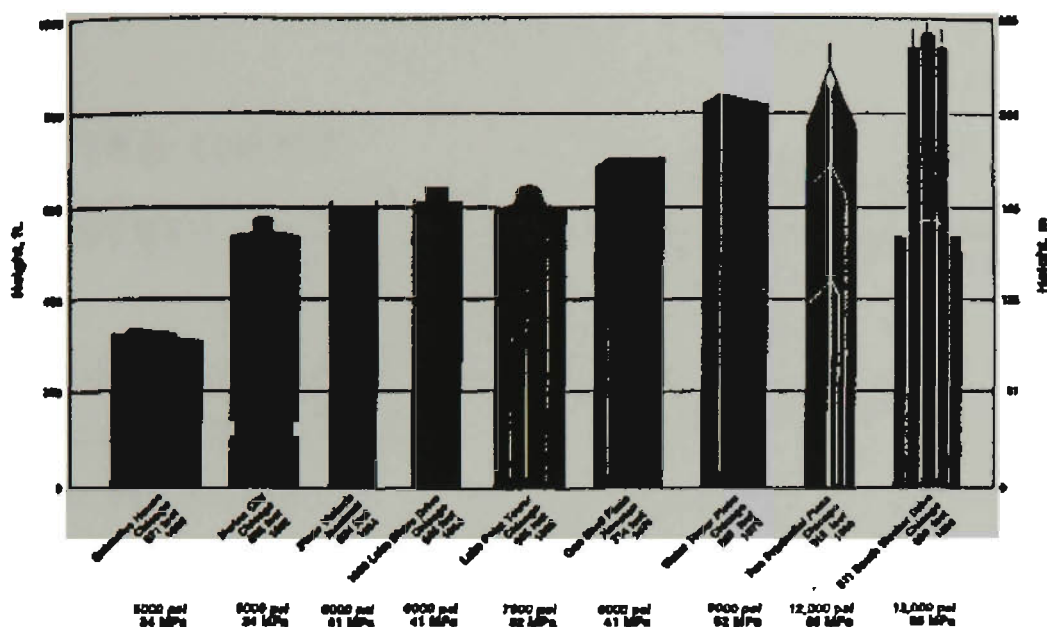


Fig. 2.4 High-strength concrete in high-rise constructions.

Astonishingly, seven out of the nine record-setting buildings illustrated in Fig. 2.4 are located in Chicago, a city that in many ways has pioneered the evolution of HSC technology. This also shows that the majority of high-rise HSC buildings were built in the regions of low seismic activity. One of the primary concerns regarding the use of HSC in the areas of high seismic is the reduced ductility of members constructed with HSC.

In most slender structures, lateral loads govern in the design of many members. The design of these members, in many cases, is not controlled by strength criteria, but by inter-storey displacement or overall lateral displacement or the stiffness criteria. The use of structural optimization techniques with the displacement-constraint problem has an attractive objective of producing the most economical structure. The basic technique of the optimisation is presented Chapter 4.

## **CHAPTER THREE**

---

### **STRUCTURAL MODELS AND DESIGN CRITERIA**

The preceding chapter revealed the significant economic advantages of using high-strength concrete (HSC) in vertical members of low-rise and high-rise buildings. Whilst the studies primarily focused on the use of HSC in the columns, it is believed that its application in structural wall elements will also be significant. The economic aspect of HSC application in structural walls, in the form of cantilever wall and coupled wall, is investigated in this study. In this chapter the design loads and criteria are outlined. This study does not follow any particular design code for structural design of walls. However, the provisions from the Building Code Requirements for Structural Concrete (ACI 318-95, 1995) and the New Zealand Standard Code of Practice for the Design of Concrete Structures (SANZ NZS 3101, 1995) are generally adopted for the design purposes.

#### **3.1 STRUCTURAL WALL SYSTEMS**

For the purpose of this study, a structural wall element is considered to be a member that contributes significantly to resisting lateral loads. Such elements may be part of a service core or a stairwell, or they may serve as a fire barrier between tenancies (Fig. 3.1). They are usually continuous down to the foundation level to which they are rigidly attached to form vertical cantilevers. Their in plane stiffness and strength makes them well suited for bracing buildings up to 35 storeys (CTBUH, 1995), while simultaneously carrying gravity loading. Ideally, the wall elements are located such that they attract an amount of gravity loading, sufficient to suppress the maximum tensile bending stresses caused by the lateral loads, resulting in minimum wall reinforcement requirement.

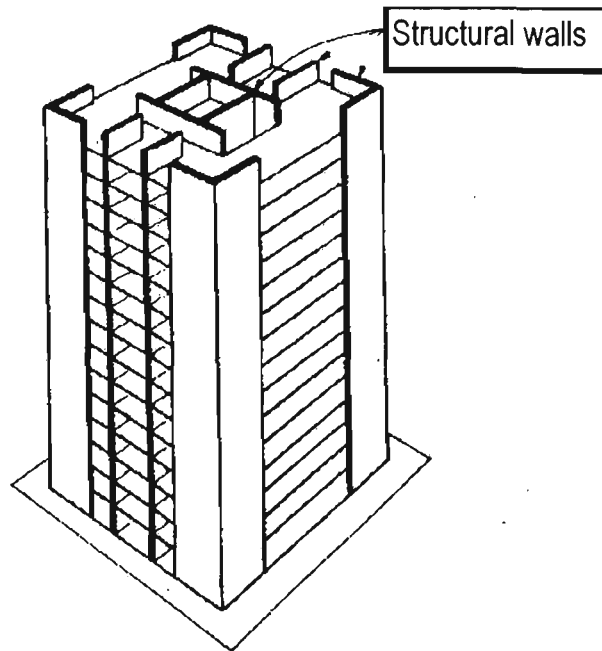


**Fig. 3.1** Structural wall building

A tall structural wall building typically comprises an assembly of structural walls whose length and thickness may change, or which may be discontinued, at stages up the height of the building. The walls can be planar or three-dimensional such as “L”, “T”, “I”, or “C” shape section, to better suit the planning and to increase their flexural stiffness. Planar walls are considered to be effective only to resist horizontal loads in the plane of the walls. However, in three-dimensional wall configuration, such as the core service walls, they are normally designed to resist the horizontal loads in both orthogonal directions.

The wall elements may be connected by flexible slab diaphragm or alternatively by flexible beams forming a coupled wall system. In the former case, each wall element forms an individual cantilever and any applied lateral load will be resisted by individual moments in each wall element, where the magnitude of the moment is proportional to the wall flexural rigidity. In the later case, the coupled wall system, when subjected to lateral loads, the connecting beam-ends are forced to rotate and displace vertically, causing the beams to deform in double curvature. The bending action induces shears in the connecting beams, which in turn induce axial forces in the walls, tension in the windward wall and compression in the leeward wall.

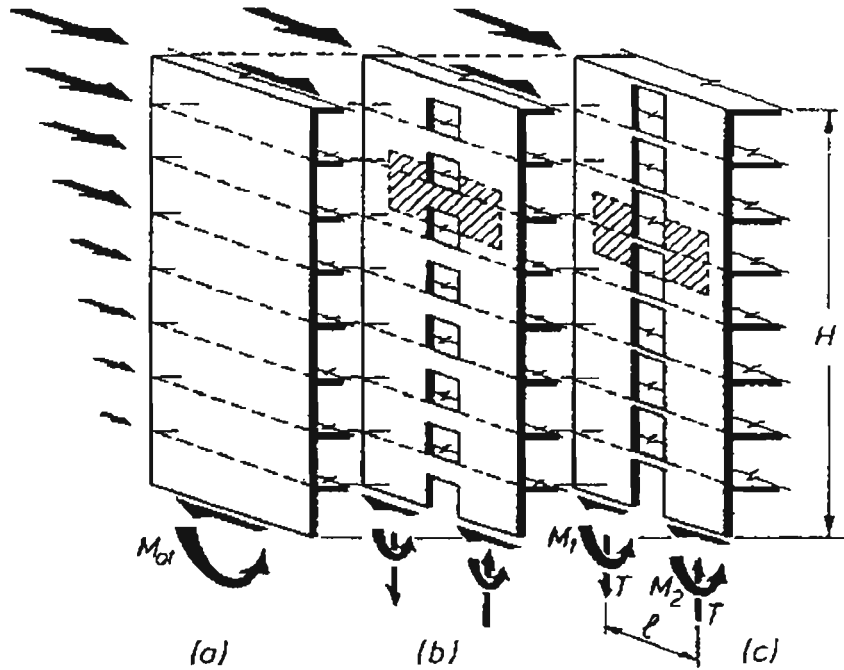


Fig 3.2 Flexural resisting mechanisms in structural walls

The external moment,  $M$ , at any level is then resisted by the sum of the bending moment,  $M_i$ , of the walls at the level, and the moment generated by the axial loads,  $N_i l_i$ , where  $l_i$  is the lever arm of the wall  $i$  to the primary axis of the wall system. i.e.

$$M = \sum M_i + \sum N_i l_i \quad (3.1)$$

These aspects are shown qualitatively in Fig. 3.2, which compares the mode of flexural resistance of coupled walls with different strength coupling beams with that of a simple cantilever wall. The action of the connecting beams is to reduce the magnitudes of the moments in the two walls by causing a proportion of the applied moment to be carried by coupled axial forces.

### 3.2 DESIGN CRITERIA

The design philosophy adopted in the modern codes has progressed from earlier working stress or ultimate strength design bases to more generally accepted probability-based approaches. This probabilistic approach, for both structural

properties and loading conditions, has led to limit states design method. The aims of the limit states method are to ensure that all structures and their constituent components are designed to sustain safely all loads and deformations that are liable to occur during construction and service, and to have adequate durability during the lifetime of the structure.

In the design of tall building structures for earthquake resistance, the limit states are translated into (Paulay & Priestley, 1992):

- (1) Serviceability limit state corresponding to low intensity earthquake (i.e. a 50-year-return-period earthquake). During small and frequent earthquakes no damage should occur to the structures and non-structural components. The appropriate design effort is to control the lateral displacements and to ensure that all components forming the structure remain essentially elastic.
- (2) Ultimate limit state. Structures should withstand an earthquake of moderate intensity (i.e. a 500-year-return-period earthquake) within economically repairable damage in the structural elements, as well as in the non-structural elements.
- (3) Survival limit state corresponding to high intensity earthquake (i.e. a 5000-year-return-period earthquake). During rare, strong feasible earthquakes, extensive damage to both structural and non-structural elements will have to be accepted. However, collapse of structure and the associated loss of life must be prevented. It must be recognised that unless structures are proportioned to possess exceptionally high level of lateral load resistance, inelastic deformations during strong earthquake are to be expected. This ability of the structure or its component to undergo the post-elastic deformation is referred to as ductility.

The following sections consider the criteria and methodology that apply to the design of tall concrete wall elements in building structures for earthquake resistance, which are: the design loads, serviceability criteria in terms of inter-storey drift, design strength of wall section, and requirements for ductility.

### 3.2.1 LOADING

#### GRAVITY LOADING

Dead load is specified as the intensity of a uniformly distributed floor load and all other permanently attached materials. The detailed values adopted are given in Table 3.1. The 150 mm slab is an equivalent slab thickness incorporating a 120 mm two-way slab spanning between nominal slab band beams.

**Table. 3.1** Design dead loads

	<b>D (kPa)</b>
150 mm Reinforced Concrete Slab	3.60
Floor Finishing	1.20
Mechanical & Electrical	0.40
<b>Total</b>	<b>5.20</b>

A live load of 2.5 kPa for office building is adopted for design purposes. However, the probability of an area being subjected to the maximum specified intensity of live load diminishes as the size of the loaded area increases. To account for the improbability of this full live load being applied simultaneously over a large area, design codes typically allow using a reduced design live load. This load is normally is given in the form:

$$L_r = \psi L \quad (3.2)$$

where  $\psi$  is a reduction coefficient which depends on the building occupancy and the type of loading,  $L$  and  $L_r$  are the code specified live load and reduced live load, respectively. Hereafter, only the symbol  $L$  is used whenever reference to live load is made, but this will imply that reduced live load will be substituted where appropriate. The coefficient reductions for office buildings adopted are 0.60 if earthquake loads are not included and 0.30 if earthquake loads are included. In addition to the coefficient  $\psi$ , a second reduction coefficient is applied to vertical members such as columns and walls that support cumulative loads of the floors above, as given in Table 3.2.

**Table 3.2** Reduction coefficients for cumulative live load

<b>Number of stories supported</b>	<b>Reduction to be multiplied to the cumulative load</b>
1	1.0
2	1.0
3	0.9
4	0.8
5	0.7
6	0.6
7	0.5
8 or more	0.4

## LATERAL LOADING

A structure shall be designed to resist a total lateral earthquake load  $V$ , which shall be assumed to act independently in orthogonal directions. The  $V$ , also called the base shear, is expressed as

$$V = CIKW \quad (3.3)$$

where  $W$  is the weight of building, which should include dead load plus the probable value of live load.

The seismic coefficient,  $C$ , represents numerically the inelastic earthquake acceleration response spectrum of a region, and is normally defined in the form of design seismic risk maps. In countries with active seismic activities, such as the United States, Japan, and Indonesia, a large area is normally divided into regions of approximately equal seismic probability. Fig 3.3 shows the divisions of Indonesia into seismic risk zones. The seismic coefficient may include the influence of soil type by specifying different curves for different soil stiffness. A design seismic coefficient curve for Jakarta, the capital city of Indonesia, which is in region 4, is shown in Fig. 3.4.

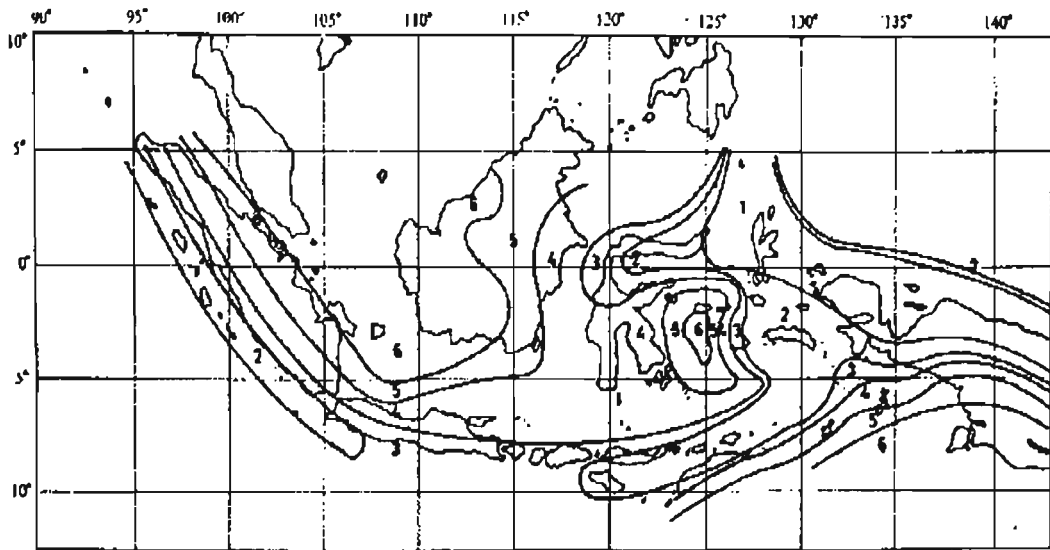


**Fig. 3.3** Indonesian seismic risk map

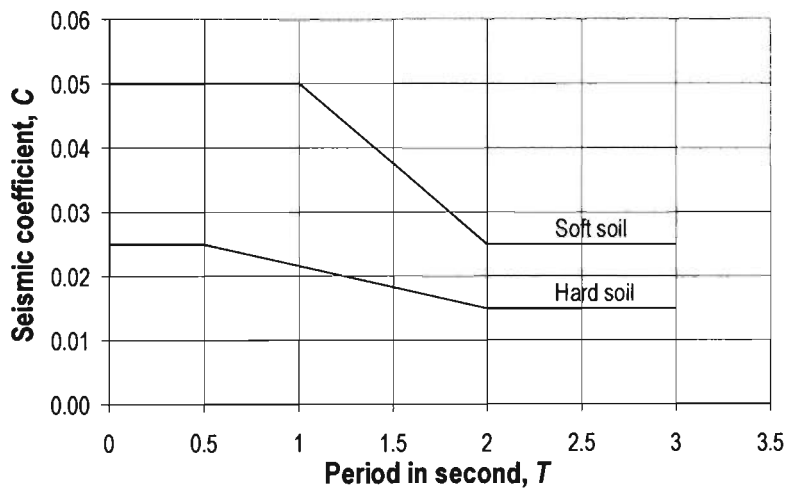


**Fig. 3.4** Seismic coefficient for region 4, Jakarta

The importance factor,  $I$ , is concerned with the need to protect essential facilities that must operate after an earthquake and is also applied to buildings where collapse could cause unusual hazard to the public. The design value for typical structures is equal to unity.

Structural factor,  $K$ , is a measure of the ability of the structural system to sustain cyclic deformations without collapse. Structures with substantial ductility and capable of dissipating energy at a substantial number of locations are assigned  $K=1.0$ , and  $K$  increases as the available ductility decreases. For the ductile cantilever and coupled wall, the values of the structural factor are taken as 1.2 and 1.0, respectively.

Having determined the value of the base shear it is necessary to distribute the base shear as effective horizontal loads at the various floor levels, in order to proceed with the analysis. The load at any level depends on the dynamic characteristics of the structural deformation, the mass at the level, and the amplitude of oscillation.

Analysis used in this study is essentially based on linear elastic analysis. Although non-linear inelastic programs are available, these are impractical and rarely employed in practice. There are two common methods for applying the dynamic earthquake loads, namely, time history analysis and response spectrum analysis. Time history method requires prescription of a specific ground motion record, which is an estimate of a future critical earthquake ground motion that can occur at a given site. This method requires several representative ground motions to be considered to allow for the uncertainty of the design motions at a site during the lifetime of a structure. Therefore it is rational to base seismic design on a range of possible earthquake ground motions rather than several single earthquakes. This is obtained by application of a response spectrum, which represents an upper-bound response of several different ground motion records.

In the absence of dynamic structural analysis programs, the distribution of the total horizontal seismic base shear over the height of the building can be derived by the following formula:

$$F_i = \frac{W_i h_i}{\sum W_i h_i} V \quad (3.4)$$

provided the buildings are regular, where  $F_i$  is the horizontal seismic load assigned to the level designated as  $i$ ,  $W_i$  is the seismic weight of the structure of level  $i$ , and  $h_i$  is the height of level  $i$  to the fixation level.

### 3.2.2 SERVICEABILITY CRITERIA

It is well established that lateral deflection or drift sustained during response to an earthquake is a major cause to both structural and non-structural damage. Studies (Freeman, 1980) showed that damage to non-structural elements occurs at inter-storey drift ratio of approximately 0.005. This drift ratio corresponds to the serviceability limit states in model codes (ICBO, 1991; CEN, 1994); this is comparable to seismic action with a higher probability of occurrence than the design seismic action. For rare, strong earthquakes, ATC provisions for seismic regulations (ATC 3-06, 1978) and New Zealand loading code NZS4203 (SANZ, 1992) suggest that inter-storey drift ratio be limited to 0.015.

For the verification of the serviceability limit state, the drifts due to the design seismic action taking into account the lower return period are calculated. NZS4203 uses a limit state factor, which has a value of 1/6 for serviceability limit state and a value of 1.0 for ultimate limit state, in the calculation of earthquake load for the two limit states. The European standard EC8 uses a reduced ultimate drift, which is a result of elastic deformation reduced by a reduction factor. The factor, which depends on the importance category of the structure, is taken as 2.0 for buildings of vital importance for civil protection and whose collapse could cause unusual hazard to the public; 2.5 for buildings of normal use and of minor importance for public safety. It is noted that the serviceability criteria adopted by EC8 are more stringent than those of NZS4203 and of many other national codes (CEB Model Code 1990 - CEB, 1993; ATC 3-06, 1978).

In this study, the inter-storey drifts are calculated from the elastic response to the design earthquake loads. These drifts shall not exceed a value defined by  $0.015 \frac{\mu}{K}$ , an equivalent drift limit due to an elastic response loading, in which  $\mu$  is the structural ductility index.

To obtain a reasonable estimate of the lateral displacement, stiffness properties of all elements of the structural wall include an allowance for the effects of cracking. These properties are based on an equivalent moment of inertia  $I_e$ , which is then related to the moment of inertia  $I_g$  of the uncracked gross cross section as given below (Paulay & Priestley, 1992)

for walls

$$I_e = \left( \frac{100}{f_y} + \frac{P_u}{f_c'} \right) I_g \approx 0.6 I_g \quad (3.5)$$

and for coupling beams

$$I_e = 0.4 I_g \left[ 1 + 3 \left( \frac{h}{l_n} \right)^2 \right] \approx 0.4 I_g \quad (3.6)$$

where  $P_u$  is axial load on the wall during an earthquake taken positive when causing compression;  $f_c$  and  $f_y$  are characteristic strength of concrete cylinder and yield strength of reinforcing steel respectively;  $h$  and  $l_n$  are depth and clear span of coupling beam.

The modulus of elasticity for the calculation of structural stiffness is taken from the formula recommended by ACI committee 363 on high-strength concrete for normal weight concretes (ACI Committee 363, 1992).

$$E_c = 3320 \sqrt{f_c'} + 6900 \text{ MPa} \quad (3.7)$$

This formula is based on work performed at Cornell University (Carrasquillo, 1981).

### 3.2.3 STRENGTH DESIGN

#### DESIGN ACTIONS

The required strength  $U$  to be provided at any section of a member in the seismic design is determined by combining the values of dead load  $D$ , live load  $L$ , and earthquake load  $E$ . This strength is defined as:

$$U = 1.05(D + L_r \pm E) \quad (3.8)$$

The design strategy adopted in this thesis is based on the philosophy of capacity design. To quote Paulay and Prestley (1992)

***“In the capacity design of structures for earthquake resistance, distinct elements of the primary lateral force resisting system are chosen and suitably designed and detailed for energy dissipation. The critical regions of these members, often termed plastic hinges, are detailed for inelastic flexural action, and shear failure is inhibited by a suitable strength differential. All other structural elements are then protected against actions that could cause failure by providing them with strength greater than that corresponding to the maximum feasible strength in the potential plastic hinge regions.”***

Design moment and shear forces are based on the recommended design envelopes proposed by Paulay & Priestley (1992) as shown in Fig. 3.5. The moment envelop in Fig. 3.5(a) is developed from the ideal or nominal flexural strength at the base, which is established from the details of the section designed and the code specified material strength properties, in the presence of a realistic axial load. The shaded moment diagram shows moments that would result from the application of lateral static force. The straight dashed line represents the maximum moment demands during the elastic as well as inelastic dynamic response to ground shaking. The plastic hinge length  $L_p$  is estimated as follows:

$$L_p = \max\left(L_w, \frac{H_w}{6}\right) \tag{3.9}$$

but

$$L_p \leq \begin{cases} 2L_w & \text{for } n \leq 6 \text{ storeys} \\ H_s & \text{for } n > 6 \text{ storeys} \\ 2H_s & \text{for } n > 6 \text{ storeys} \end{cases}$$

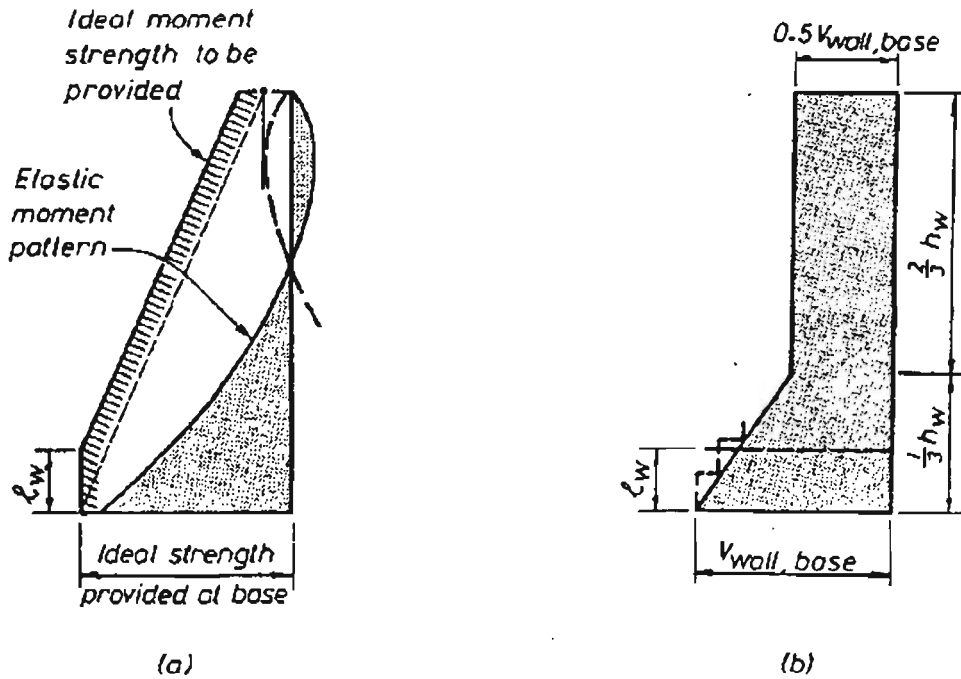


Fig. 3.5 Recommended design actions for structural wall (a) Moment; (b) Shear

The shear demand  $V_{w,base}$  in Fig. 3.5(b) is obtained as

$$V_w = \omega_v \phi_{o,w} V_u \tag{3.10}$$

where  $V_u$  is the shear demand derived from code specified lateral force;  $\omega_v$  is the dynamic magnification factor, for  $n$  storeys to be taken as

$$\omega_v = 0.9 + \frac{n}{10} \quad \text{for } n \leq 6 \tag{3.11}$$

$$\omega_v = 1.3 + \frac{n}{30} \quad \text{for } n > 6 \tag{3.12}$$

and the flexural overstrength factor  $\phi_{o,w}$  is

$$\phi_{o,w} = \frac{M_{o,w}}{M_u} \quad (3.13)$$

in which  $M_u$  is the moment resulting from code specified forces and  $M_{o,w}$  is the flexural overstrength defined as

$$M_{o,w} \geq \frac{\lambda_o}{\phi} M_u \quad (3.14)$$

where  $\lambda_o$  is the overstrength factor, taken as 1.25 for strength of reinforcing steel  $f_y < 400$  MPa and 1.40 for  $f_c \geq 400$  MPa (SNI T-15-1991, 1991); and  $\phi$  is a strength reduction factor.

## FLEXURAL STRENGTH

The analytical calculation of flexural strength of a column and wall section is based on the traditional concepts of equilibrium and strain compatibility, consistent with the plane section hypothesis. A computer program RCDESIGN97, developed by the author (Bong, 1997), is employed to calculate the flexural strength of the wall sections. The methodology used in RCDESIGN97 is described in Appendix C.

## SHEAR STRENGTH

Design for shear strength for a wall section follows the guidance given by Paulay and Prestley (1992) and is summarised in this section. The shear strength of a section is given by:

$$V_i = V_c + V_s \quad (3.15)$$

where  $V_c = v_c b_w l_w$  is the contribution of concrete and  $V_s$  is the contribution of shear reinforcement,  $b_w$  and  $l_w$  are the effective width and depth of the wall cross section, respectively.

The contribution of the concrete is taken as (1) for all regions except plastic hinges  $v_c = 0.27\sqrt{f'_c + N_u/4A_g}$ ; (2) for plastic hinge regions  $v_c = 0.6\sqrt{N_u/A_g}$ . The contribution of shear reinforcement with the area  $A_v$  and spacing  $s$  to the total shear strength is given by  $V_s = A_v f_y (d/s)$ .

To ensure that premature diagonal compression failure will not occur in the web before the onset of yielding of the web reinforcement, the nominal shear stress needs to be limited. Recommended limitations are (1) in general  $v_i \leq 0.2f'_c \leq 6 \text{ MPa}$ ; (2) in plastic hinge regions  $v_i = (0.22\phi_{o,w} / \mu_\Delta + 0.03)f'_c \leq 0.16f'_c$ , where  $v_i = V_i / 0.8b_w l_w$ .

### 3.2.4 DUCTILITY

It is well understood in seismic design that the action of a seismic excitation on an oscillation system can be resisted either with large restoring forces and responding within the elastic range or with smaller restoring forces and undergoing large plastic deformation. The ability of a system to undergo plastic deformation without excessive stiffness degradation whilst maintaining strength is characterised as ductility.

It is generally uneconomic to design structures to respond to seismic loads in the elastic range. The inelastic response force level is less than the corresponding elastic response by a factor  $R$ . For long period structures, period greater than 0.7 seconds, the force reduction factor is approximately equal to the displacement ductility factor, which is defined as the ratio of the ultimate displacement at failure to the yield displacement deformation. However, for structures to respond inelastically, they should possess adequate displacement ductility.

The displacement ductility capacity of walls depends on the rotational capacity of the plastic hinge at the base. It is convenient to express the displacement ductility in terms of curvature ductility capacity, which can readily be evaluated when the wall section is designed for strength. A detailed study of the parameters related to ductility capacity is given by Paulay and Prestley (1993).

Paulay and Prestley presented a method that ensures a minimum curvature ductility capacity by limiting the compression zone depth. The maximum compression depth,  $c_c$ , corresponding to a development of a desired displacement capacity factor  $\mu_\Delta$ , taking into account variations in aspect ratio  $A_r$  and the yield strength of the tension reinforcement  $f_y$  is given as:

$$c_c = \frac{k_c M_{o,u}}{(\mu_\Delta - 0.7)(17 + A_r)\lambda_o f_y M_E} l_w \quad (3.16)$$

where  $k_c = 3400$  MPa. Eq. (3.16) ensure a minimum curvature ductility be sustained without the provision of confining reinforcement in the compression region. However, when the computed neutral axis depth,  $c$ , is larger than critical value  $c_c$ , at least a portion of the compression region of the wall section needs to be confined. It is suggested that the length of the wall section to be confined should not be less than  $\alpha c$ , where

$$\alpha = (1 - 0.7c_c / c) \geq 0.5 \quad (3.17)$$

where  $c_c/c < 1$ . The lower limit (i.e., 0.5) is given in case  $c$  is only a little larger than  $c_c$ , leading to an impractical area to be confined.

### 3.3 CONCLUDING REMARKS

The design of structural systems for tall buildings typically needs to satisfy the serviceability, strength, and survival limit states. The serviceability limit state criteria normally corresponds to the inter-storey drift, as it often causes the damage of non-structural elements. Design guidance for strength design and satisfying ductility requirement is also given. This chapter provides the basis for the structural design of walls in Chapters 6, 7, and 8. The next chapter will discuss the basic techniques of structural optimisation for structural wall systems based on the principle of virtual work. A more practical technique for optimising the structural wall optimisation will be presented in Chapter 5.

## CHAPTER FOUR

---

### STRUCTURAL OPTIMIZATION

The preceding chapter concluded that the design of tall building structures for earthquake resistant needs to satisfy the serviceability limit state, ultimate limit state, and survival limit state. At the early stage of design process, normally the designer is to determine the member cross sectional sizes. In determining the initial cross sectional sizes, consideration is often given to the serviceability criteria. Also as the building structure increases in height, the stiffness criteria becomes increasingly important compared to strength criteria in the design of the individual members. Despite many codes providing guidance for selecting the beam sizes and slab thicknesses for general structural conditions, the selection of column sizes and wall thicknesses has been an iterative procedure, especially when buildings are subjected to lateral loadings. Therefore it becomes essential to develop an efficient method for column and wall size selections. This can normally be accomplished by utilising structural optimisation techniques.

This chapter outlines the development of a basic technique of structural optimization for lateral load resisting structural systems subject to a displacement constraint. The method, which uses the well-known principle of virtual work, provides a necessary parameter, the displacement participation factors (DPF) for solving the optimisation problems. To illustrate the optimization method, examples are presented at the end of the chapter. In the next chapter, a practical optimisation technique will be derived from this optimisation technique, which is very useful in the construction practice of tall buildings.

## 4.1 PRINCIPLE OF VIRTUAL WORK: UNIT LOAD METHOD

It is possible to analyse determinate structures by solving three equations of statical equilibrium ( $\sum V = 0$ ,  $\sum H = 0$  and  $\sum M = 0$ ). However, with most real structures, which are statically indeterminate with the presence of redundant members, it is not possible to analyse these structures with the three equations of equilibrium alone. In one of the analysis methods (eg. flexibility method), it is necessary to consider relative member deformation before a solution of the structure can be attained. These deformations provide the basic equations of compatibility that, in addition to the three equations of equilibrium, allow the solution of the unknown effects and the internal forces and moments upon which the subsequent structural design is based.

There are two basic approaches to the analysis of structural deformations, the strain energy and virtual work. The principle of virtual work can be further divided into two categories: the principle of virtual displacements and principle of virtual forces. The principle of virtual forces, as sometimes referred to as the unit load method, is commonly used in developing classical methods of structural analysis. This section outlines the principle of this method.

Principle of virtual work: In any structural system in equilibrium, the external virtual work done by the external virtual forces under the actual displacement is equal to the internal virtual work done by the virtual stresses under the actual strains.

Two systems of loading are required when using this method. The first system is the real loading the structural system is subjected to. The second system consists of the same structure subjected to a unit load at the point and direction of the desired displacement.

According to the principle of virtual work, the external virtual work is equal to the unit virtual load multiplied by the actual displacement  $D$  in the direction of the virtual load. It is written as

unit load  $\times D$

The internal virtual work is equal to the resultant of the internal forces, resulting from the application of the unit virtual load in the second system, multiplied by the actual deformation in the first system. ie.

$$\sum_{i=1}^m u_i d_i$$

where  $u_i$  is the internal forces in member  $i$  due to the unit virtual load,  $d_i$  is the deformation in member  $i$  due to the actual loads, and  $m$  is the total number of members in the structure.

Equating the work of the external and internal forces gives the fundamental equation of the unit load method:

$$D = \sum_{i=1}^m u_i d_i \quad (4.1)$$

The quantity  $d_i$  appearing in Eq.(4.1) can be expressed in terms of member properties. For a member with length  $L_i$ , flexural moment of inertia  $I_i$ , and modulus of elasticity  $E_i$ , the flexural deformation is given by the formula

$$d_{M,i} = \int_0^{L_i} \frac{U_{M,i} dx}{E_i I_i}$$

in which  $U_{M,i}$  represents the flexural moment in element  $i$  due to the actual load. Similarly, the expressions of the axial and shear deformations are

$$d_{N,i} = \int_0^L \frac{U_{N,i} dx}{E_i A_i} \qquad d_{V,i} = \int_0^L \frac{U_{V,i} dx}{G_i A_i}$$

where  $U_{N,i}$  and  $U_{V,i}$  are the axial and shear force caused by actual loads;  $A_i$  is the cross sectional area; and  $G_i$  is the shear elastic material modulus.

Substituting these relations into Eq.(4.1), the displacement in the direction of the virtual load is

$$D = \sum_{i=1}^m \left( \int_0^L \frac{u_{M,i} U_{M,i}}{E_i I_i} + \int_0^L \frac{u_{V,i} U_{V,i}}{E_i A_i} + \int_0^L \frac{u_{N,i} U_{N,i}}{G_i A_i} \right) dx \quad (4.2)$$

or more simply

$$D = \sum_{i=1}^m \delta_i \quad (4.3)$$

where  $\delta_i$  is the deformation of member  $i$  that contributes to the displacement at the point and direction of the unit load, sometimes referred to as displacement participation factors (DPF).

Usually not all of the components of Eq.(4.2) are required in the calculation of displacements. In a truss with hinged joints, with loads at the joints only, there will be no shear, torsional and bending deformations and therefore only the axial component needs to be considered. In a rigid frame where axial and bending deformations dominate, the shear deformation component can be ignored.

## 4.2 STRUCTURAL OPTIMIZATION TECHNIQUES

The problem of finding the minimum volume (weight) design of a lateral load-resisting framework, having  $m$  members, to satisfy lateral drift constraint can be generally stated as:

minimise

$$V_{\text{total}} = \sum_{i=1}^m v_i \quad (4.4)$$

subject to

$$D_{\text{design}} = \sum_{i=1}^m \delta_i \quad (4.5)$$

where  $v_i$  is the volume of member  $i$ . On the assumption that the materials are elastic and the changes in cross sectional area and moment of inertia are proportional to the volume change of the member, then Eq.(4.4) and Eq.(4.5) can be expressed as

$$V'_{\text{total}} = \sum_{i=1}^m \alpha_i v_i \quad (4.6)$$

and

$$D'_{\text{design}} = \sum_{i=1}^m \frac{\delta_i}{\alpha_i} = D_{\text{design}} \quad (4.7)$$

The constrained optimization problem in Eq.(4.6) and Eq.(4.7) can be transformed into an unconstrained problem by introducing the Lagrange multiplier  $\lambda$ .

$$V'_{\text{total}} = \sum_{i=1}^m \alpha_i v_i + \lambda \cdot \left( \sum_{i=1}^m \frac{\delta_i}{\alpha_i} - D'_{\text{design}} \right) \quad (4.8)$$

Differentiating Eq.(4.8) with respect to the coefficient  $\alpha$  and  $\lambda$ , and setting the derivatives to zero lead to local extremes.

$$\frac{\partial V'_{\text{total}}}{\partial \alpha} = v_i - \lambda \frac{\delta_i}{\alpha_i^2} = 0 \quad (4.9)$$

and

$$\frac{\partial V'_{\text{total}}}{\partial \lambda} = \sum_{i=1}^m \frac{\delta_i}{\alpha_i} - D'_{\text{design}} = 0 \quad (4.10)$$

From Eq. (4.9),  $\alpha_i$  can be written as:

$$\alpha_i = \left( \lambda \frac{\delta_i}{v_i} \right)^{0.5} \quad (4.11)$$

rearranging Eq. (4.11) gives

$$\lambda^{-1} = \frac{\left( \frac{\delta_i}{\alpha_i} \right)}{(\alpha_i v_i)} \quad (4.12)$$

where  $\frac{\left( \frac{\delta_i}{\alpha_i} \right)}{(\alpha_i v_i)}$  is the strain energy density (also known the sensitivity index) of element  $i$ . Thus for the optimization problem above, the optimum is achieved when the strain energy density is equal for each element of the structure.

One disadvantage with the above optimality criteria is its difficulty to identify the optimising values for the design variables, essential for a complete solution. To achieve such a solution the displacement constraint Eq.(4.10) must be active at the optimum (if the constraint function,  $c(\alpha_i)$  or  $\left( \sum_{i=1}^m \frac{\delta_i}{\alpha_i} - D'_{\text{design}} \right) = 0$ , the constraint is said to be active, otherwise it is inactive). By using Eq.(4.10) the optimising design variables,  $\alpha$ , can be replaced to give

$$D'_{\text{design}} = \sum_{i=1}^m \delta_i \div \lambda \left( \frac{\delta_i}{v_i} \right)^{0.5} = \frac{1}{\lambda} \sum_{i=1}^m (\delta_i v_i)^{0.5} \quad (4.13)$$

and the optimising value for the Lagrange multiplier can now be extracted:

$$\lambda^{0.5} = \frac{\sum_{i=1}^m (\delta_i v_i)^{0.5}}{D'_{\text{design}}} \quad (4.14)$$

The optimising values for the design variables can now be found by using Eq.(4.10) to provide the solution:

$$\alpha_i = \frac{\left(\frac{\delta_i}{v_i}\right)^{0.5} \sum_{i=1}^m (\delta_i v_i)^{0.5}}{D'_{\text{design}}} \quad (4.15)$$

and thus optimum displacement and volume for each element is given by:

$$\delta'_i = \frac{\delta_i}{\alpha_i} = \frac{(\delta_i v_i)^{0.5}}{\sum_{i=1}^m (\delta_i v_i)^{0.5}} D'_{\text{design}} \quad (4.16)$$

and

$$v'_i = \alpha_i v_i = \frac{(\delta_i v_i)^{0.5} \sum_{i=1}^m (\delta_i v_i)^{0.5}}{D'_{\text{design}}} \quad (4.17)$$

The path followed has permitted a direct exploitation of the optimality criteria to achieve a complete optimal solution to the design problem. This is made possible due to the basic simplicity of the problem.

Similarly, the problem of minimising the displacement without changing the total volume may be expressed as:

minimise

$$D'_{\text{total}} = \sum_{i=1}^m \frac{\delta_i}{\alpha_i} \quad (4.18)$$

subject to

$$V'_{\text{design}} = \sum_{i=1}^m \alpha_i v_i \quad (4.19)$$

Transforming Eq.(4.18) and Eq.(4.19) into the unconstrained equation, it becomes

$$D'_{\text{total}} = \sum_{i=1}^m \frac{\delta_i}{\alpha_i} + \lambda \cdot \left( \sum_{i=1}^m \alpha_i v_i - V'_{\text{design}} \right) \quad (4.20)$$

Differentiating Eq. (4.19) with respect to the coefficient  $\alpha$ , and setting the derivative to zero, the values of  $\alpha_i$ , which minimise the  $D_{\text{total}}$  can be found. ie.

$$\frac{\partial D'_{\text{total}}}{\partial \alpha} = -\frac{\delta_i}{\alpha_i^2} + \lambda \cdot v_i = 0 \quad (4.21)$$

to give

$$\alpha_i = \left( \frac{1}{\lambda} \cdot \frac{\delta_i}{v_i} \right)^{0.5} \quad (4.22)$$

Substituting Eq. (4.21) into Eq. (4.18), and extracting the Lagrange multiplier gives

$$\lambda^{0.5} = \frac{\sum_{i=1}^m (\delta_i v_i)^{0.5}}{V'_{\text{design}}} \quad (4.23)$$

Eq. (4.21) can be rewritten as

$$\alpha_i = \frac{\left( \frac{\delta_i}{v_i} \right)^{0.5}}{\sum_{i=1}^m (\delta_i v_i)^{0.5}} V'_{\text{design}} \quad (4.24)$$

The optimum displacement and volume for each element therefore are given by

$$\delta'_i = \frac{\delta_i}{\alpha_i} = \frac{(\delta_i v_i)^{0.5} \sum_{i=1}^m (\delta_i v_i)^{0.5}}{V'_{\text{design}}} \quad (4.25)$$

and

$$v'_i = \alpha_i v_i = \frac{(\delta_i v_i)^{0.5}}{\sum_{i=1}^m (\delta_i v_i)^{0.5}} V'_{\text{design}} \quad (4.26)$$

In conclusion, the volume (weight) of member  $i$ , whose section is to be changed to minimise the displacement at the point of the unit load, can be obtained by allocating the total volume (weight) in proportion to the square root of the product of  $\delta_i$  and  $v_i$ . These simple formulas can be used intuitively to achieve the design objective, which is to obtain the optimum volume (weight) or displacement.

### 4.3 ILLUSTRATIVE EXAMPLES

Three examples are presented to illustrate the efficiency of the optimisation technique. The first example is a standard structure frequently used for verifying optimisation algorithms, whereas the other examples are a simple reinforced concrete cantilever wall and coupled wall.

#### 4.3.1 18-BAR TRUSS

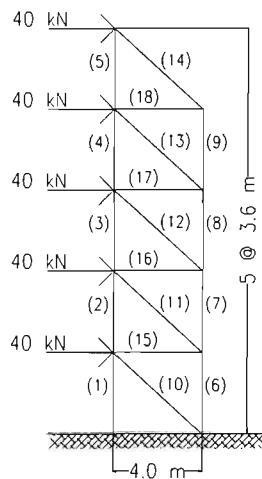


**Fig. 4.1** 18-bar truss

A simple statically determinate 18-bar plane truss ( $E = 200,000$  MPa) shown in Fig. 4.1 will be analysed and designed to satisfy a drift ratio limit of 0.25% at the top (450 mm). Initially all members have the same volume. ( $12,000 \text{ cm}^3$ ). A lateral load of 40 kN per storey is applied to this structure. From the static analysis using the uniform cross section, a lateral displacement of 0.52 m equal to 0.29% of the height of the structure is obtained. The DPFs are calculated in Table 4.1 and the initial strain energy density is shown in Fig. 4.2.

**Table 4.1** Calculation of optimum volumes for 18-bar truss example

Member	$L_i$ (cm)	$A_i$ (cm <sup>2</sup> )	$V_i$ (cm <sup>3</sup> )	$u_{N,i}$ (kN)	$U_{N,i}$ (kN)	$\delta_i$ (cm)	$\alpha_i$ (1/cm)	$V'_i$ (cm <sup>3</sup> )	$\delta'_i$ (cm)		
01	360	33	12000	4.500	540	1.312	2.12	25460	0.618		
02	360	33	12000	3.600	360	0.700	1.55	18594	0.452		
03	360	33	12000	2.700	216	0.315	1.04	12473	0.303		
04	360	33	12000	1.800	108	0.105	0.60	7201	0.175		
05	360	33	12000	0.900	36	0.017	0.24	2940	0.071		
06	360	33	12000	-3.600	-360	0.700	1.55	18594	0.452		
07	360	33	12000	-2.700	-216	0.315	1.04	12473	0.303		
08	360	33	12000	-1.800	-108	0.105	0.60	7201	0.175		
09	360	33	12000	-0.900	-36	0.017	0.24	2940	0.071		
10	538	22	12000	-1.345	-269	0.437	1.22	14690	0.357		
11	538	22	12000	-1.345	-215	0.349	1.09	13139	0.319		
12	538	22	12000	-1.345	-161	0.262	0.95	11379	0.276		
13	538	22	12000	-1.345	-108	0.175	0.77	8291	0.226		
14	538	22	Volumes whose DPF > 0.291 are increased							9	0.160
15	400	30	12000	1.000	160	0.107	0.60	7259	0.176		
16	400	30	12000	1.000	120	0.080	0.52	6287	0.153		
17	400	30	12000	1.000	80	0.053	0.43	5133	0.125		
18	400	30	12000	1.000	40	0.027	0.30	3630	0.088		
			216000				5.164			185251	4.500

During the redesign cycle the structure will be optimised for the minimum volume (weight). The optimum design found using the optimality criteria algorithm is calculated in Table 4.1. Fig. 4.2 illustrates that the final optimal strain energy density profile is equal to  $0.024 \times 10^{-3}$ , which is significantly different from the initial profile. Based on the theory of strain energy density, the members with cross sectional areas with magnitude of strain energy densities greater than  $0.024 \times 10^{-3}$  or DPFs greater than 0.291 cm are increased and conversely, for the members with strain energy density less than  $0.024 \times 10^{-3}$  are decreased

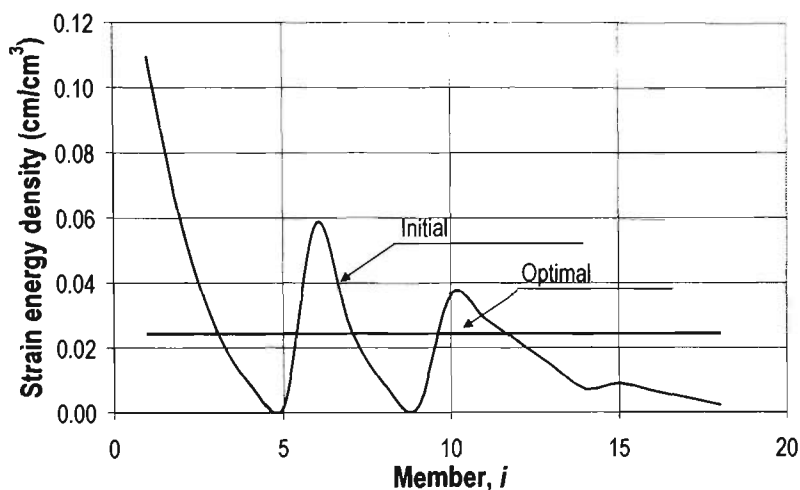


Fig. 4.2 Strain energy density of 18-bar truss example

### 4.3.2 30-STOUREY CANTILEVER WALL

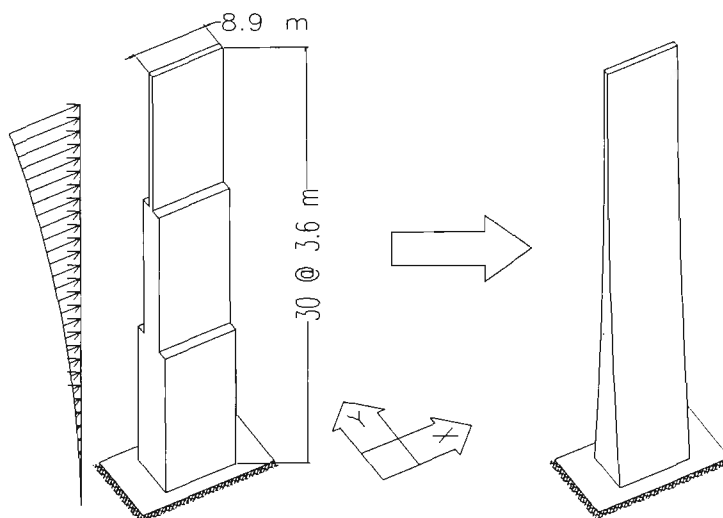


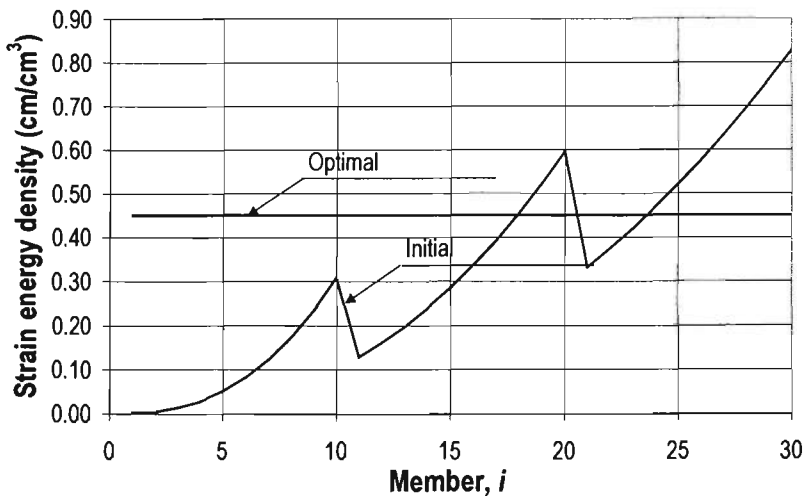
Fig. 4.3 30-storey cantilever wall; model and the optimum shape

Fig. 4.3 shows a 30-storey cantilever wall. The wall is modelled using 30 concrete panel elements. In the optimisation process, the volume of the wall is minimised subject to the constraint that the displacement at the top is equal to a value  $D_{\text{design}}$ . Initially the wall is assumed to consist of three 10-panel elements each of 400, 700, and 1000 mm thick. Taking the wall's length of 9000 mm (Aspect ratio,  $A_r = 12$ ), the initial volume is  $680.4 \text{ m}^3$ . By setting the  $D_{\text{design}}$  to 270 mm (drift ratio = 0.25%), the total base shear corresponding to a seismic loading is found to be 974 kN.

During the redesign process the structure is optimised for the minimum volume (weight) with the same displacement. The initial DPFs are obtained from the ETABS™-DISPAR™ analysis. The description of the programs ETABS™ and DISPAR™ is given in Sections 5.2. The optimum volumes and modified DPFs, as calculated from Eq. (4.17) and Eq. (4.16) respectively, are shown in Table 4.2. The total volume calculated is  $600 \text{ m}^3$ , which is about 88% of the initial volume. Member strain energy density profiles before and after the optimisation are shown in Fig. 4.4.

**Table 4.2** Calculation of optimum volumes for cantilever wall example

Member	$v_i$ (m <sup>3</sup> )	$\delta_i$ (cm)	$\alpha_i$	$v'_i$ (m <sup>3</sup> )	$\delta'_i$ (cm)	Member	$v_i$ (m <sup>3</sup> )	$\delta_i$ (cm)	$\alpha_i$	$v'_i$ (m <sup>3</sup> )	$\delta'_i$ (cm)
01	10.500	0.021	0.067	0.700	0.315	16	22.679	7.620	0.864	19.584	8.824
02	14.000	0.070	0.105	1.475	0.664	17	22.654	8.903	0.934	21.157	9.533
03	12.714	0.178	0.176	2.241	1.010	18	22.668	10.314	1.005	22.779	10.264
04	13.107	0.367	0.249	3.267	1.472	19	22.671	11.857	1.077	24.426	11.005
05	12.863	0.656	0.336	4.328	1.950	20	22.677	13.538	1.151	26.103	11.761
06	12.915	1.059	0.427	5.509	2.482	21	32.383	10.751	0.858	27.797	12.524
07	12.992	1.585	0.520	6.760	3.046	22	32.425	12.127	0.911	29.542	13.311
08	12.977	2.245	0.620	8.041	3.623	23	32.393	13.605	0.965	31.275	14.091
09	12.966	3.047	0.722	9.364	4.219	24	32.380	15.186	1.020	33.035	14.885
10	12.942	3.999	0.828	10.717	4.829	25	32.382	16.871	1.075	34.821	15.689
11	22.636	2.920	0.535	12.112	5.457	26	32.392	18.658	1.131	36.625	16.502
12	22.665	3.649	0.598	13.548	6.104	27	32.409	20.547	1.186	38.444	17.321
13	22.731	4.478	0.661	15.030	6.772	28	32.378	22.535	1.243	40.241	18.131
14	22.649	5.413	0.728	16.495	7.432	29	32.395	24.620	1.299	42.073	18.957
15	22.660	6.458	0.795	18.022	8.120	30	32.405	26.799	1.355	43.902	19.781
							678.60	270.08		599.41	270.08



**Fig. 4.4** Strain energy density profiles of cantilever wall example

### 4.3.2 30-STOREY COUPLED WALL

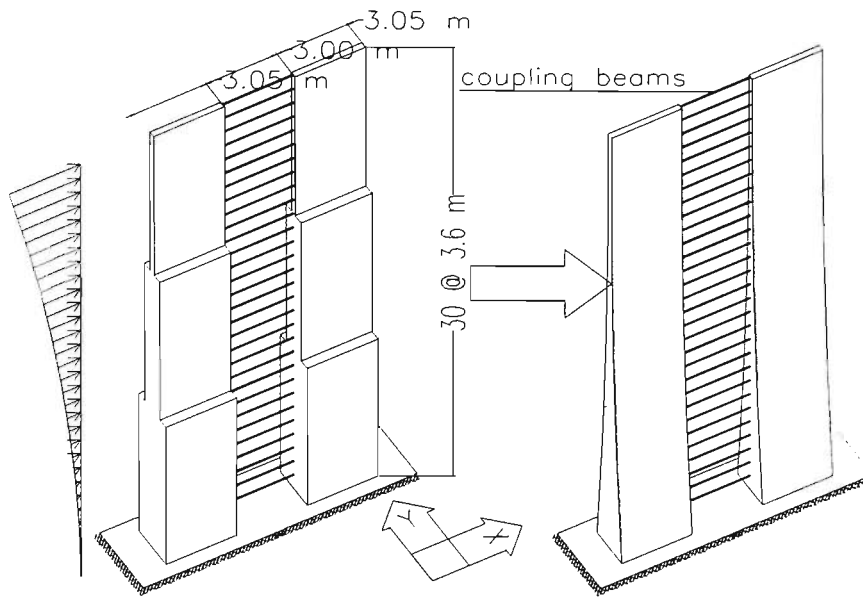


**Fig. 4.5** 30-storey coupled wall; model and the optimum shape

This example is a 30-storey reinforced concrete coupled wall. The walls are modelled using 30 concrete panel elements of 3000 mm length x 3600 mm height (one storey height). The coupling beams have a fixed depth of 900 mm. Both the thickness of the walls and the width of the beams vary with height. The initial wall thicknesses are assumed to consist of three 10-panel elements each of 200, 500, and 800 mm thick. The initial beam width is 450 mm. This gives the initial volumes of  $324 \text{ m}^3$  for the walls and  $36.45 \text{ m}^3$  for the beams. The base shear corresponding to a seismic loading is found to be 286 kN.

The design criteria are the same as in Example 4.2. The volume of the walls and coupling beams are minimised subject to a displacement at the top of 270 mm (drift ratio of 0.25%). Again the initial DPFs are obtained from the ETABS<sup>TM</sup>-DISPAR<sup>TM</sup> analysis. The optimum volumes and modified displacement participation factors, as calculated from Eq. (4.17) and Eq. (4.16) respectively, are listed in Table 4.3. The total optimum volumes are  $305 \text{ m}^3$  and  $31 \text{ m}^3$ , respectively, for the walls and coupling

beams, which is 94% of the initial volume. Member strain energy density profiles before and after the optimisation are shown in Fig. 4.6.

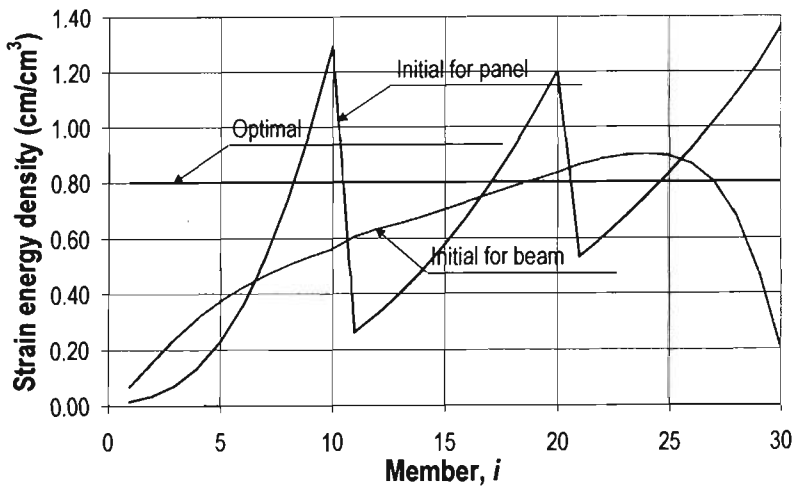
**Table 4.3** Calculation of optimum volumes for the coupled wall example

Panel	$v_i$ (m <sup>3</sup> )	$\delta_i$ (cm)	$\alpha_i$	$v'_i$ (m <sup>3</sup> )	$\delta'_i$ (cm)
01	2.188	0.035	0.141	0.309	0.248
02	2.171	0.076	0.209	0.454	0.364
03	2.151	0.157	0.302	0.649	0.520
04	2.154	0.293	0.412	0.887	0.711
05	2.166	0.496	0.534	1.158	0.928
06	2.159	0.775	0.669	1.445	1.158
07	2.159	1.138	0.811	1.751	1.404
08	2.159	1.591	0.959	2.070	1.659
09	2.160	2.141	1.112	2.402	1.926
10	2.161	2.792	1.270	2.743	2.199
11	5.399	1.420	0.573	3.093	2.479
12	5.393	1.769	0.640	3.450	2.765
13	5.401	2.166	0.707	3.820	3.062
14	5.399	2.613	0.777	4.195	3.363
15	5.405	3.113	0.848	4.581	3.672
16	5.402	3.668	0.920	4.972	3.985
17	5.398	4.281	0.995	5.369	4.304
18	5.402	4.954	1.070	5.778	4.632
19	5.399	5.691	1.147	6.191	4.963
20	5.402	6.493	1.225	6.615	5.302
21	8.634	4.602	0.815	7.040	5.644
22	8.647	5.188	0.865	7.481	5.997
23	8.643	5.817	0.916	7.920	6.349
24	8.642	6.490	0.968	8.365	6.705
25	8.641	7.207	1.020	8.814	7.066
26	8.642	7.968	1.072	9.268	7.430
27	8.637	8.775	1.126	9.723	7.794
28	8.643	9.637	1.179	10.193	8.171
29	8.641	10.585	1.236	10.682	8.563
30	8.637	11.729	1.302	11.242	9.011
	162.04	123.66		152.66	122.37

Beam	$v_i$ (m <sup>3</sup> )	$\delta_i$ (cm)	$\alpha_i$	$v'_i$ (m <sup>3</sup> )	$\delta'_i$ (cm)
01	1.203	0.083	0.293	0.353	0.283
02	1.215	0.192	0.444	0.539	0.432
03	1.215	0.294	0.549	0.668	0.535
04	1.213	0.382	0.627	0.760	0.609
05	1.213	0.455	0.684	0.830	0.665
06	1.214	0.516	0.728	0.884	0.709
07	1.214	0.567	0.763	0.927	0.743
08	1.215	0.611	0.792	0.962	0.771
09	1.215	0.649	0.816	0.992	0.795
10	1.214	0.681	0.837	1.016	0.814
11	1.215	0.736	0.869	1.056	0.846
12	1.215	0.768	0.888	1.079	0.865
13	1.214	0.793	0.903	1.096	0.879
14	1.216	0.823	0.919	1.117	0.896
15	1.215	0.854	0.936	1.138	0.912
16	1.214	0.886	0.954	1.158	0.928
17	1.214	0.919	0.972	1.180	0.946
18	1.214	0.952	0.989	1.201	0.963
19	1.215	0.984	1.005	1.221	0.979
20	1.214	1.014	1.021	1.239	0.994
21	1.215	1.052	1.039	1.263	1.012
22	1.216	1.076	1.051	1.277	1.024
23	1.215	1.090	1.058	1.285	1.030
24	1.215	1.096	1.061	1.289	1.033
25	1.216	1.088	1.057	1.285	1.030
26	1.216	1.054	1.040	1.264	1.013
27	1.215	0.977	1.001	1.217	0.976
28	1.215	0.831	0.924	1.122	0.900
29	1.213	0.586	0.776	0.942	0.755
30	1.213	0.245	0.502	0.609	0.488
	36.43	22.25		30.97	24.82

Note: The above values are for one panel



**Fig. 4.6** Strain energy density profiles for coupled wall

#### 4.4 CONCLUDING REMARKS

This chapter presented a single displacement/volume constrained optimisation technique, which forms the basis for the solution of practical problems encountered in structural design office, which is the member-linking technique.

Generally, a single constraint optimisation problem is written as:

minimise  $f(x)$

subject to  $g(x) \leq 0$

In the case of a displacement constraint, the function  $g(x)$  is the form of:

$D_{\text{design}} - \sum_{i=1}^m \delta_i = 0$ , in which the  $\delta$  is the displacement participation factors, which can

be calculated from the principle of virtual work.

The derived optimising formulas provide a means for the design engineers to calculate the optimum values efficiently. Simple spreadsheets as demonstrated in the working examples, and in the following chapters, perform the computations satisfactorily. The spreadsheets can be used intuitively and easily be modified as the number of structure element increases.

In the next chapter, the methodology and techniques to carry out the thesis objectives are presented. Founded upon the optimisation techniques in this chapter, the member-linking technique is derived. Similar examples to those in this chapter are also presented to illustrate this technique. The program ETABS™ and DISPAR™ for the structural analysis and calculating the DPFs are also described.

## **CHAPTER FIVE**

---

### **RESEARCH METHODOLOGIES AND PARAMETERS**

In Chapter 3, the design loading and criteria for the structural design were established. The primary objective of this study is to assess the economic benefit of using high-strength concrete (HSC) for structural walls in tall buildings. This chapter describes the methods and techniques adopted to achieve this objective. For structural analysis and design purposes, the computer program ETABS™ and DISPAR™ are used. The capacities and limitations of these programs are briefly discussed. The basic technique of structural optimisation presented in the previous chapter is extended by using the so-called member-linking technique. In deriving these formulae, the issue of HSC is incorporated. Finally an approximate method of numerical analysis is introduced and applied to verify an example.

#### **5.1 METHODOLOGY OF MEMBER-LINKING TECHNIQUE**

Once design loading for a particular wall structure is determined, the design process is to perform structural analysis and design using different concrete strengths. The structural design as mentioned in Chapter 3 will need to satisfy three limit states: serviceability limit state, ultimate limit state, and survival limit state.

With increasing building heights, serviceability limit states, in terms of lateral deflection and inter-storey drift, become increasingly important and subsequently often govern the final design of the principle structural elements. Based on this understanding, the initial selection of cross sectional dimensions adopted is to satisfy these serviceability criteria. The ultimate limit states and deformation capacities will be checked as a post process and if found to be inadequate the process is repeated with a revised sizing.

The optimisation technique outlined in the preceding chapter provides an efficient and systematic method for finding the optimum sizing of structural members for a system with a single displacement constraint. However, in the design of tall buildings for lateral loading, the design criterion is often given by the inter-storey drift rather than the total lateral deflection. Therefore, due to the simplicity of the derived optimisation formulae for the single displacement problem, the proposed method will be used as an approximate solution for the inter-storey constraint problem. This method is found to be conservative, as the ratio of the total lateral displacement to the total structural height is less than the maximum inter-storey drift ratio. However, it should be noted that this optimisation technique produces continuous changes in the cross sectional dimension for the structural members.

It is well understood in the building industry the undesirability of frequently changing member sizes. It typically lengthens the construction time as well as increases the formwork costs. In addition to the resulting time, slower construction increases the holding costs in terms of interest and furthermore delays the time for financial return from rental income. Recognising this issue, an optimisation process that links several members of the same length to a single representative design variable is derived. The developed member-linking method has similar formulation to the basic optimisation process outlined in the previous chapter. This formulation is discussed in detail in Section 5.3.1.

The member-linking method requires the positioning of each transition up the height of the structure to be chosen. A preliminary study by the author (Bong *et al.*, 1997) revealed that these transition points should be positioned such that each group is equal in height, independent of the concrete grade. However, this is only true if there is no restriction for the minimum cross sectional size. In many cases, by making all groups equal in height, the section size or the wall thickness at the upper-most group may become much less than the minimum requirement. To avoid this situation, the number of members for upper-most group should be increased such that its cross sectional size

is not less than the minimum requirement, whilst proportionally decreasing the number of members in the other groups.

This technique has been limited to one material property. However, as different concrete grades may be used in a wall at different levels, the member-linking method needs to introduce concrete strength as a parameter, which is achieved by introducing the material modulus of elasticity in the optimisation process. This is discussed in detail in Section 5.3.2.

The member-linking method can be applied to cantilever walls and coupled walls. For a single cantilever wall system, the member sizes can be adjusted without changing the member forces. For coupled walls and other non-proportional walls, the design formulations are only approximate since any change in the member sizing will cause the redistribution of internal forces. Theoretically, an iteration process is required to obtain the optimum volume. However, many structures are force insensitive, where changes in member forces are insignificant even with significant changes in member size. For these force insensitive structures, a single cycle of member size adjustment is sufficiently accurate for design purposes.

Once the cross sectional dimensions have been determined from the optimisation formulae, the costs associated with material savings and gains in lettable area are quantified. A detailed discussion of the cost analysis is given in Section 5.8, where two cases are considered: (1) single concrete strength is used throughout the wall height; (2) two concrete strengths are utilised, in which the higher strength concrete is used in the lower zones of the wall and the lower strength concrete is used in the upper zones. The design procedures for the two cases are shown in Fig. 5.1 and Fig. 5.2. in the form of flow-charts.

For indeterminate structures, iterations are normally required in the structural analysis. This study adopts two analysis-design cycles for the calculation of optimum cross sectional areas.

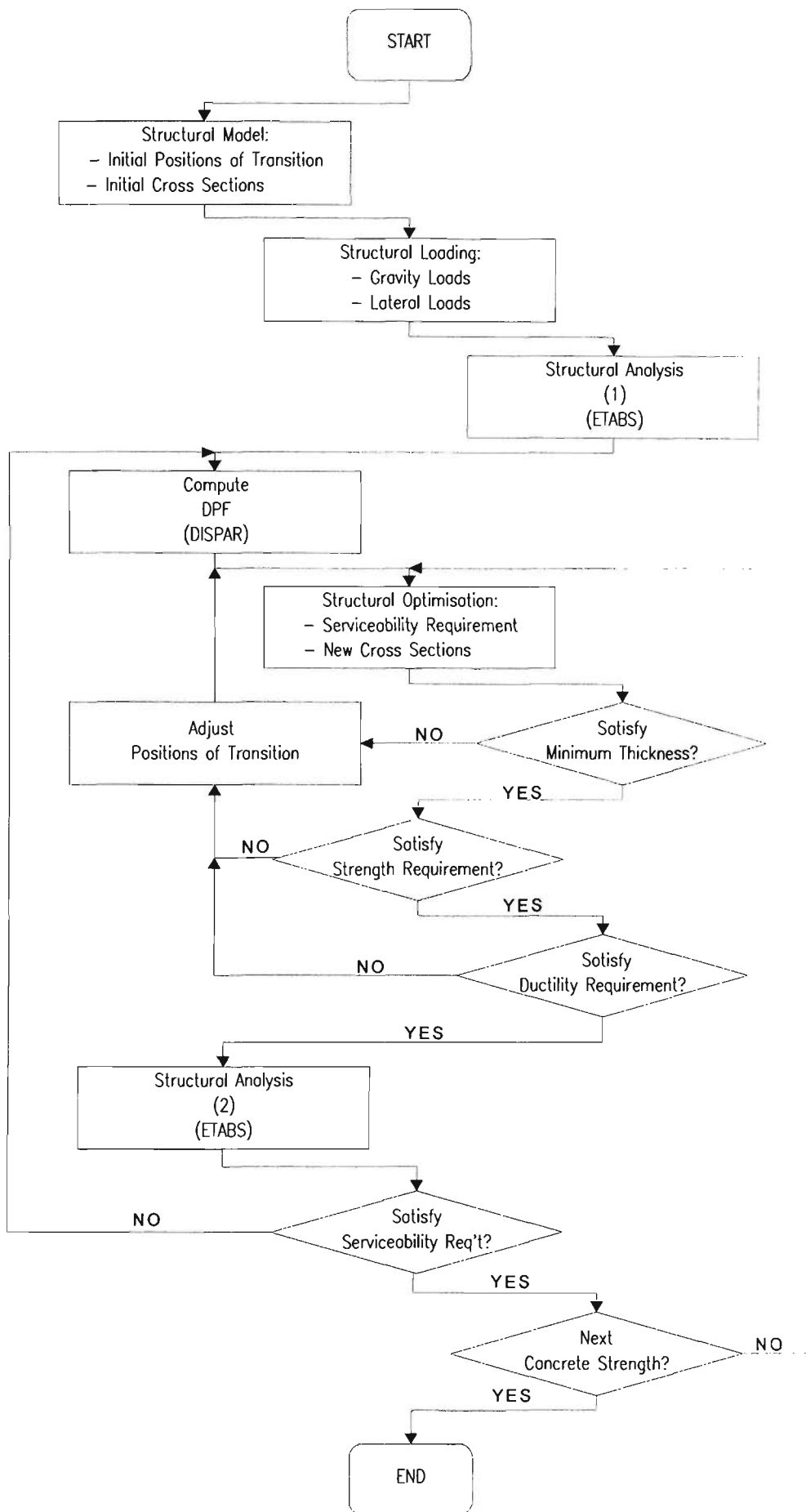


Fig. 5.1 Procedure for Single Concrete Strength System

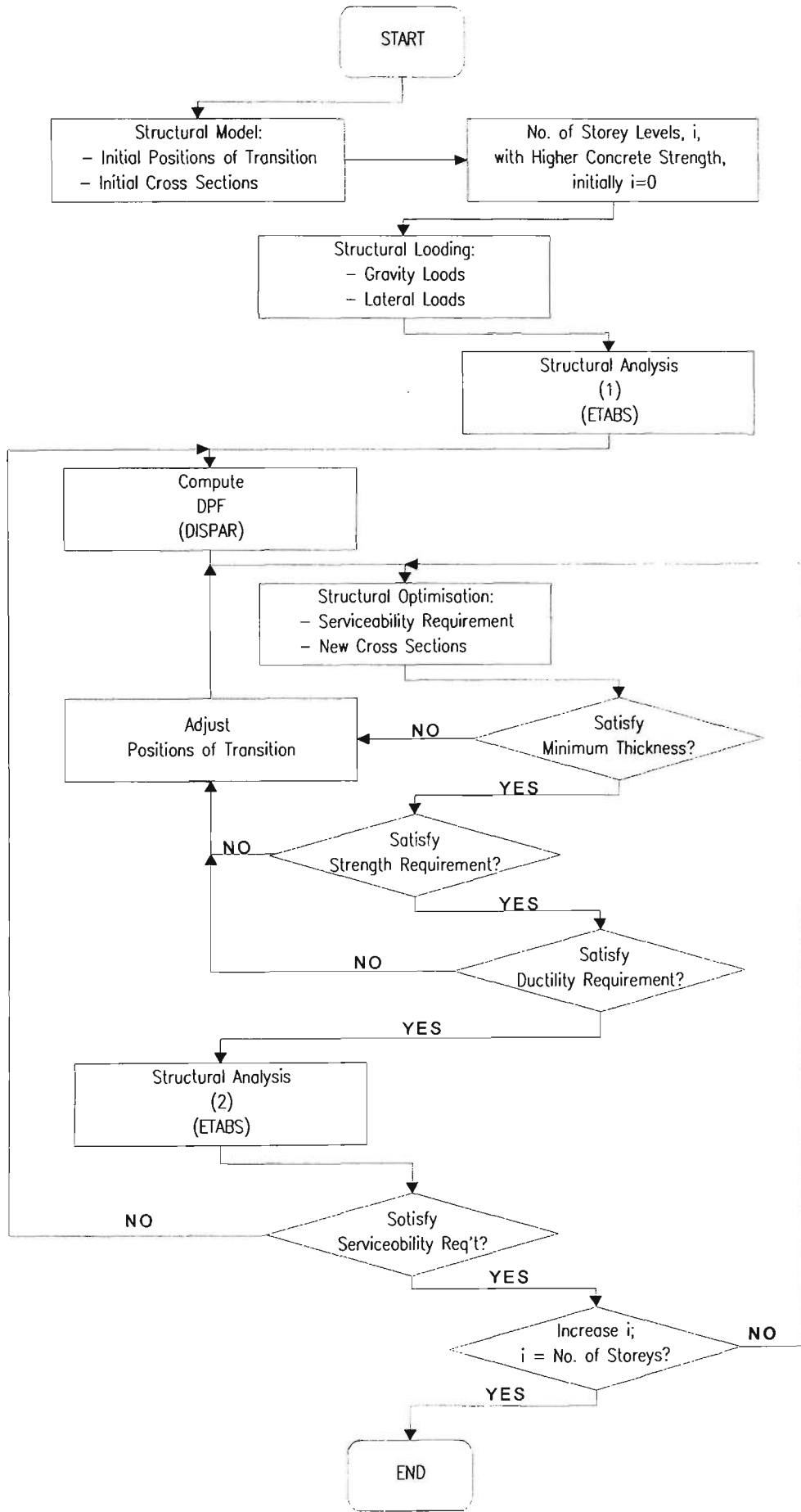


Fig. 5.2 Procedure for Variable Concrete Strength System

## 5.2 ETABS™ AND DISPAR™

There are a number of computer software packages available for the structural analysis of building structures (e.g. ETABS, STAAD-III). In addition to the analysis capabilities, some commercial packages provide additional design features to satisfy member strength requirements in accordance with the relevant design standards, in the form of post-processors. In recent years, several practicing engineers (Velivasakis & DeScenza, 1983; Chan, 1993; Charney, 1994) have developed software for sizing members to satisfy stiffness criteria.

The procedure for obtaining the optimum design values (volume), using the techniques described in Sections 4.2 and 5.3, requires the determination of deformation of each element that contributes to the total displacement at the point of interest. These deformations referred to as Displacement Participation Factors or DPFs can be calculated using the unit load method described in Section 4.1. In this study, computer software packages, ETABS™ and DISPAR™ will be used for the structural analysis and design purposes and to obtain the necessary parameter, DPF, for the structural optimisation process.

ETABS™ (Habibullah, 1987) is a special purpose software for the linear and non-linear analysis of building structures. The building is idealised as an assemblage of column, beam, brace and wall elements interconnected by rigid horizontal floor diaphragm slab at each floor level. The basic frame geometry is defined with reference to a simple three-dimensional grid system.

The wall structures in this study are modeled with a set of panel elements, and beams in the case of coupled wall. In ETABS, a special panel element is implemented for the modelling of general wall configurations, which may be planar or three-dimensional such as the core elevator walls. This panel element is based on an isoparametric finite element membrane formulation with the in-plane rotational stiffness being defined. Therefore, only beams that frame into panel element, in the plane of the wall, will

receive full continuity. Each panel is defined between any two-column lines and any two consecutive levels.

DISPAR™ (Charney, 1994), which is a special purpose post-processor for ETABS, works together with the results from one or two ETABS runs to calculate the DPF for each structural element, including the breakdown of each member's contribution in terms of axial, flexural, shear and torsional participation. The theoretical background of DISPAR in computing the DPFs is based on the principle of virtual work as described in Chapter 4. The DPF is important for solving the optimisation problem with displacement constraints.

### **5.3 VARIABLE-LINKING TECHNIQUE**

The optimization techniques presented in the previous chapter concluded that for a structure with a given displacement constraint, the volume of the material will be a minimum when the material is distributed such that all elements have the same strain energy density or sensitivity coefficient. The solutions of the optimization problems above are complex and often undesirable in the content of practical design. As the structural wall examples demonstrated in Sections 4.3.2 and 4.3.3, the member sizes are continuously changing. These changes are discouraged, as they are not only impractical but also often costly.

In the minimum volume (weight) design problem subject to a single displacement constraint with a restricted number of transitions, the basic optimisation theory in the previous chapter is extended by the use of a member-linking technique. This technique allows several members to be linked and represented by a single design variable. Since the solution of the optimisation problem is characterised by a single displacement constraint, the optimising values for the design variables and the Lagrangian Multiplier are directly available. This section outlines the formulation of the member-linking technique.

Based on the assumption that the change of stiffness is proportional to the change of volume, the relationship of individual optimum and initial values of the design variables can be written as:

$$v'_i = \alpha v_i \quad \text{and} \quad \delta'_i = \frac{\delta_i}{\alpha} \quad (5.1)$$

or

$$v'_i \delta'_i = v_i \delta_i \quad (5.2)$$

In the member-linking technique, members of equal length may be linked into a group having the same cross sectional properties. For a group  $n$  of  $m$  members, Eq. (5.2) can be rewritten as

$$[v']_{m,n} [\delta']_{m,n} = [v]_{m,n} [\delta]_{m,n} \quad (5.3)$$

or

$$v'_{m,n} [\delta']_{m,n} = [v]_{m,n} [\delta]_{m,n} \quad (5.4)$$

Recalling the theorem of strain energy density and applying it to the member-linking technique, it says: for a structure in which member-linking technique is employed, for a given deflection constraint, the volume of material will be a minimum when the material is distributed such that the strain energy density is equal for each group in the structure. i.e.

$$\frac{[\delta']_{m,n}}{[v']_{m,n}} = \lambda^{-1} \quad (5.5)$$

Substituting the group volume  $[v']_{m,n}$  from Eq. (5.5) into Eq. (5.4) and solving for the group DPF,  $[\delta']_{m,n}$ , yield

$$[\delta']_{m,n} = \left( \frac{m}{\lambda} [v]_{m,n} [\delta]_{m,n} \right)^{0.5} \quad (5.6)$$

The total displacement is the sum of all group displacement participation factors.

$$D_{\text{design}} = \sum \left( \frac{m}{\lambda} [v]_{m,n} [\delta]_{m,n} \right)^{0.5} \quad (5.7)$$

While it appears that the target displacement  $D_{\text{target}}$  may be calculated from Eq. (5.7) by substituting the Lagrange multiplier from Eq. (4.14), it is intuitively obvious that such is not the case, because the strain energy density for each member in each group will no longer be equal. This deficiency, which results in a larger displacement, needs to be justified.

To obtain the desired target displacement, the Lagrange multiplier is adjusted such that

$$D_{\text{target}} = \sum \left( \frac{m}{\lambda'} [v]_{m,n} [\delta]_{m,n} \right)^{0.5} \quad (5.8)$$

Dividing Eq. (5.8) by Eq. (5.7) gives

$$\lambda' = \left( \frac{D_{\text{design}}}{D_{\text{target}}} \right)^2 \cdot \lambda = k^2 \lambda \quad (5.9)$$

Thus, the optimum volumes for each group and member are given by

$$[v']_{m,n} = \left( m \lambda' [v]_{m,n} [\delta]_{m,n} \right)^{0.5} \quad (5.10)$$

and

$$v'_{m,n} = \left( \frac{\lambda'}{m} [v]_{m,n} [\delta]_{m,n} \right)^{0.5} \quad (5.11)$$

The volumes in Eq. 5.10 and Eq. 5.11 can easily be calculated using a spreadsheet such as the one shown in Table. 5.1. The spreadsheet also shows the calculation process.

## 5.4 ILLUSTRATIVE EXAMPLES

The three examples presented in Chapter 4 are again used to illustrate the optimisation technique with the member-linking strategy. The design loading, design criteria, and initial member properties are unchanged.

### 5.4.1 18-BAR TRUSS

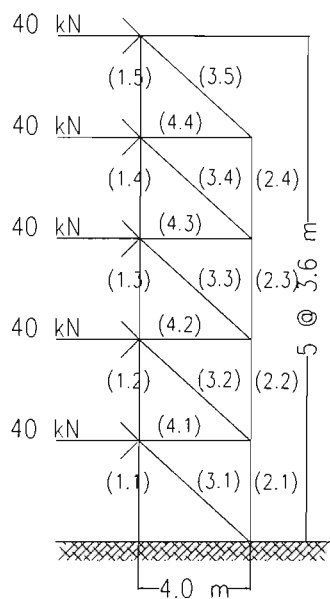


**Fig. 5.3** 18-bar truss

Fig. 5.3 shows the grouped member numbering. The values of Eq. (5.6), Eq. (5.11), and the recalculated DPFs are listed in Table 5.1. The initial strain energy density, calculated from Eq. (3.13), is  $0.0243 \times 10^{-3}$ . This gives a  $k$  value, the square of the

ratio of calculated displacement to desired displacement, as defined in Eq. (5.9) of 0.903.

As shown in the last column of Table 5.1, the values of strain energy density at optimum are not equal, but the average values for each group are. For comparison the initial and final strain energy density values are plotted in Fig. 5.4.

**Table 5.1** Calculation of optimum volumes for 18-bar truss example

Member	$v_i$ (cm <sup>3</sup> )	$\delta_i$ (cm)	$\delta'_i$ (cm)	$v'_i$ (cm <sup>3</sup> )	DPF <sub>i</sub> (cm)	Sl <sub>i</sub> (x1e3)
1.1	12000	1.312		17218	0.915	0.053
1.2	12000	0.700		17218	0.488	0.028
1.3	12000	0.315		17218	0.219	0.013
1.4	12000	0.105		17218	0.073	0.004
1.5	12000	0.017	1.889	17218	0.012	0.001
2.1	12000	0.700		13117	0.640	0.049
2.2	12000	0.315		13117	0.288	0.022
2.3	12000	0.105		13117	0.096	0.007
2.4	12000	0.017	1.152	13117	0.016	0.001
3.1	12000	0.437		12594	0.416	0.033
3.2	12000	0.349		12594	0.333	0.026
3.3	12000	0.262		12594	0.250	0.020
3.4	12000	0.175		12594	0.166	0.013
3.5	12000	0.087	1.382	12594	0.083	0.007
4.1	12000	0.107		6352	0.202	0.032
4.2	12000	0.080		6352	0.151	0.024
4.3	12000	0.053		6352	0.101	0.016
4.4	12000	0.027	0.558	6352	0.050	0.008
	216000	5.164	4.981	226933	4.500	

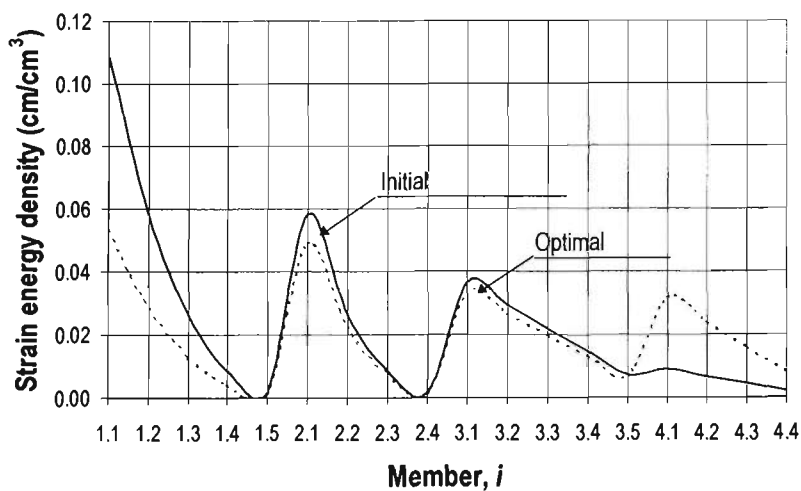


**Fig. 5.4** Strain energy density of 18-bar truss example

### 5.4.2 30-STOREY CANTILEVER WALL

In optimising the 30-storey cantilever wall employing the member-linking technique, the positions of the transition are kept the same. Based on the strain energy density of  $0.451 \times 10^{-3}$  (Section 4.3.2) the displacement calculated from Eq. (4.7) is 278 cm, therefore the  $k$  value is 0.971. Recalculating the strain energy density and substituting it into Eq. (5.11) gives the optimum volumes as shown in Table 5.2. The total volume with the linking technique is  $636 \text{ m}^3$ , which is 93% of the initial volume.

**Table 5.2** Calculation of optimum volumes for cantilever wall example

Member	$v_i$ (m <sup>3</sup> )	$\delta_i$ (cm)	$\delta'_i$ (cm)	$v'_i$ (m <sup>3</sup> )	PF <sub>i</sub> (cm)
1.01	10.500	0.021		6.356	0.043
1.02	14.000	0.070		6.356	0.143
1.03	12.714	0.178		6.356	0.363
1.04	13.107	0.367		6.356	0.750
1.05	12.863	0.656		6.356	1.340
1.06	12.915	1.059		6.356	2.161
1.07	12.992	1.585		6.356	3.235
1.08	12.977	2.245		6.356	4.582
1.09	12.966	3.047		6.356	6.219
1.10	12.942	3.999	27.788	6.356	8.162
2.01	22.636	2.920		20.039	3.307
2.02	22.665	3.649		20.039	4.133
2.03	22.731	4.478		20.039	5.072
2.04	22.649	5.413		20.039	6.131
2.05	22.660	6.458		20.039	7.315
					continue...
2.06	22.679	7.620		20.039	8.631
2.07	22.654	8.903		20.039	10.085
2.08	22.668	10.314		20.039	11.683
2.09	22.671	11.857		20.039	13.431
2.10	22.677	13.538	87.613	20.039	15.334
3.01	32.383	10.751		37.248	9.349
3.02	32.425	12.127		37.248	10.545
3.03	32.393	13.605		37.248	11.830
3.04	32.380	15.186		37.248	13.205
3.05	32.382	16.871		37.248	14.670
3.06	32.392	18.658		37.248	16.224
3.07	32.409	20.547		37.248	17.867
3.08	32.378	22.535		37.248	19.596
3.09	32.395	24.620		37.248	21.409
3.10	32.405	26.799	162.850	37.248	23.304
	678.60	270.08		636.43	270.12

Reanalysing the structure using the resulting optimum member sizes using ETABS™ and DISPAR™ results in the DPFs listed in Table 5.2. The total displacement confirms with 270 cm. The strain energy densities are shown in Fig. 5.5.

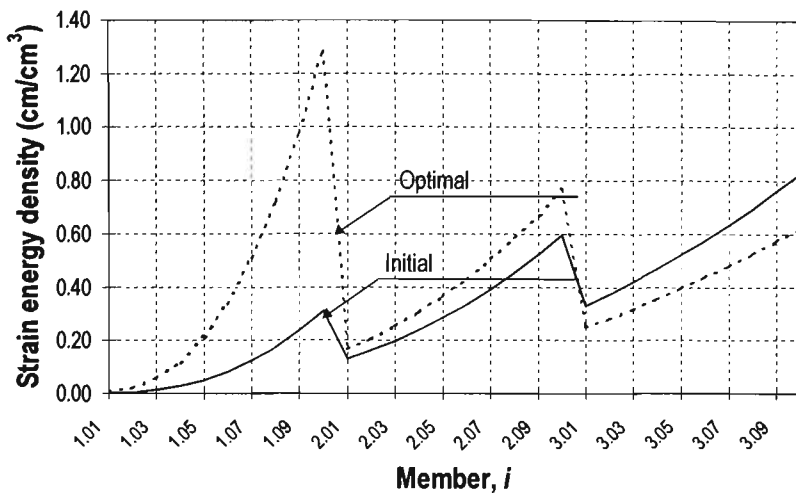


**Fig. 5.5** Strain energy density of cantilever wall example

### 5.4.3 30-STOREY COUPLED WALL

As per the previous example, the positions of the transition are kept the same. Based on the strain energy density of  $0.802 \times 10^{-3}$  (Section 4.3.3) the displacement calculated from Eq. (4.7) is 277 cm, therefore the  $k$  value is 0.975. Recalculating the strain energy density and substituting it into Eq. (5.09) gives the optimum volumes as shown in Table 5.3. The total volume using the linking technique is  $1073 \text{ m}^3$ , which is 95% of the initial volume.

Reanalysing the structure using the resulting optimum member sizes using ETABS™ and DISPAR™ results in the DPFs listed in Table 5.3. The total displacement confirms with 270 cm. The strain energy densities are shown in Fig. 5.6.

## 5.5 APPROXIMATE METHOD

The optimisation technique presented in the previous section is to optimise structures with predetermined group members. Often, inadequate information in the optimisation formulas causes difficulty in selecting suitable group members. In the absence of an efficient tool, the decision is often made by the structural engineer based on intuition and experience.

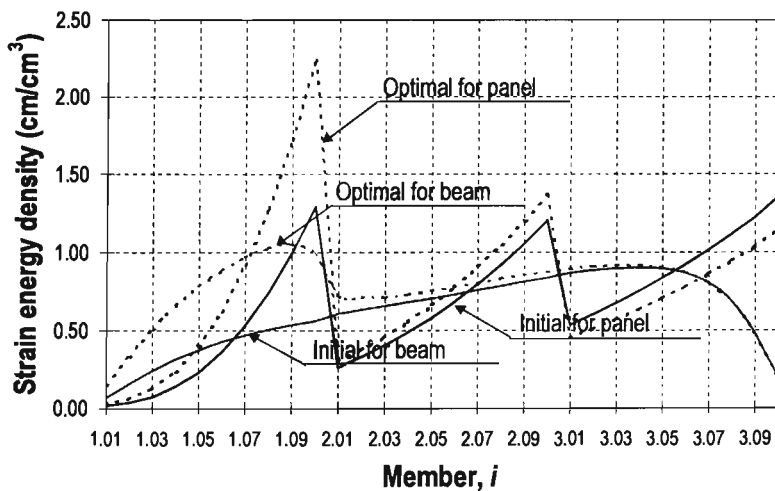
**Table 5.3** Calculation of optimum volumes for coupled wall example

Panel	$v_i$ (m <sup>3</sup> )	$\delta_i$ (cm)	$\delta'_i$ (cm)	$v'_i$ (m <sup>3</sup> )	PF <sub>i</sub> (cm)
1.1	2.188	0.035		1.641	0.047
1.2	2.171	0.076		1.641	0.100
1.3	2.151	0.157		1.641	0.207
1.4	2.154	0.293		1.641	0.386
1.5	2.166	0.496		1.641	0.653
1.6	2.159	0.775		1.641	1.020
1.7	2.159	1.138		1.641	1.498
1.8	2.159	1.591		1.641	2.094
1.9	2.160	2.141		1.641	2.817
1.10	2.161	2.792	12.822	1.641	3.680
2.1	5.399	1.420		5.064	1.514
2.2	5.393	1.769		5.064	1.886
2.3	5.401	2.166		5.064	2.309
2.4	5.399	2.613		5.064	2.786
2.5	5.405	3.113		5.064	3.319
2.6	5.402	3.668		5.064	3.911
2.7	5.398	4.281		5.064	4.565
2.8	5.402	4.954		5.064	5.283
2.9	5.399	5.691		5.064	6.068
2.10	5.402	6.493	39.570	5.064	6.923
3.1	8.634	4.602		9.406	4.226
3.2	8.647	5.188		9.406	4.765
3.3	8.643	5.817		9.406	5.343
3.4	8.642	6.490		9.406	5.961
3.5	8.641	7.207		9.406	6.619
3.6	8.642	7.968		9.406	7.319
3.7	8.637	8.775		9.406	8.062
3.8	8.643	9.637		9.406	8.857
3.9	8.641	10.585		9.406	9.737
3.10	8.637	11.729	73.501	9.406	10.809
	162.04	123.66	125.89	161.11	122.76

Beam	$v_i$ (m <sup>3</sup> )	$\delta_i$ (cm)	$\delta'_i$ (cm)	$v'_i$ (m <sup>3</sup> )	PF <sub>i</sub> (cm)
1.1	1.203	0.083		0.840	0.125
1.2	1.215	0.192		0.840	0.278
1.3	1.215	0.294		0.840	0.424
1.4	1.213	0.382		0.840	0.551
1.5	1.213	0.455		0.840	0.657
1.6	1.214	0.516		0.840	0.743
1.7	1.214	0.567		0.840	0.814
1.8	1.215	0.611		0.840	0.866
1.9	1.215	0.649		0.840	0.886
1.10	1.214	0.681	6.566	0.840	0.830
2.1	1.215	0.736		1.180	0.853
2.2	1.215	0.768		1.180	0.838
2.3	1.214	0.793		1.180	0.839
2.4	1.216	0.823		1.180	0.857
2.5	1.215	0.854		1.180	0.884
2.6	1.214	0.886		1.180	0.914
2.7	1.214	0.919		1.180	0.946
2.8	1.214	0.952		1.180	0.978
2.9	1.215	0.984		1.180	1.006
2.10	1.214	1.014	9.219	1.180	1.029
3.1	1.215	1.052		1.205	1.074
3.2	1.216	1.076		1.205	1.091
3.3	1.215	1.090		1.205	1.100
3.4	1.215	1.096		1.205	1.101
3.5	1.216	1.088		1.205	1.088
3.6	1.216	1.054		1.205	1.047
3.7	1.215	0.977		1.205	0.963
3.8	1.215	0.831		1.205	0.811
3.9	1.213	0.586		1.205	0.564
3.10	1.213	0.245	9.412	1.205	0.232
	36.43	22.25	25.20	32.25	24.39

Note: The above values are for one panel



**Fig. 5.6** Strain energy density of coupled wall example

This section proposes an approximate numerical method for solving an optimisation problem with non-predetermined group members. This method finds the local optimum values for a volume function by solving its partial derivatives. It is well understood that for a given function of  $n$  variables, differentiating the function with respect to the variables and setting the derivatives to zero, result in a set of non-linear equations. Solving these nonlinear equations and substituting the resulting values to the initial function provide the local optimum values for that function. Following this principle, the method is derived below.

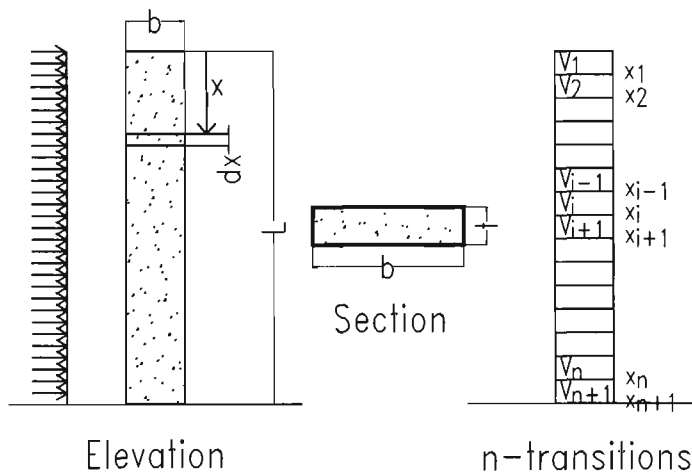


**Fig. 5.7** Transition locations in a cantilever member

A displacement participation factor  $\delta$  of an element of length  $dx$  (Fig. 5.7) undergoing flexural deformation only is given by

$$\delta_x^M = \int \frac{Mm}{EI} dx = \frac{k_x}{v_x} \tag{5.12}$$

where  $v_x$  is the volume of the element and  $k_x = \int \frac{Mm}{r^2 E} d^2x$

Following a successful analysis using ETABS™ and DISPAR™ of a structure having  $m$  elements, the  $k_x$  for each element can be calculated from the resulting  $\delta$  and the initial volume  $v_x$ . A function equation  $f(x)$  may then be formulated by curve-fitting the values of  $k_x$ .

The displacement at the point of virtual unit load is the sum of the  $\delta$ , i.e.

$$D = \sum \delta_x = \int_0^{x_1} \frac{1}{v_x} f(x) = \frac{g(x)}{v_x} \quad (5.13)$$

where

$$g(x) = \int_0^x f(x)$$

Rewriting the Eq. (5.13) for a structure with  $n$  transitions or  $n+1$  elements gives

$$D = \int_0^{x_1} \frac{1}{v_1} f(x) + \dots + \int_{x_n}^{x_{n+1}} \frac{1}{v_{n+1}} f(x) \quad (5.14)$$

or

$$D = \sum_{i=1}^{n+1} \frac{1}{v_i} (g(x_i) - g(x_{i-1})) \quad (5.15)$$

Having the displacement function formulated, the problem of finding the optimum volume (weight) of a lateral resisting structure having  $n$  transitions can be stated as

minimise

$$V_{total} = \sum_{i=1}^{n+1} v_i (x_i - x_{i-1}) \quad (5.16)$$

subject to

$$D_{design} = \sum_{i=1}^{n+1} \frac{1}{v_i} (g(x_i) - g(x_{i-1})) \quad (5.17)$$

where  $v_i$  is the volume per linear length of element  $i$  and  $g(x_i) = \int_0^{x_i} f(x)$ .

By substituting the  $v_{n+1}$  from Eq. 5.17 into Eq. 5.16, the volume function can be written as

$$V_{total} = f(x_i, v_i) \quad \text{where } i = 1 \text{ to } n \quad (5.18)$$

Differentiating Eq. 5.18 with respect to  $x_i$  and  $v_i$  gives a set of  $2n$  nonlinear equations. Setting these derivative equations to zero and solving for the optimising variables, the optimum locations of transition and volumes are given by the  $x_i$  and  $v_i$ , respectively.

$$\begin{aligned} \frac{\partial f(x_i, v_i)}{\partial x_i} &= 0 \\ \frac{\partial f(x_i, v_i)}{\partial v_i} &= 0 \end{aligned} \quad (5.19)$$

Given that the transition locations are determined, the above differentiating problem can be turned into an  $n+1$  simultaneous equation problem with  $n+1$  unknowns. These unknowns can be obtained from solving Eq. 5.17 plus  $n$  equal strain density equations given as

$$\frac{1}{x_1 v_1^2} g(x_1) = \frac{1}{(x_{i+1} - x_i) v_{i+1}^2} [g(x_{i+1}) - g(x_i)] \quad \text{where } i = 1 \text{ to } n \quad (5.20)$$

## 5.6 EXAMPLE OF APPROXIMATE METHOD

To illustrate the optimisation techniques, The example given in Section 5.4.2 of a 30-storey structure will be redesigned for optimum volume and positions of transition. The  $k_x$  values defined as the multiplication of DPF and volume are listed in Table 5.4.

Curve-fitting the values of  $k_x$  to obtain  $f(x)$ :

$$f(x) = 2.81335x^0 - 1.84931x^1 + 0.57748x^2 + 0.016379x^3$$

and the integration is given by:

$$g(x) = 2.81335x^1 - 0.92466x^2 + 0.19249x^3 + 0.0040946x^4$$

**Table 5.4**  $k_x$  values

Member	$v_1$ (m <sup>3</sup> )	$\delta t$ (cm)	$k_i$ (cm/m <sup>3</sup> )
1.01	12.960	0.021	0.272
1.02	12.960	0.070	0.907
1.03	12.960	0.178	2.307
1.04	12.960	0.367	4.756
1.05	12.960	0.656	8.502
1.06	12.960	1.059	13.725
1.07	12.960	1.585	20.542
1.08	12.960	2.245	29.095
1.09	12.960	3.047	39.489
1.10	12.960	3.999	51.827
2.01	22.680	2.920	66.226
2.02	22.680	3.649	82.759
2.03	22.680	4.478	101.561
2.04	22.680	5.413	122.767
2.05	22.680	6.458	146.467
			continue...
2.06	22.680	7.620	172.822
2.07	22.680	8.903	201.920
2.08	22.680	10.314	233.922
2.09	22.680	11.857	268.917
2.10	22.680	13.538	307.042
3.01	32.400	10.751	348.332
3.02	32.400	12.127	392.915
3.03	32.400	13.605	440.802
3.04	32.400	15.186	492.026
3.05	32.400	16.871	546.620
3.06	32.400	18.658	604.519
3.07	32.400	20.547	665.723
3.08	32.400	22.535	730.134
3.09	32.400	24.620	797.688
3.10	32.400	26.799	868.288
	680.40	270.08	7762.87

For the sake of simplicity, only one transition will be considered for the example. The optimisation functions can then be written as

minimise

$$v(x) = v_1 x_1 + v_2 (x_2 - x_1) \quad \text{where } x_2 = 30 \tag{5.21}$$

subject to

$$\frac{1}{v_1} g(x_1) + \frac{1}{v_2} [g(x_2) - g(x_1)] = 270 \text{ cm} \tag{5.22}$$

Solving Eq. (5.22) for  $v_1$  and substituting the  $v_1$  into Eq. (5.21) gives

$$v(x) = \left\{ \begin{array}{l} x \left[ \frac{v_2(0.20473x^4 + 9.62450x^3 - 46.23300x^2 + 14.06679x)}{0.20473x^4 + 9.62450x^3 - 46.23300x^2 + 14.06679x + 1350v_2 - 388303} \right] \\ + [v_2(30 - x)] \end{array} \right\} \quad (5.23)$$

Differentiating Eq. (5.23) with respect to  $x$  and  $v_1$ , and setting the derivatives to zero, the  $v_2$  can now be extracted Using the mathematical software DERIVE<sup>®</sup> from Soft Warehouse, Inc., the derivatives are

$$v_2 = \frac{1}{13500} [0.61419x^4 + 19.24900x^3 - 46.23300x^2 + 388303] \quad (5.24)$$

$$v_2 = \frac{1}{13500} \left[ \begin{array}{l} x \left( \begin{array}{l} +0.04191x^6 + 5.19827x^5 + 229.649x^4 \\ +6057.12x^3 + 107061x^2 - 538382x + 1820726 \end{array} \right) \\ -0.20473x^4 - 9.62450x^3 + 46.2333x^2 - 140.668x + 388303 \end{array} \right] \quad (5.25)$$

With the computer software Mathematica from Wolfram Research, Inc., the variable  $x$  can be solved by equating Eq. (5.24) and Eq. (5.25). The  $v_2$  and  $v_1$  are then given by Eq. (5.24) and Eq. (5.22) respectively. The total volume  $V$  is calculated from Eq.(5.21). The resulting values are:

$$x = 13.71, \quad v_1 = 9.60 \text{ m}^3, \quad v_2 = 33.40 \text{ m}^3, \quad V = 676 \text{ m}^3$$

Next, suppose the position  $x$  is given. The problem of finding the optimum volume  $V$  is defined as:

satisfying

$$\frac{1}{x_1 v_1^2} g(x_1) = \frac{1}{(x_2 - x_1) v_2^2} [g(x_2) - g(x_1)] \quad \text{where } x_2 = 30 \quad (5.26)$$

subject to

$$\frac{1}{v_1} g(x_1) + \frac{1}{v_2} [g(x_2) - g(x_1)] = 270 \text{ cm} \quad (5.27)$$

Since there are only two unknowns,  $v_1$  and  $v_2$ , they can be obtained by solving two equations, Eq. (5.26) and Eq. (5.27), simultaneously. The volume  $V$  is then calculated using Eq. (5.21). The volume  $V$  as a function of  $x$  is shown in Fig. 5.8. The figure also confirms that the most optimum volume is achieved at the position between levels 13 and 14.

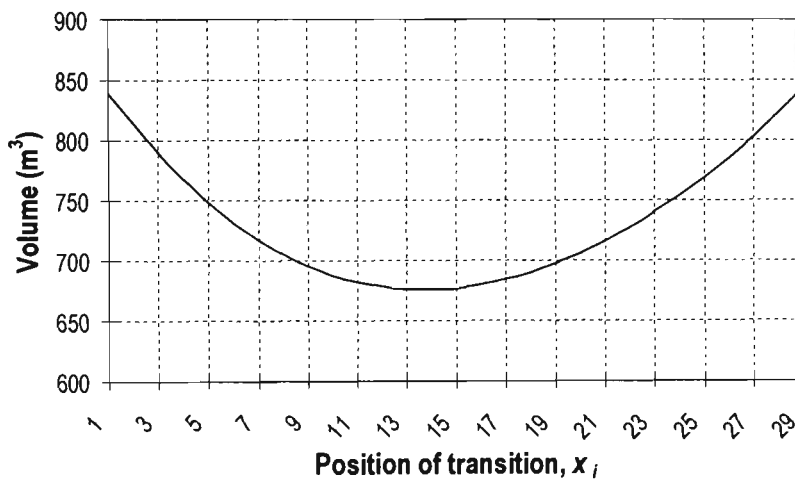


**Fig. 5.8** Optimum volumes at different transition positions

The 30-storey cantilever wall example in Section 5.4.2 can be solved similarly. Given the positions  $x_i$ , the problem is to find the three values of  $v_i$ . This requires three non-singular equations, which are given by two strain energy density equations and one constrain function.

$$\frac{1}{x_1 v_1^2} g(x_1) = \frac{1}{(x_2 - x_1) v_2^2} [g(x_2) - g(x_1)] \tag{5.28}$$

and

$$\frac{1}{x_1 v_1^2} g(x_1) = \frac{1}{(x_3 - x_1) v_3^2} [g(x_3) - g(x_1)] \tag{5.29}$$

and

$$\frac{1}{v_1} g(x_1) + \frac{1}{v_2} [g(x_2) - g(x_1)] + \frac{1}{v_3} [g(x_3) - g(x_2)] = 270 \text{ cm} \tag{5.30}$$

Solving Eq. (5.28), Eq. (5.29), and Eq. (5.30) gives

$$v_1 = 6.31 \text{ m}^3 ; v_2 = 20.09 \text{ m}^3 ; v_3 = 37.25 \text{ m}^3 ; V = 636 \text{ m}^3$$

which differs insignificantly from the ones calculated in Section 5.4.2.

## 5.7 VARIABLE CONCRETE STRENGTHS

The previous optimisation technique is applied to structures with a uniform concrete strength. However, if the design objective is to achieve a target displacement, it is obvious that increasing the concrete strength will decrease the volume of the structural members, due to the increase associated with stiffness. A method that incorporates concrete strengths in an optimisation process is presented as follows:

Generally, a member DPF,  $\delta$ , can be expressed as (Eq. 4.2)

$$\delta_i = \int_0^L \left( \frac{u_{M,i} U_{M,i}}{E_i I_i} + \frac{u_{V,i} U_{V,i}}{G_i A_i} + \frac{u_{N,i} U_{N,i}}{E_i A_i} \right) dx \quad (5.31)$$

For an element having constant cross sectional properties, Eq. (5.31) can be written as:

$$\delta_i = \frac{1}{E_i V_i} \int_0^L \left( \frac{u_{M,i} U_{M,i}}{r_i} + (2 + 2\mu_i) \frac{u_{V,i} U_{V,i}}{1} + \frac{u_{N,i} U_{N,i}}{1} \right) L_i dx \quad (5.32)$$

or more simply

$$\delta_i = \frac{K_i}{E_i V_i} \quad (5.33)$$

where  $K_i$  is a constant for a particular member and loading. Eq. (5.33) asserts that the multiplication of  $\delta$ ,  $V$ , and  $E$  should stay the same in spite of the changes made to either of those individual values.

Therefore, the relationship between the optimum values and the initial ones may be expressed as:

$$\delta'_i \cdot V'_i \cdot E'_i = \delta_i \cdot V_i \cdot E_i \quad (5.34)$$

then

$$\delta'_i \cdot V'_i = \frac{\delta_i \cdot V_i}{E'_i / E_i} \quad (5.35)$$

Eq. (5.35) indicates that if either the initial  $\delta$  or  $V$  is replaced with its value divided by  $E'_i / E_i$  prior to the optimisation process, not only do the resulting optimum,  $\delta'$  and  $V'$ , maintain the constant of  $\delta \cdot V \cdot E$ , but also they satisfy the optimality theorem of equal sensitivity index.

This is a desirable realisation as it also applies to the member-linking technique. In this technique, the relationship between the initial and optimum values is written as (Eq. 5.4)

$$[v']_{m,n} [\delta']_{m,n} [E']_{m,n} = [v]_{m,n} [\delta]_{m,n} [E]_{m,n} \quad (5.36)$$

which may also be written as

$$[v']_{m,n} [\delta']_{m,n} = \frac{[v]_{m,n} [\delta]_{m,n}}{[E']_{m,n} / [E]_{m,n}} \quad (5.37)$$

Eq (5.35) is identical to Eq. (5.37), therefore it shall conclude similarly.

## 5.8 PARAMETERS IN COST ANALYSIS

The aim of a structural design in any project must be to produce the most economical design whilst satisfying code requirements and building owner's brief. The economical design of a building requires optimisation with regard to material cost, construction time and, in the case of office building, maximisation of rentable floor space. In a single cost analysis, the examination incorporating all these factors can be complex. Normally, assumptions are needed in order to simplify the analysis.

This research study analyses the cost benefits of utilising HSC in structural walls. Parameters included in the comparative studies are the wall construction cost and the capitalised income of rentable floor space gains.

A typical construction cost of a structural wall comprises of: (1) concrete supply and placing; (2) reinforcement supply and placing; and (3) formwork supply and operation. The cost of each item is obtained from a survey of several concrete suppliers and quantity surveyors in Melbourne and from the article "Current Construction" published in 1997. A summary of the findings is given in Table 5.5. They reflect the average costs in Australia's metropolitan area in 1997.

**Table 5.5** Components of wall construction cost.

Concrete (MPa)	f c 040	f c 050	f c 060	f c 070	f c 080	f c 090	f c 100	f c 110	f c 120
- supply	138.00	148.00	162.00	180.00	202.00	228.00	258.00	292.00	330.00
- place	48.00	48.00	48.00	48.00	48.00	48.00	48.00	48.00	48.00
- total (\$ per m <sup>3</sup> )	186.00	196.00	210.00	228.00	250.00	276.00	306.00	340.00	378.00
<b>Reinforcement; supply and place</b>				1385.00	\$ per ton				
<b>Formwork; supply and operation</b>				60.00	\$ per m <sup>2</sup>				

However, due to the variability of reinforcement content, an assumption is made with regard to the cost of the steel reinforcement. With high strength concrete, the amount of reinforcing steel may increase as the result of using a thinner wall. However, from

experience, the percentage increase of reinforcing steel is usually low for wall construction. Fig. 5.9 illustrates the significance of the cost increase as the concrete strength increases. It assumes that the percentage of the reinforcing steel increases linearly with concrete strength.

Fig. 5.9 shows that at 0.025% increment of reinforcement content, i.e. 0.4% for 40 MPa increases to 0.6% for 120 MPa concrete, the reinforcing steel volume, therefore the cost, remains constant with respect to the concrete strength. At 0.00% and 0.05% increment, the percentages of cost increase can be as high as (-)35% and 28%, respectively. (-) indicates a cost decrease. For simplicity, this study makes assumption that the cost of reinforcement does not change with concrete strength.

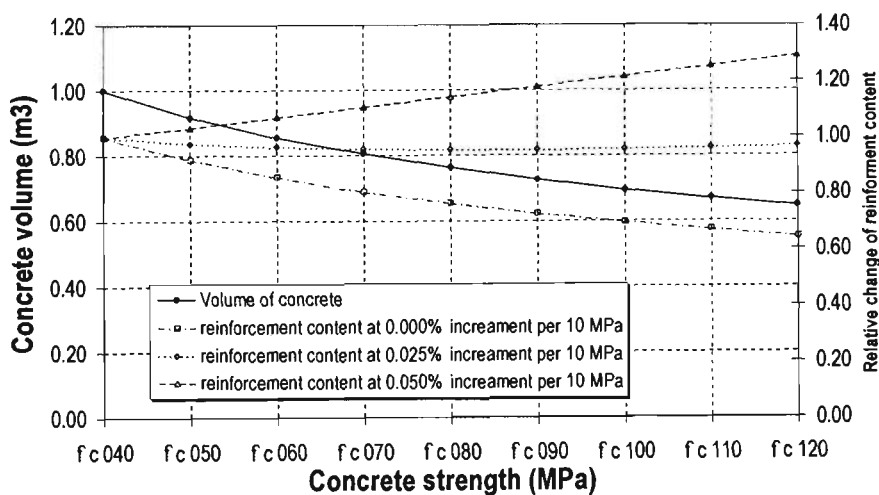


**Fig. 5.9** Variability of reinforcement contents with concrete strength.

Calculation of the capitalised income of rentable floor space variation is done on the following basis: For example, one square metre may derive a nett rental income of \$300 per annum. At a yield of 6%, this area capitalises at  $\$300/0.06 = \$5,000$ . i.e. the value of one square metre is \$5,000. However, this capitalised value can vary significantly depend on the economy, locality, quality of building and many more factors. For the purpose of the research study, a wide range of capitalised values is selected to represent the various conditions. The chosen values are: 1000, 2000, 3000, 4000, 6000, and 8000 dollars per square metre.

The cost benefits associated with construction time will not be included in the cost analysis. However, it is worth pointing out that the early stripping of formwork of building elements built from HSC may reduce the construction time and formwork rental resulting in significant cost savings. To illustrate the benefit of faster construction, considering a 50-storey building having 60000 m<sup>2</sup> of rentable space, a single day reduction in construction time would correspond to approximately \$50,000 cost benefit, in terms of savings on interest costs (Martin, 1989). It can be easily shown that investments in HSC to speed up construction will have a favourable return for even moderate time saving.

Thus, the construction cost, comprising the concrete and formwork components, and the benefit from capitalising the rental income, form the basis for the cost comparative studies in the next two chapters. It has also been demonstrated that the formulated member-linking optimisation technique provide a useful method to compute the optimum cross sections, using uniform and variable concrete strengths. Founded on the derived formulas, it is convenient to put these formulas into a Microsoft™ Excel© spreadsheet. This will be demonstrated in the following chapters.

## CHAPTER SIX

---

### USE OF HSC IN RECTANGULAR WALLS

The preceding chapter described the methodology and techniques to carry out the objectives of the research. In this chapter, the financial benefits of utilising high-strength concrete (HSC) in wall elements for high-rise buildings are examined. The use of HSC in C-shaped walls is evaluated in Chapter 7. The analysis and design of these structures are subjected to the design loads and criteria described in Chapter 3.

Two types of structural walls are investigated: a single cantilever wall and a coupled wall system. Material costs and capitalisation costs associated with rental space, described in the previous chapter, form the basis for the cost comparative study. The study will identify the cost-benefits associated with the use of higher strength concrete. In walls where two concrete strengths are used, the position for the concrete strength transition is shown to be an important parameter to gain maximum cost benefits.

Due to the higher strength and stiffness property of HSC, the resulting wall thickness as required to resist a given load can be significantly less. Consequently, the inertial loads due to earthquake are lower as a result of the reduced mass of the wall providing further savings. Finally the requirements for strength and ductility are checked and comments on the overall analysis are given.

## 6.1 CANTILEVER WALL

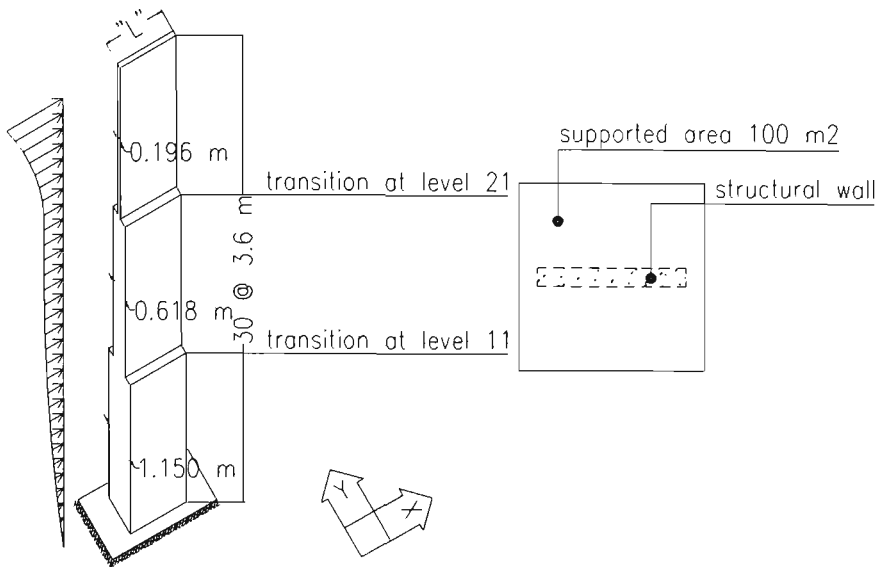


**Fig. 6.1** Cantilever wall model

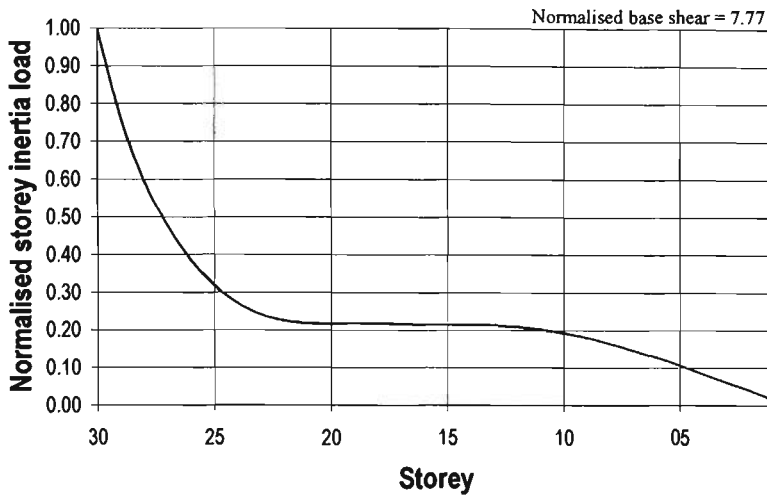
### 6.1.1 STRUCTURAL MODEL AND LOADING

Fig. 6.1 illustrates a cantilever wall with its rectangular cross section. The wall is designed to support seismic load resulting from a mass equivalent to  $100 \text{ m}^2$  of floor area for a 30-storey building with an inter-storey height of 3.6 m. The thickness for the wall is initially assigned to be 1.150, 0.618, and 0.196 m with the corresponding transitions occurring at the levels 11 and 21 (Section 5.3.2). The initial concrete strength is assigned to be 40 MPa. The cross sectional length,  $L$ , is based on a deflection criteria such that the inter-storey drift ratio, when subjected to the design seismic load, is approximately  $0.015K/\mu = 0.375\%$ , where  $K$  is the structural factor and  $\mu$  the ductility factor.

The resulting distribution of storey inertia load, resulting from a dynamic response spectrum analysis, is shown in Fig. 6.2. The base shear is then from Eq. (3.3):

$$V_{\text{base}} = CIK(W_f + W_w) \quad (6.1)$$

where  $W_f$  is 595 kN, and  $W_w$  is  $1697L$  kN.



**Fig. 6.2** Design seismic loads

Assuming  $C = 0.025$ , a wall length of 8.9 m is found to satisfy all the above criteria. This corresponds to a total concrete volume of  $629 \text{ m}^3$ , with a base shear equal to 824 kN, structural time period equal to 4.22 seconds. The displacement at the top is 239 mm.

## 6.1.2 UNIFORM CONCRETE STRENGTHS

### 6.1.2.1 VOLUME vs NUMBER OF THICKNESS TRANSITIONS

Given the model and loading, the optimum volumes may be calculated using the formulae given in the previous chapters. The structure is deemed to satisfy the inter-storey criterion if the displacement at the top is maintained to 240 mm. A Microsoft™ Excel® spreadsheet is set up to perform the computation. A typical spreadsheet layout is illustrated in Fig. 6.3.

Fig. 6.4 illustrates the optimal concrete volumes for various concrete strengths with differing number of wall thickness transitions, hereafter only referred to as thickness transitions. For comparison purposes, an ideal theoretical optimal solution is shown. The principal observation is the significance of the volume reduction with increasing concrete strength and the insignificance of the effect of number of transitions on the total volume.

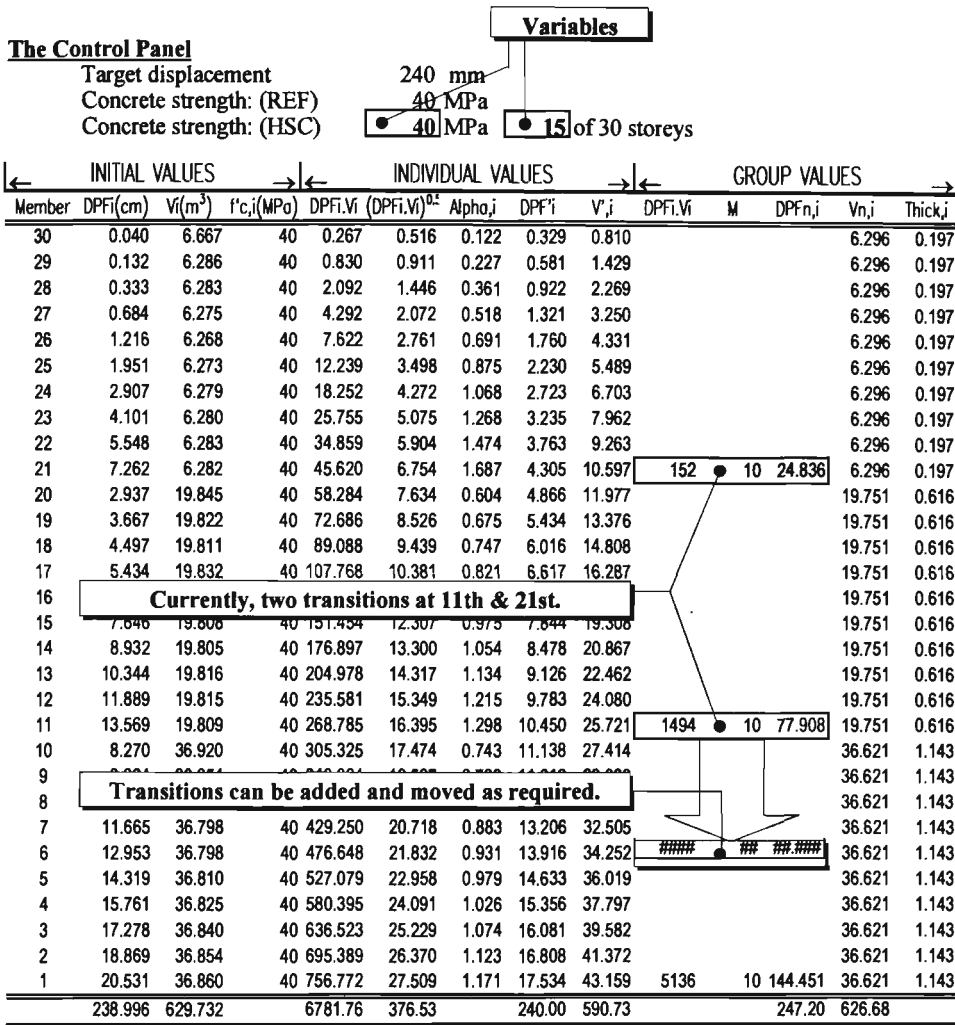


Fig. 6.3 Spreadsheet for optimum volume calculations

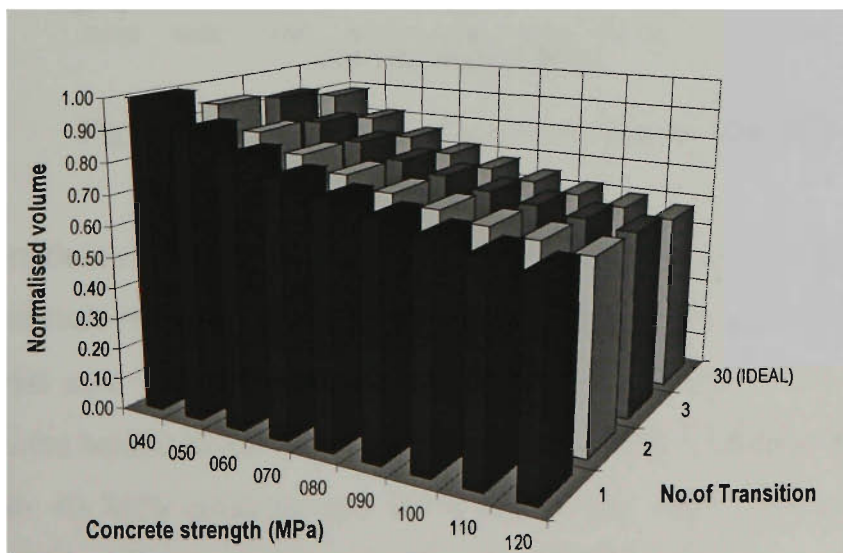


Fig 6.4 Optimum volumes with uniform concrete strengths

The average reduction in the concrete volume is 24% corresponding to an increase in concrete strength from 40 MPa to 80 MPa. However, only a reduction of 1.48% is obtained for an increase in number of thickness transitions from 2 to 3. When one considers the substantial cost increase, associated with construction delay, for introducing each transition, it is clear that use of higher strength concrete is an effective means of minimising concrete volume.

### 6.1.2.2 COST ANALYSIS

Following the above figures, a cost comparative study is carried out adopting only the results from two thickness transitions. The results of the cost study are shown in Fig. 6.5 for varying capitalisation values.

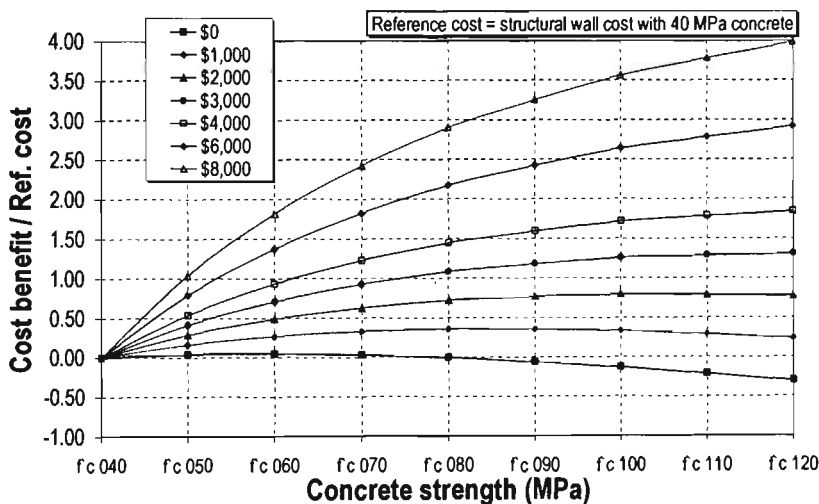


Fig. 6.5 Cost-benefits with uniform concrete strengths

The cost benefit is calculated by capitalising the rentable floor space gain from the use of higher concrete strengths, which results in thinner walls, and the cost differential from material cost associated with higher concrete strength. This cost benefit is presented as the benefit divided by a reference cost, which is taken as the material cost of wall with 40 MPa concrete and 0.4% reinforcing steel. The cost of concrete, reinforcing steel, and formwork have been given in Section 5.8.

The results also show that on the basis of construction cost only, ignoring the capitalisation costs, as illustrated by the zero value, the cost benefits of using low concrete strengths is negligible. On the other hand, despite a significant reduction in concrete volume for very high-strength concretes, the wall construction cost increases. The benefit of using higher strength concrete only becomes apparent if the capitalisation value of the rentable floor space gain is taken into consideration.

Fig. 6.5 also indicates that the cost benefit of using very high-strength concrete for buildings attracting low financial returns diminishes. For example, for buildings yielding not more than \$2000/m<sup>2</sup>, there is no benefit using concrete strength exceeding 80 MPa. However, for the higher yielding buildings, corresponding to prestigious buildings located in central business districts of most cities, there is a notable financial benefit, which increases as the concrete strength increases. For example, for a building capitalising \$6000/m<sup>2</sup>, utilising 80 MPa for the wall will gain a cost benefit corresponding to 2.17 times the material cost of the 40 MPa wall, a significant amount.

### **6.1.3 VARIABLE CONCRETE STRENGTHS**

Although high cost benefits are achieved by using HSC, its application typically requires more extensive quality control, both in production and during construction, consequently resulting in additional cost. For this reason, a means to utilise various concrete strengths at different storey levels has the attractive objective of providing the most appropriate alternative. A study investigating the cost benefit of utilising two concrete strengths for the wall is carried out in the next section.

#### **6.1.3.1 VOLUME vs NUMBER OF LOWER STOREYS UTILISING HSC**

The calculation to determine optimal concrete volumes is carried out using the same worksheet as illustrated in Fig. 6.3. For increasing concrete strength, the optimum

volume is computed for increasing number of storeys utilising higher strength concrete. Typical volume changes are shown in Fig. 6.6.

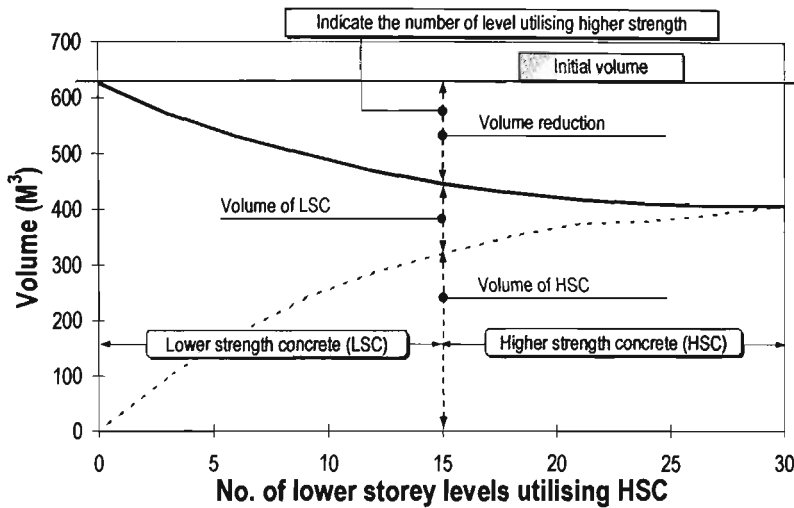


**Fig. 6.6** Typical volume changes with variable concrete strengths

Fig. 6.6 illustrates a case of utilising 120 MPa high strength concrete up to the mid-height of the building, with the remainder using 40 MPa normal strength concrete. It clearly demonstrates the significant total volume reduction, reducing from 626 m<sup>3</sup> to 445 m<sup>3</sup>, in which the volume of 120 MPa concrete amounts to 320 m<sup>3</sup>. The volume of the initial concrete strength being replaced by the HSC is  $626 - (445 - 320) = 501$  m<sup>3</sup>.

For various concrete strengths, the results of relative volume reduction are shown in Fig. 6.7. Also shown in the figure are the percentage reductions achievable at various storey levels. It shows that on average, more than 80% of the maximum volume reduction is achievable when HSC is used up to the mid wall height, independent to the concrete strength.

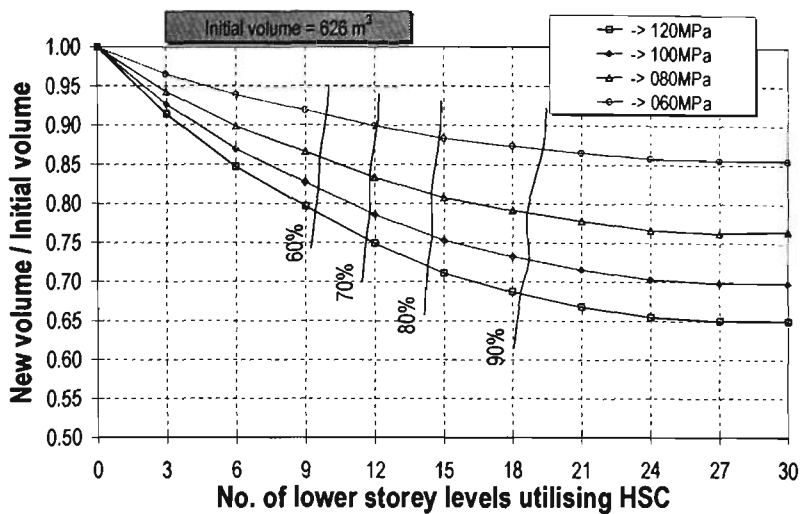


Fig 6.7 Volume reduction with variable concrete strengths

### 6.1.3.2 COST ANALYSIS

The cost comparative study of the above wall is carried out similarly to the cost study for the uniform concrete strength. The results for replacing a reference concrete strength, 40 MPa, with a higher concrete strength, 120 MPa, are shown in Fig. 6.8. Results for utilising other concrete strengths are given in Appendix A.

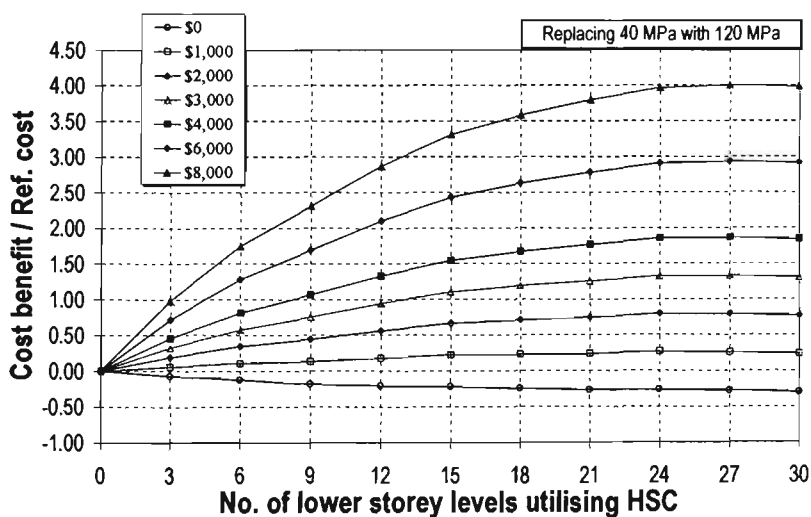
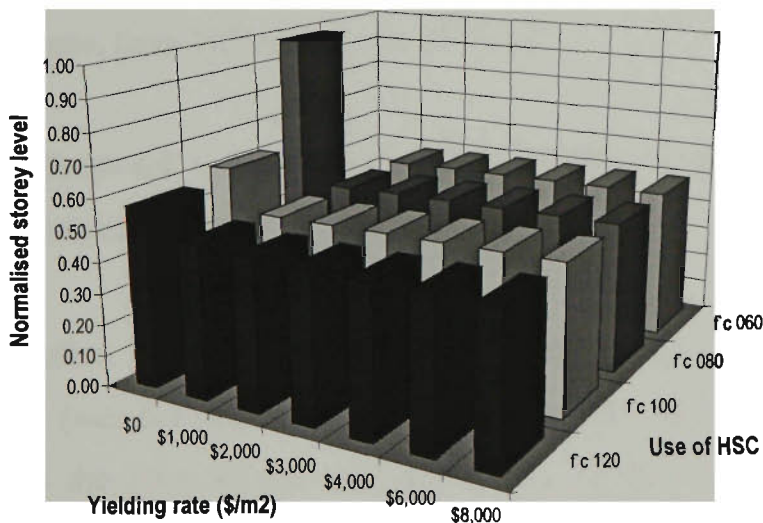


Fig. 6.8 Cost-benefits with variable concrete strengths

As expected, there is a penalty in the wall cost associated with replacing a lower strength concrete with a higher strength concrete. However, the benefit from the

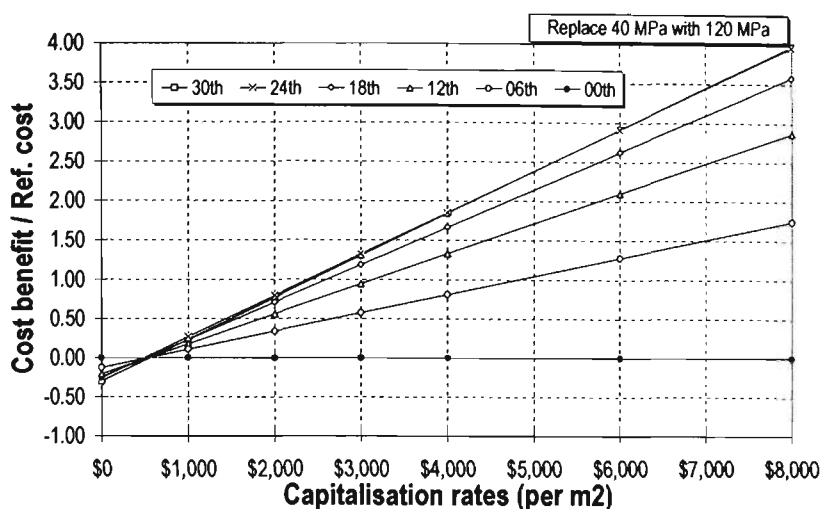
capitalised income, resulting from an increase in rentable area, far exceeds the cost penalty of the material cost. It is also observed that there is no significant gain in cost benefit by extending the higher strength concrete much beyond two-thirds of the wall height, particularly for buildings yielding low rentals. The main gain is achieved by introducing HSC up to the mid-height.

Fig 6.9 shows the positions of concrete grade transitions to achieve 80% of possible maximum benefit, plotted for different concrete strengths and yield rates. It can be seen that the transition position is consistently near the mid-height. The only exception is where only material cost is considered. This suggests that a convenient transition for concrete strength is at approximately mid-height of the wall, as there is no significant cost benefit in using higher strength concrete above this level.



**Fig. 6.9** Concrete strength transitions at 80% maximum

Fig. 6.8 shows the cost benefit for various capitalisation rates and varying number of storeys utilising higher strength concrete. A variant of this chart, which looks at the cost benefit from the capitalisation value perspective illustrated in Fig. 6.10 reveals an interesting trend. It indicates that the total benefit gain increases linearly with the yield rate, irrespective to the number of storeys utilising HSC. The corresponding plots for other concrete grades is included in Appendix A.



**Fig. 6.10** Cost-benefits versus capitalisation yield rate

The tangent slope of the lines indicates the rate of change of the benefit with respect to yield rate. It clearly illustrates the insignificance of the increment of the slope as the storey level increases, from 18<sup>th</sup> level to the 30<sup>th</sup> level.

#### 6.1.4 IMPLICATION OF WALL THICKNESS OPTIMISATION TO DESIGN SEISMIC LOAD

As mentioned earlier, for buildings subjected to earthquake loading, a decrease in concrete volume (weight) implicates a reduction in the magnitude of the design seismic load. As the mass of the wall contributes significantly towards the total structural mass (40 MPa wall represents 46% of the total mass), a moderate reduction of seismic load can be expected. The design of such buildings is an iterative process, based on the procedure shown in Fig. 6.11(a).

The effect of the wall volume reduction to the design seismic loads can be quantified by considering the reduced mass of the wall as a portion of the total contributing mass. Hence, the percentage reduction in the seismic load is:

$$\frac{W_f + W_{w,opt}}{W_f + W_{w,ini}} \times 100\%$$

where the subscripts 'opt' and 'ini' indicate optimum and initial states, respectively. Therefore, the concrete volume should be reduced as well. This volume reduction is expected to be in the same order as the reduction in the seismic loading. A simplified method of the calculation process is illustrated in Fig. 6.11(b), adopting three iterations.

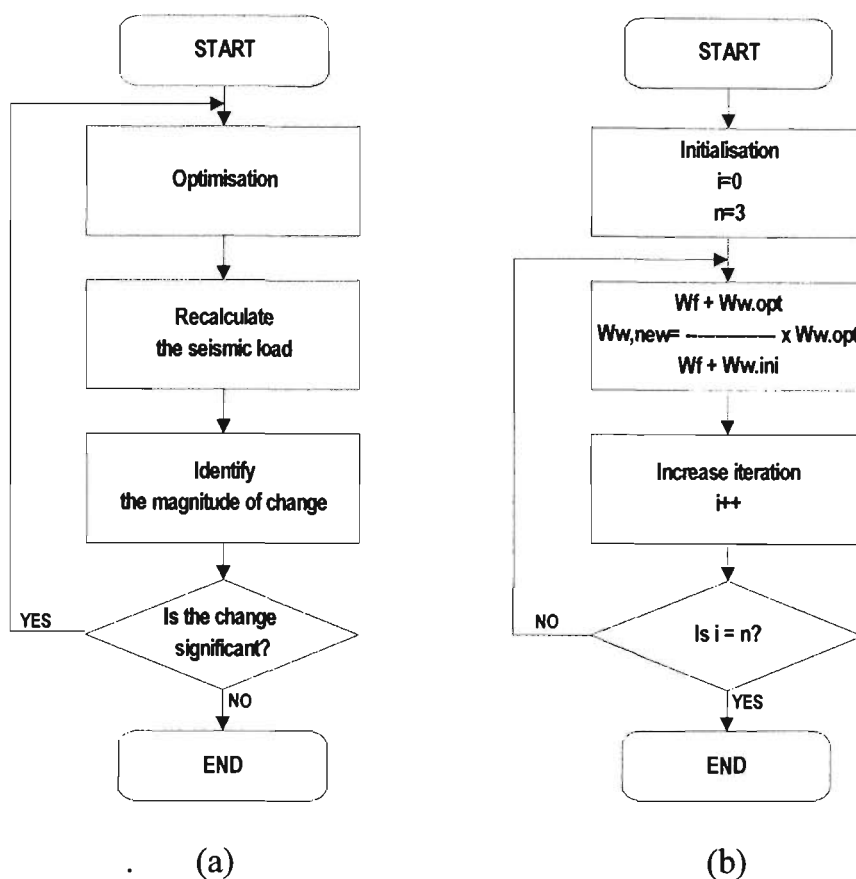


Fig. 6.11 Redesign process due to reduced seismic loads

To investigate the significance of the decrease in seismic loading to the total cost benefit, a cost comparative study is performed, only the case where HSC is used up to mid-height of the wall is considered.

Fig. 6.12 shows the volume reduction with progressive iterations. It clearly illustrates the insignificance of iterating beyond three iterations and that the volume computed according to Fig. 6.11(b) is comparable to the volume at iteration 5.

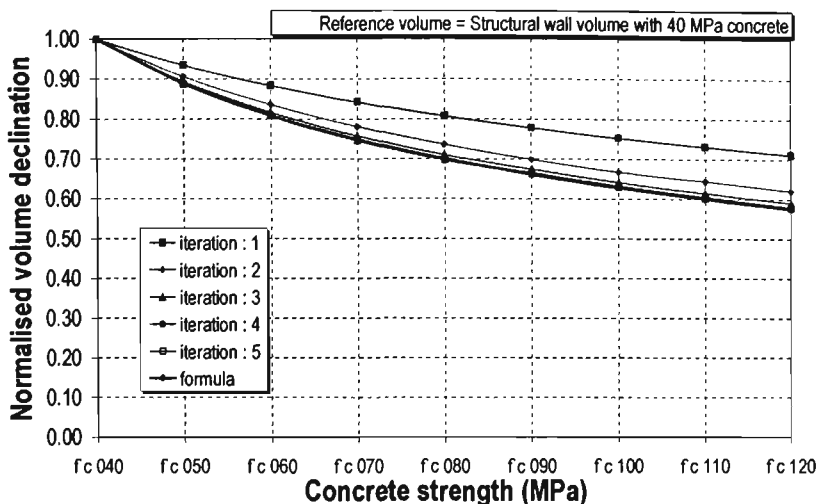


Fig. 6.12 Volume reduction due to reduced seismic loads

To illustrate the significance of the volume change due to the decreased seismic loads, a chart similar to Fig. 6.5 is reproduced in Fig. 6.13. The differences of the benefit gains are shown in Fig. 6.14.

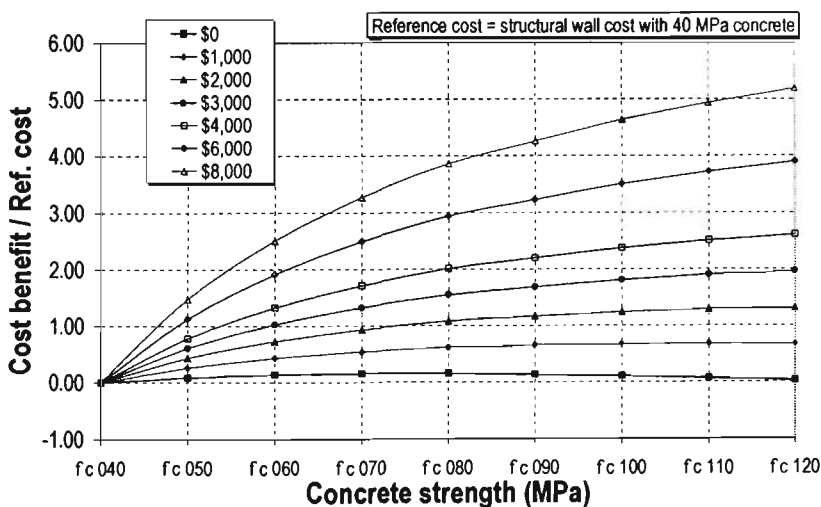
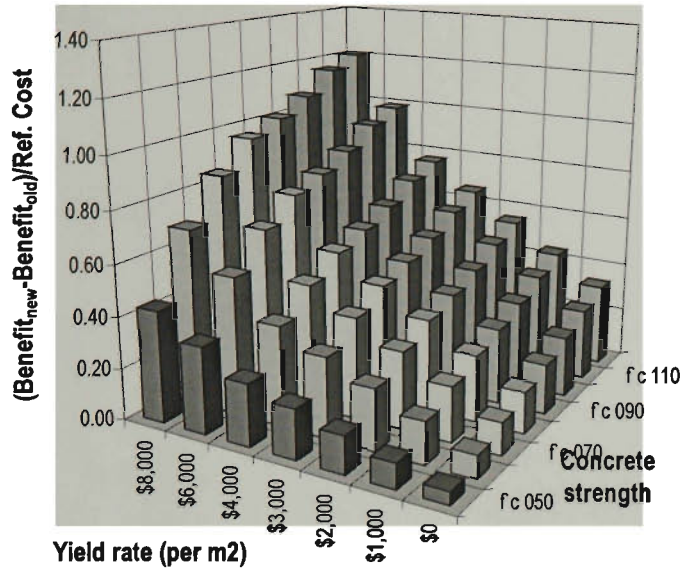


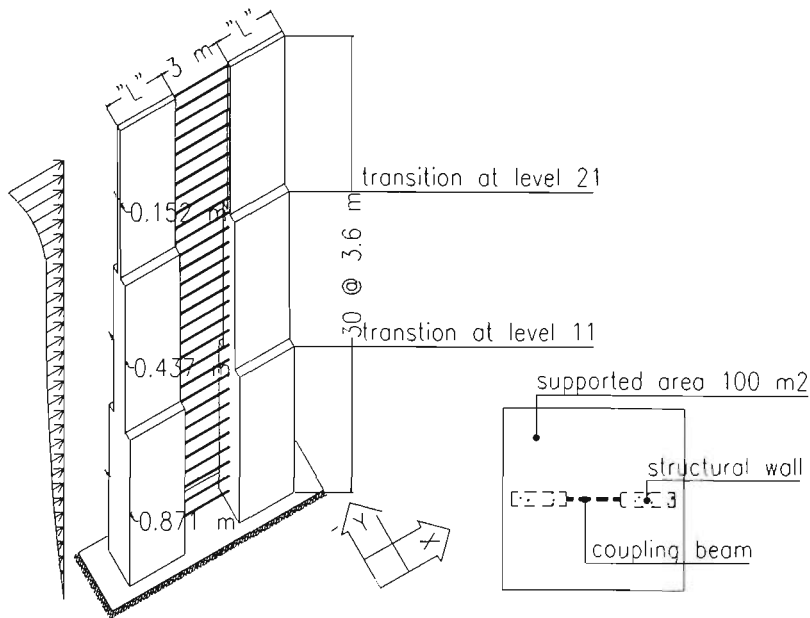
Fig. 6.13 Cost-benefits due to reduced seismic loads

Fig. 6.14 shows that the further gains resulting from the thinner walls, subsequently smaller seismic loads, increase with increasing concrete strength and increasing capitalisation yield rate.



**Fig. 6.14** Addition cost-benefits due to reduced seismic loads

## 6.2 COUPLED WALL



**Fig. 6.15** Coupled wall model

### 6.2.1 STRUCTURAL MODEL AND LOADING

Fig. 6.15 shows a rectangular coupled wall for a 30-storey building with an inter-storey height of 3.6 m. The design parameters and criteria are similar to the design for the cantilever wall model in Section 6.1. The wall is designed to resist seismic loading equivalent to a storey weight  $5.95 \text{ kN/m}^2$  over an area of  $100 \text{ m}^2$ . The initial concrete strength is taken 40 MPa. The wall thickness and the beam width are taken as 0.871, 0.469, 0.152 m and 0.446, 0.437, 0.311 m, respectively, with the corresponding transitions occurring at levels 11 and 21 (Section 5.3.3). The cross sectional length is based on satisfying an inter-storey drift ratio criterion of 0.375%.

The distribution of storey inertia load resulting from the dynamic response spectrum analysis is shown in Fig. 6.16. The base shear is defined in Eq. (6.1) where  $W_w = 1288L \text{ kN}$ . Assuming  $C = 0.025$ , a wall length of 3.05 m is found to satisfy all the criteria. This corresponds to a total concrete volume of  $360 \text{ m}^3$ , with a base shear equal to 662 kN and structural time period equal to 4.20 seconds. The displacement at the top is 268 mm.

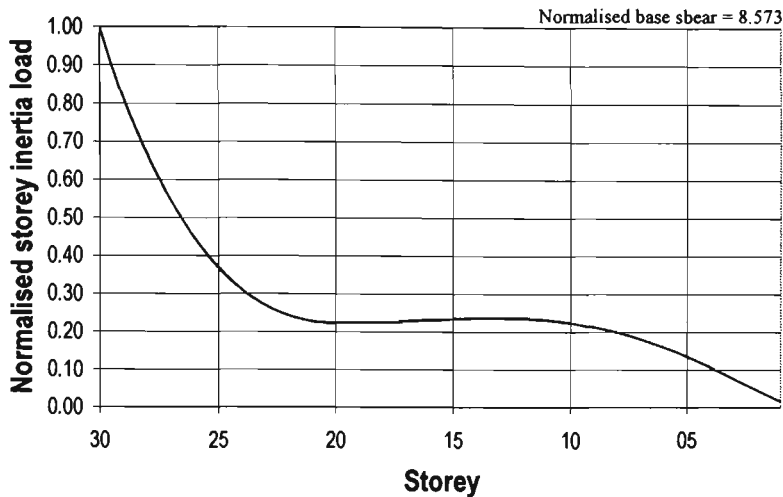


**Fig. 6.16** Design seismic loads

## 6.2.2 UNIFORM CONCRETE STRENGTHS

The analysis for the optimum volumes is carried out using a similar spreadsheet shown in Fig. 6.3. The coupled wall is deemed to satisfy the inter-storey criterion if the displacement at the top is maintained at 268 mm. The adjusted spreadsheet for the member sizing of the coupled wall is shown in Fig. 6.17.

The optimum concrete volumes for various concrete strengths with differing number of thickness transitions are illustrated in Fig. 6.18. An ideal theoretical optimal solution is also given for comparison purposes. Similar trends of volume reduction to that of cantilever wall model are observed for the coupled wall. The average reduction in the concrete volume is 23%, corresponding to an increase in concrete strength from 40 MPa to 80 MPa, while the reduction obtained by increasing the number of thickness transition from 2 to 3 is only 1%.

Fig. 6.19 illustrates the cost benefits of the cost comparison study for the coupled wall for different concrete strengths and capitalisation rental values. The figure shows similar trends as illustrated in Fig. 6.5 for the cantilever wall model. For example, utilising 80 MPa concrete for the coupled wall, in a building with a capitalisation value of \$6000/m<sup>2</sup>, provides a cost benefit 1.9 times the 40 MPa wall material costs.



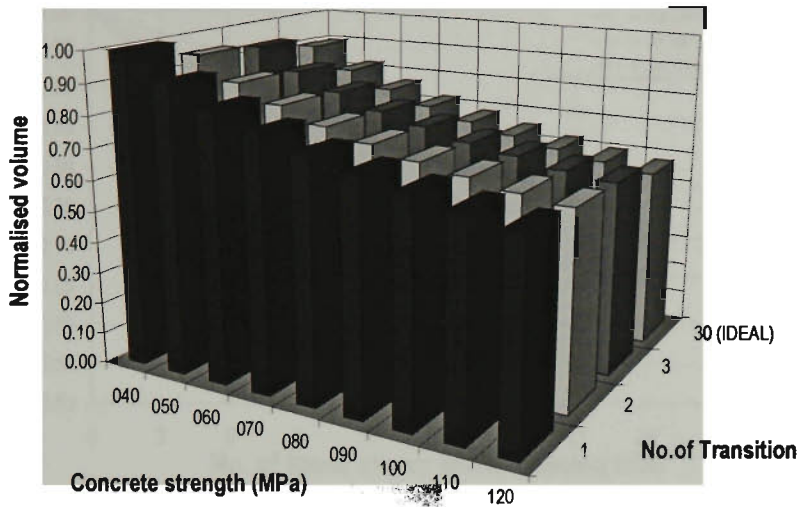


Fig. 6.18 Optimum volumes with uniform concrete strengths

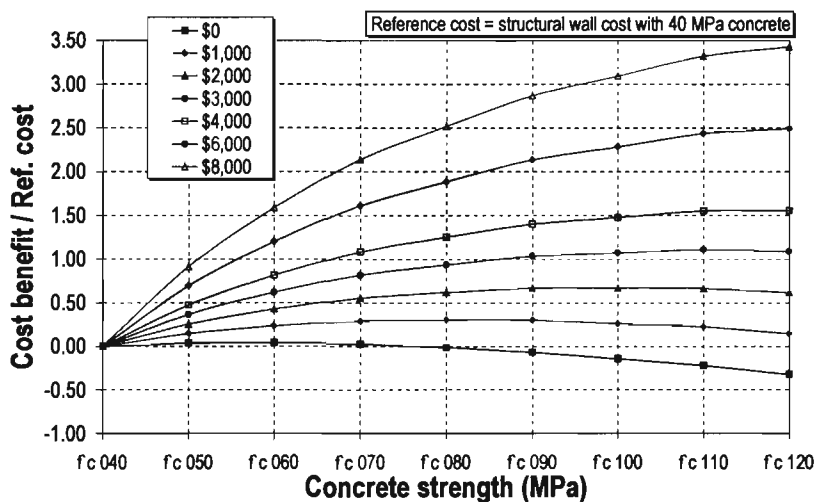


Fig. 6.19 Cost-benefits with uniform concrete strengths

### 6.2.3 VARIABLE CONCRETE STRENGTHS

Introducing HSC in structural walls can reduce the concrete volume significantly, even though the extent of the reductions varies up the height of the building. The results of the volumetric calculations, employing the member-linking optimisation technique, for various concrete strengths are shown in Fig. 6.20.

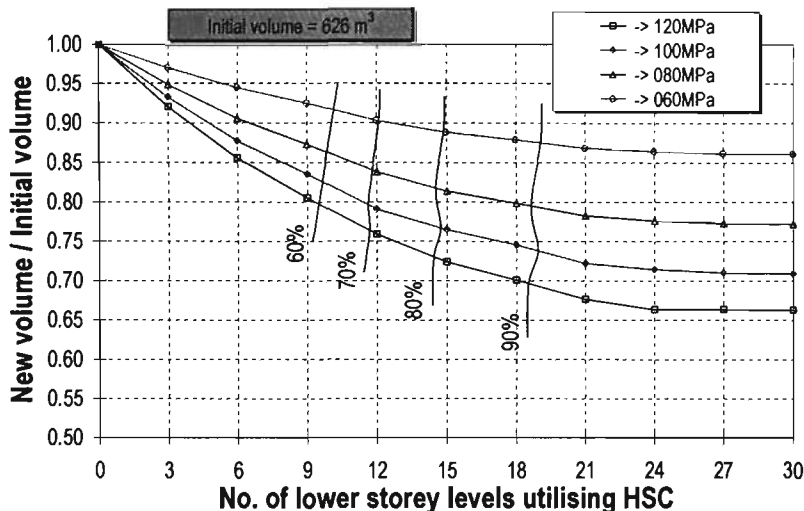


Fig. 6.20 Volume reduction with variable concrete strength

The results of the cost benefits analysis for replacing 40 MPa concrete with 120 MPa concrete are shown in Fig. 6.21. Results for utilising other concrete strengths are given in Appendix A. As expected, the main gain in cost benefits is obtained by using HSC up to the mid-height of the building. The cost benefits further increase with increasing capitalisation rates.

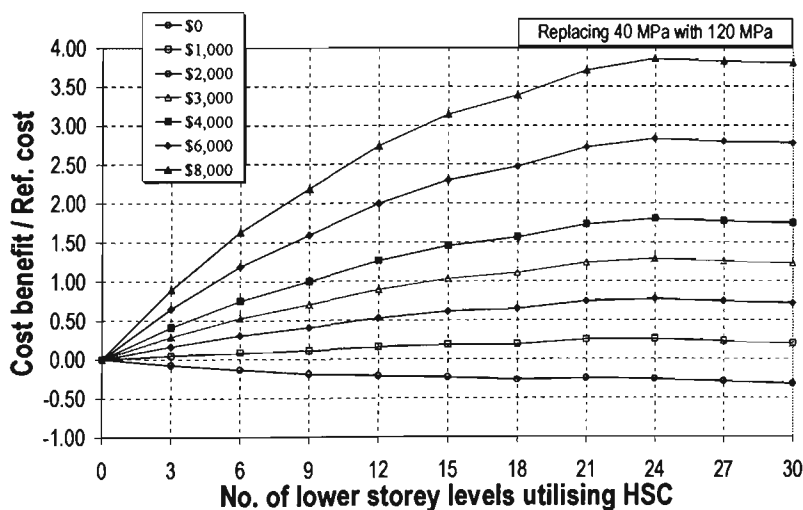


Fig. 6.21 Cost-benefits with variable concrete strengths

Fig.6.22 illustrates the linear relationships of the cost benefits and capitalisation values. The corresponding charts for other concrete grades are also given in Appendix A.

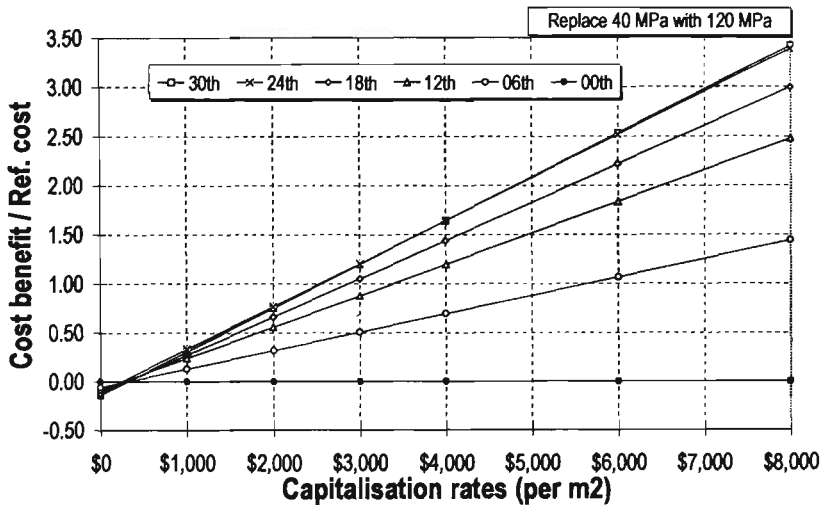


Fig. 6.22 Cost-benefits versus capitalisation yield rate

Fig. 6.23 shows the positions of concrete grade transitions for achieving 80% of the maximum benefits. The figure also suggests that the convenient transition for concrete strength is at the mid-height of the wall. The exceptions are where the capitalisation values of additional floor space benefits are ignored.

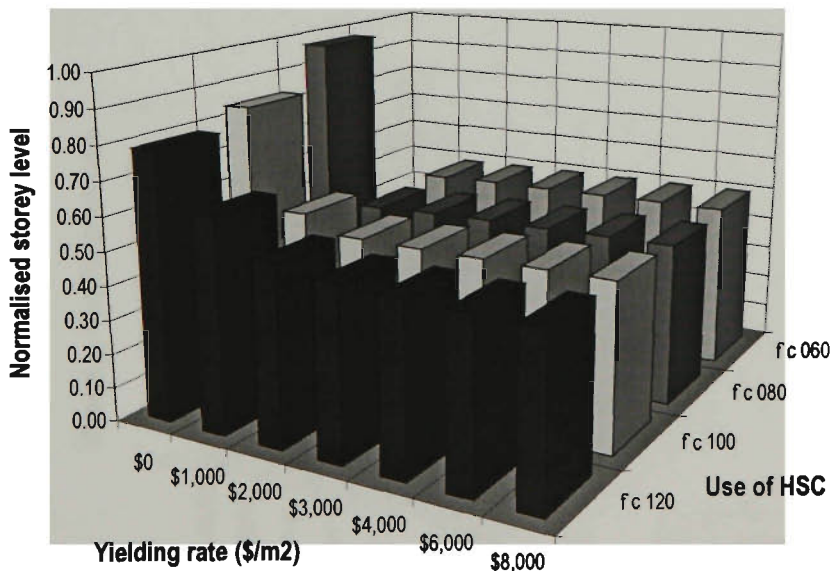


Fig. 6.23 Concrete strength transitions at 80% maximum benefit

## 6.2.4 IMPLICATION OF WALL THICKNESS OPTIMISATION TO DESIGN SEISMIC LOAD

To illustrate the additional benefits of using HSC, associated with concrete volume reduction, in buildings designed for seismic loading, a cost benefit diagram that takes into account the reduced seismic loads is developed and illustrated in Fig. 6.24. The magnitudes of the additional benefit gains are given in Fig. 6.25.

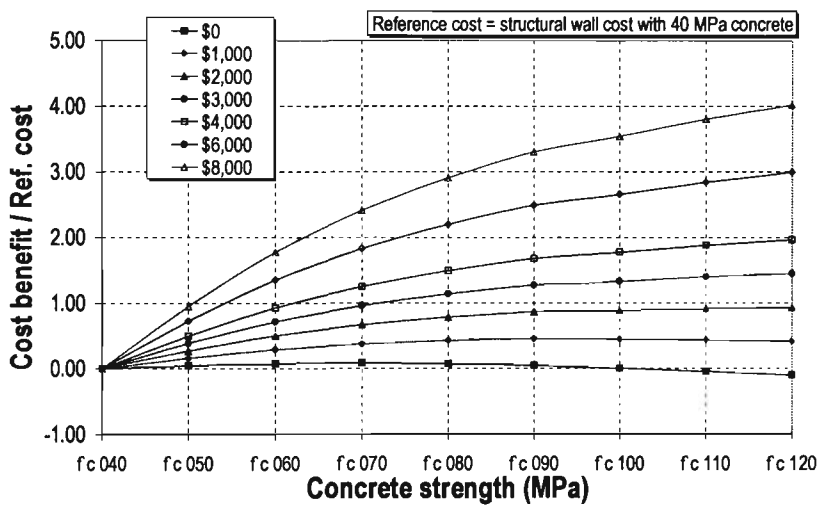


Fig. 6.24 Cost-benefits due to reduced seismic loads

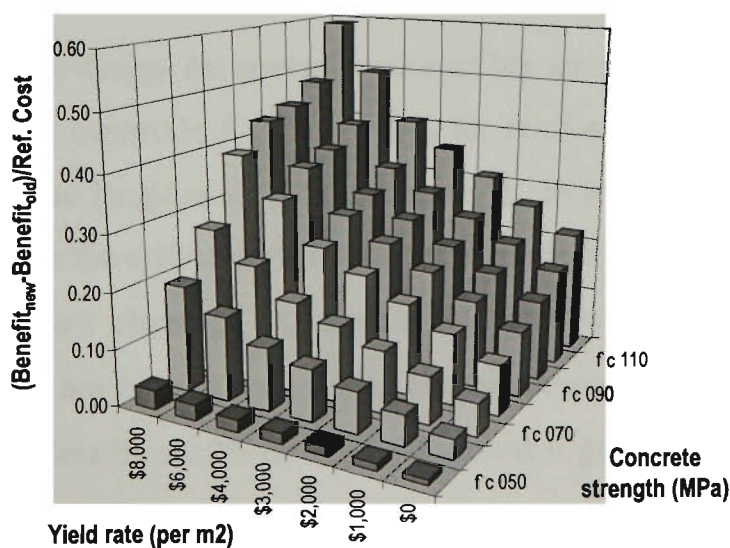


Fig. 6.25 Additional cost-benefits due to reduced seismic loads

It can be concluded from Fig. 6.25 that the additional gains from reduction in design seismic loading far exceeds the amount of benefit achievable by using higher concrete strength beyond the mid-height of the wall. For example, for a building with a capitalisation value of \$6000/m<sup>2</sup>, the benefit gain from using HSC throughout the height of the wall, without taking into consideration the additional benefit from reducing seismic loading, is 1.9 times material cost. On the other hand, the benefit with the reduced seismic loading amounts to 2.20 times material costs, despite the fact that HSC is used to mid-height of the wall, inferring a significant benefit.

### 6.3 STRENGTH AND DUCTILITY

Design check for strength and ductility of the rectangular wall sections are given in this section. This study makes no attempt to optimise the amount of steel reinforcement or the structural cost of the reinforcement. The study is limited to satisfying the strength limit states by checking the section capacity against the design actions using an acceptably low reinforcement content. The check for the ductility performance is made at the potential plastic hinge regions, which for this example is the wall within the lowest two floors.

The general rules for design for strength and ductility are given in Sections 3.2.3 and 3.2.4. Provisions of Eurocode 8 (CEN, 1994) for reinforcement details are adopted and summarised. The longitudinal reinforcement,  $\rho_v$ , in boundary elements shall not be less than 0.4%. In the critical region, this reinforcement shall be greater than 1.0%. Outside the boundary elements,  $\rho_v$  may be reduced to 0.2%, however the total reinforcement shall not be less than 0.4%. The transverse reinforcement,  $\rho_h$ , at any section shall not be less than 0.2% or  $0.5\rho_v$ , whichever is greater.

### 6.3.1 CANTILEVER WALL

Fig. 6.26 shows the moment-axial interaction diagrams for the cantilever model. For each concrete strength, three curves are given corresponding to three different cross sections, representing the wall with two thickness transitions. All curves are designed using a minimum steel reinforcement of 0.4%. The details of the cross sections are given in Table 6.1.

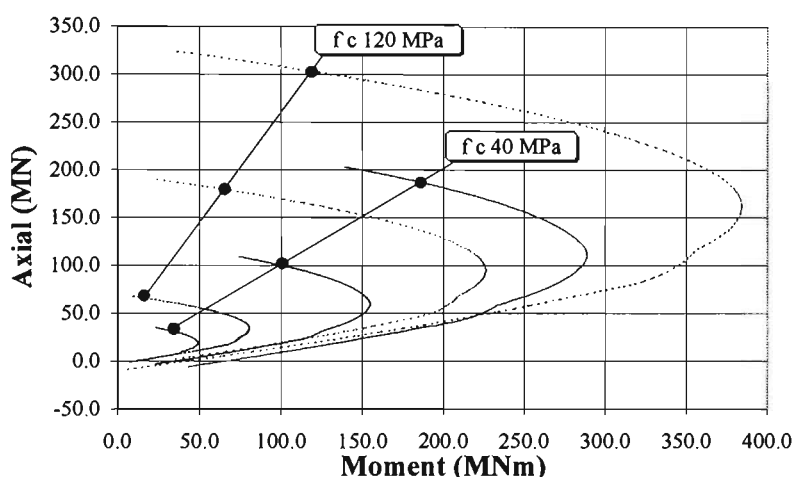


Fig 6.26 Moment-axial interaction diagram (a) cantilever wall; (b) coupled wall

Table 6.1 Details of designed cross sections

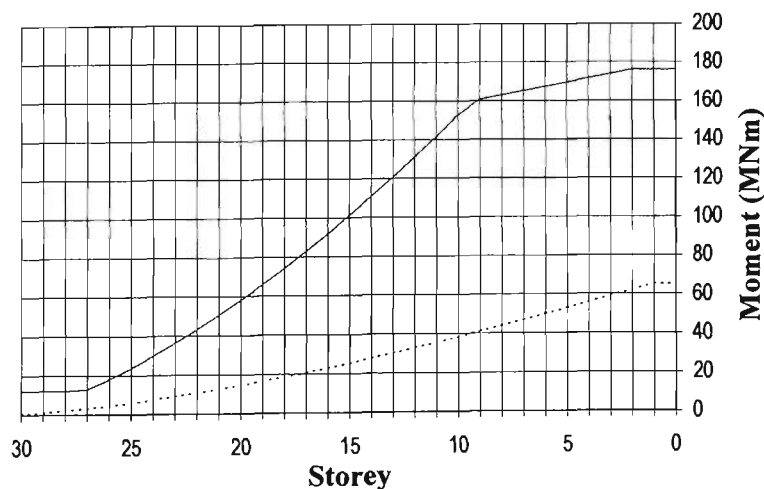
Dimension	Reinforcement detail of 40 MPa concrete		
	Flange	Web	Ratio
8900x196	2x6 of dia. 22.47 mm	32 of dia. 10.05mm	0.42%
8900x616	2x6 of dia. 39.83 mm	32 of dia. 17.81mm	0.42%
8900x1150	2x6 of dia. 54.42 mm	32 of dia. 24.34mm	0.42%
Dimension	Reinforcement detail of 120 MPa concrete		
	Flange	Web	Ratio
8900x158	2x6 of dia. 20.17 mm	32 of dia. 09.02mm	0.42%
8900x444	2x6 of dia. 33.82 mm	32 of dia.15.12mm	0.42%
8900x756	2x6 of dia. 44.12 mm	32 of dia.19.73mm	0.42%

It can be seen from the diagram that the flexural-axial capacity for higher concrete strength, especially at high axial load levels, is significantly larger in comparison to the lower concrete strength. However, the difference of the moment capacity between the two concrete strengths diminishes as the axial load level decreases. At the

condition where the walls are subjected to pure bending moment, the moment capacity of lower concrete strength is in fact larger than that of the higher concrete strength. This is well understood since, for a given reinforcement ratio, the larger cross section corresponding to lower strength concrete gives larger steel reinforcement content compared to the reinforcement content given by smaller cross section with higher strength concrete.

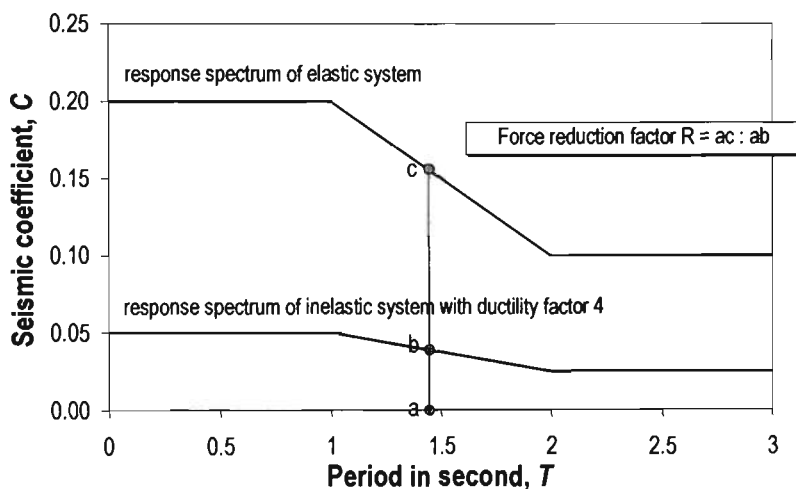
Sections 6.1 and 6.2 have demonstrated that HSC provides significant cost-benefits for the wall in satisfying the deflection criteria. The purpose of this section is to confirm that the optimum HSC wall cross sections satisfying the serviceability limit state in term of deflection criteria shall also possess adequate strength to satisfy the strength limit state.

Fig. 6.27 shows the elastic moments obtained from the inelastic response spectrum loading and moment envelop developed according to the procedure described in Section 3.2.3. The figure illustrates that despite the fact that the base section has been designed with a minimum reinforcement, the flexural moment capacity is significantly greater than the elastic moment, giving a significant large moment envelop as well. However, the design moments, which is the envelop moments, do not need to be greater than the moments resulted from elastic response spectrum loading.



**Fig. 6.27** Moment envelop

A typical inelastic response spectrum is illustrated in Fig. 6.28. It is shown that the inelastic response force level is less than the corresponding elastic response by a factor of  $R$ . For long period structures, the force reduction factor,  $R$ , is equal to  $\mu/K$ , in which  $\mu$  is the ductility factor and  $K$  the structural factor. The maximum moment limitation is corresponding to the moments developed from elastic response spectrum, hence the walls are expected to respond in the elastic range.



**Fig. 6.28** Typical inelastic response spectra

Fig. 6.29 shows the moments and the corresponding axial forces for the 30 storey levels, and the flexural-axial capacity diagrams for the three different cross sections. It can be seen from the figure that all design forces fall within the section capacity envelop for each corresponding curve. For example, the first 12 points of the design forces in Fig. 6.29, corresponding to storey levels 19 to 30, are within the capacity envelop of  $8900 \times 158 \text{ mm}^2$  cross section, and the next 9 points, corresponding to storey levels 10 to 18, are within the capacity of  $8900 \times 444$  cross section, etc.

The flexural-axial diagrams in Fig. 6.29 are developed using a 1.24% steel reinforcement ratio. This reinforcement may be reduced as the design forces get smaller at higher levels for each transition. However, the attempt to minimise the reinforcement content and the cost saving associated with it are beyond the scope of this study.

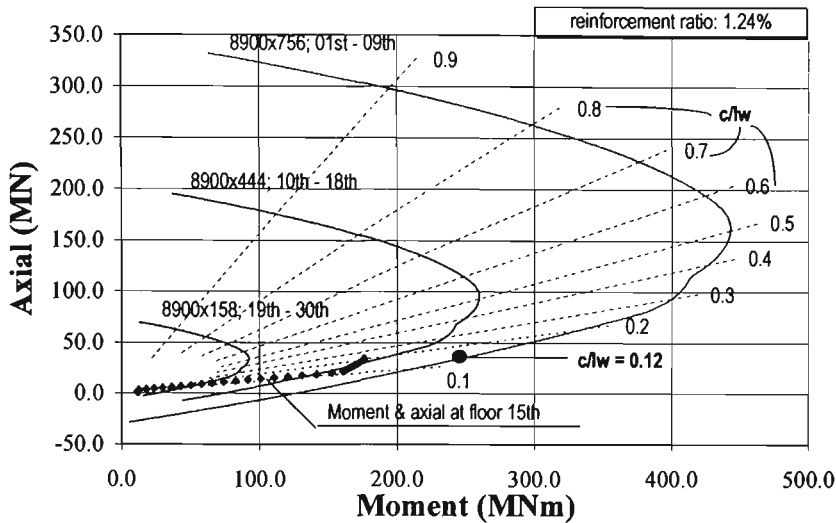


**Fig. 6.29** Design for flexural-axial strength

It was stated in Section 3.2.4 that the structural wall is deemed to possess adequate ductility level if the actual neutral axis depth is less than critical neutral axis depth,  $c_c$ , as derived from Eq. (3.16). From the elastic and nominal moments at the first floor, and the wall aspect ratio,  $A_r = 12$ , this critical neutral axis depth is found to be  $0.24l_w$ . From Fig. 6.29 the actual neutral axis depth corresponding to design forces at the first floor is found to be  $0.12l_w$ , which is less than the critical value.

The shear demand as calculated according to Eq. (3.15) and the shear strengths of the wall section are tabulated in Table 6.2. It is shown that the contribution of concrete alone exceeds the design shear. Therefore, only minimum shear reinforcement needs to be provided, and is not found to be a governing criterion.

**Table 6.2** Design for shear strength

Floor	$V_{,w}$ (MN)	$\phi.V_c$ (MN)	$\phi.V_s$ (MN)
30th	1.71	2.33	0.72
01st	5.12	6.25	3.43

### 6.3.2 COUPLED WALL

The elastic moment and design moment envelop for the coupled wall are shown in Fig. 6.30. Due to a large flexural-axial capacity of the wall section at the first floor, the design moment envelop is developed from the elastic response moments, which is  $\mu/K$  times the inelastic response moments. The comparison between the design forces and section capacities for flexural and axial strength is shown in Fig. 6.31. It can be seen that the section capacity of the wall section with a minimum reinforcement far exceeds the required strength, at all floor levels.

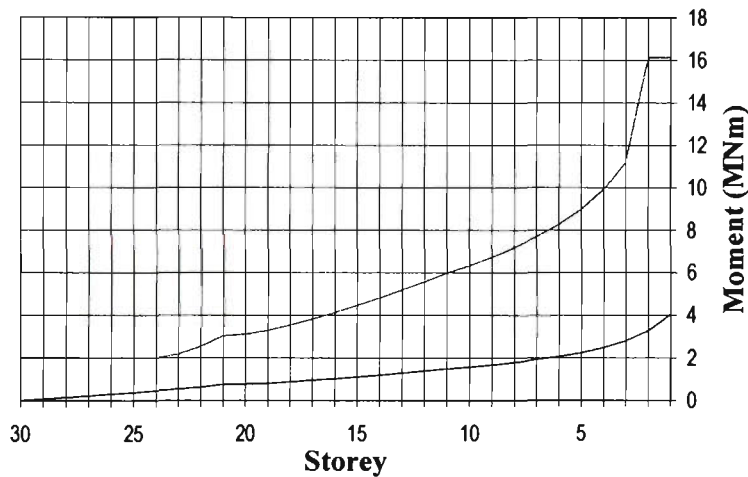


Fig. 6.30 Moment envelop

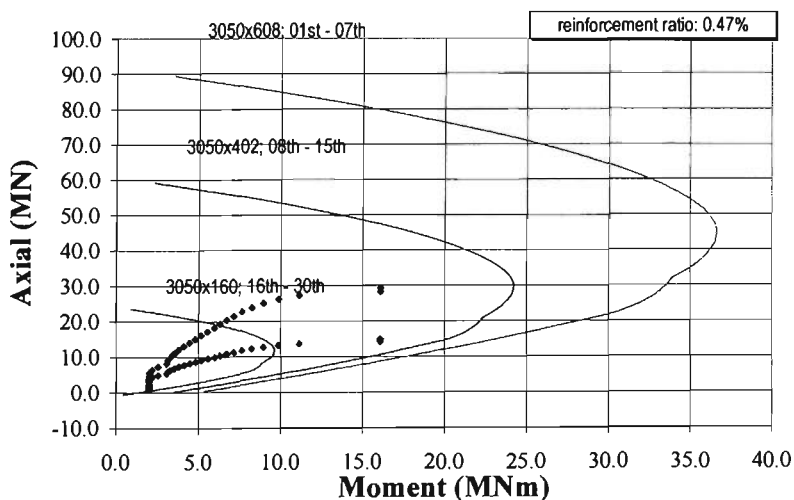


Fig. 6.31 Design for flexural-axial strength

The design for the shear strength is checked at the two extreme ends and summarised in Table 6.3. It is also noted that the contribution of shear strength of concrete alone exceeds the required shear strength. Also shown in the table is the shear strength calculated using minimum 0.2% transverse reinforcement.

**Table 6.3** Design for shear strength

Floor	$V_w$ (MN)	$\phi.V_c$ (MN)	$\phi.V_s$ (MN)
30th	0.16	1.01	0.25
01st	1.39	3.09	0.95

Since the walls are designed to behave elastically, there is no need to give special consideration for the ductility behaviour of the coupled wall.

## 6.4 CONCLUDING REMARKS

In this chapter, volumetric optimisation and cost analysis have been carried for a cantilever wall and a coupled wall system. The results show the significant volume reduction due to the increase of concrete strength compared to the reduction due to the increase of number of wall thickness transitions. Despite the significant reduction in the concrete volume, the construction cost of the walls with HSC increases. The benefit of using HSC only becomes apparent if the floor space gained through wall thickness reduction is capitalised, to obtain a net financial benefit for the building owner.

A utilisation of various concrete strengths at different floor levels also has an attractive objective of providing a most cost effective solution. The results of the cost comparative study showed that the cost-benefits of extending the use of HSC beyond two-third of the wall height are minimal. It was also shown that up to 80% benefits could be achieved by using HSC up to the mid-height of the wall.

Furthermore, in earthquake resistant structures, the thinner walls with HSC reduce the magnitude of seismic loading, providing further cost-benefits. The results reveal that benefits increase with increasing concrete strength and capitalisation yield rate.

The study confirms that from the examples given, the strength limit state is found to be not critical and that the optimisation process can be adequately based on displacement constraint alone.

In the next chapter, similar analyses will be carried out for three-dimensional “C” shape core walls. These walls are normally designed to resist horizontal loads from both orthogonal directions, as opposed to these two-dimensional rectangular shape walls.

## CHAPTER SEVEN

---

### USE OF HSC IN COUPLED “C” SHAPE CORE WALLS

The preceding chapter discussed the cost-benefits of using high-strength concrete (HSC) in rectangular walls. The walls are designed primarily to resist lateral loads in the direction parallel to the walls. In three dimensional wall configurations, such as “C” shape core elevator walls, they are typically designed to resist lateral loads from two orthogonal directions. The cost-benefit study of the coupled “C” shape wall is discussed in this chapter.

#### 7.1 MULTIPLE-DIRECTION DISPLACEMENT CONSTRAINT PROBLEM

The structural optimisation technique outlined in Chapter 4 is for solving a single-direction displacement constraint problem. Due to the requirement of solving the problem for both orthogonal directions, the technique presented in Chapter 4 needs to be modified to solve the problem with multiple-direction displacement constraints.

There are several methods of dealing with the multiple-direction displacement constraint problems, such as using Lagrangian multipliers (e.g. Venkayya *et al.*, 1973; Chan *et al.*, 1995). A simpler approach is to use the weighed values (Xie & Steven, 1997) of strain energy density or sensitivity index contribution of each direction. The modified values of strain energy density may be given in the form

$$\lambda_i^{-1} = \sum_{j=1}^l \omega_j |\lambda_{ij}^{-1}| \quad (7.1)$$

and defined as the strain energy density for the  $i$ th element. In the above equation,  $\lambda_{ij}^{-1}$  is the strain energy density of the  $i$ th element for loading direction  $j$  ( $l=2$ ) and the weighting parameter  $\omega_j$  is given as

$$\omega_j = \frac{\sum \delta'_{ij}}{D'_{\text{design}}} \quad (7.2)$$

in which  $\delta'_{ij}$  is the optimum displacement participation factor (DPF) of the  $i$ th element caused by loading direction  $j$ , and  $D'_{\text{design}}$  is the design displacement at the point of interest.

When the total displacement (sum of all element DPFs) is far below the design value, the corresponding weighing parameter will be small, thus the corresponding strain energy density in Eq. (7.1) will be of little significance.

## 7.2 STRUCTURAL MODEL AND LOADING

Fig. 7.1 shows a "C" shape core wall of a 40-storey building with an inter-storey height of 3.6 m. The wall will be designed for a seismic loading corresponding to a floor area of 40x40 m<sup>2</sup>. The distribution of base shear is derived by application of Eq. (3.3). With the initial concrete strength at 40 MPa, wall thicknesses of 0.650, 0.500, 0.350, and 0.200 m are adopted for the first, second, third, and fourth 10 storeys, respectively, and beam dimension of 500 mm wide by 950 mm deep, the displacement at the top is 285 mm for both directions. The corresponding base shear and the first mode structural time period are 11723 kN and 4.578 seconds, respectively.

## 7.3 UNIFORM CONCRETE STRENGTHS

The optimum cross sections of the structural elements are calculated using the spreadsheet shown in Fig. 7.2. In the optimisation process, the displacement at the top

is maintained unchanged, and thus the adjusted strain energy density can be approached by using the average value of two load conditions, corresponding to the lateral load application in the two orthogonal directions.

$$\lambda_i^{-1} = \frac{1}{2} (|\lambda_{i1}^{-1}| + |\lambda_{i2}^{-1}|) \quad (7.3)$$

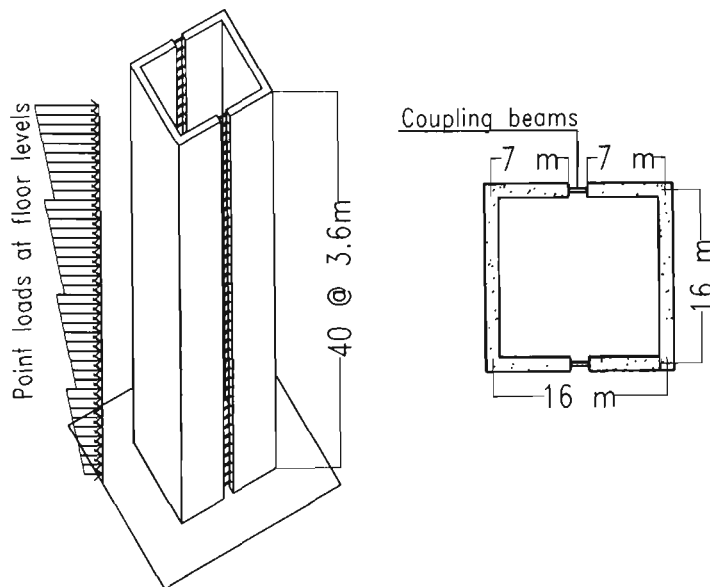


**Fig. 7.1** Coupled "C" shape core walls model

With these strain energy densities, the optimal concrete volumes for various concrete strengths with differing number of wall thickness transitions are calculated following the optimisation procedure outlined in Chapters 4 and 5, with the results shown in Fig. 7.3. A reanalysis with these new optimum cross sections results in total displacements of 280 mm and 284 mm, respectively, for the X and Y-directions, giving differences of less than 2%.

It can be seen from Fig. 7.2 that the volume reduction obtained by increasing concrete strength is much more significant than increasing the number of thickness transitions. The volume reduction corresponding to an increase in concrete strength from 40 MPa to 80 MPa amounts to 23%, whereas the reduction is only 1% for an increase in transitions from 2 to 3.

**CONTROL PANEL**  
 Target displacement 285 mm  
 Concrete strength [REF] 40 MPa  
 Concrete strength [HSC] 120 MPa  
 20 of 40 storeys  
 Variables

←		PANEL - FLANGE (VALUES X 4)				PANEL - WEB (VALUES X 2)				COUPLING BEAM (VALUES X 2)				→				
Level	DPF	V	f'c	Alpha	DPF	V	f'c	Alpha	DPF	V	f'c	Alpha	DPF	V	M	DPFn	Vn	Thick
40	0.01	5.04	40	0.12	0.07	0.62	40	0.09	0.12	1.04	40	0.34	0.04	0.32			0.81	0.428
39	0.02	5.04	40	0.17	0.10	0.87	40	0.13	0.17	1.49	40	0.44	0.05	0.42			0.81	0.428
38	0.03	5.04	40	0.22	0.13	1.10	40	0.13	0.17	1.49	40	0.52	0.06	0.49			0.81	0.428
37	0.04	5.04	40	0.28	0.16	1.33	40	0.13	0.17	1.49	40	0.60	0.07	0.57			0.81	0.428
36	0.06	5.04	40	0.31	0.19	1.58	40	0.13	0.17	1.49	40	0.67	0.08	0.64			0.81	0.428
35	0.08	5.04	40	0.37	0.22	1.86	40	0.13	0.17	1.49	40	0.74	0.08	0.70			0.81	0.428
34	0.11	5.04	40	0.43	0.25	2.15	40	0.13	0.17	1.49	40	0.79	0.09	0.76			0.81	0.428
33	0.14	5.04	40	0.49	0.28	2.46	40	0.13	0.17	1.49	40	0.85	0.10	0.81			0.81	0.428
32	0.18	5.04	40	0.55	0.33	2.79	40	0.13	0.17	1.49	40	0.90	0.10	0.86			0.81	0.428
31	0.23	5.04	40	0.62	0.37	3.12	40	0.13	0.17	1.49	40	0.94	0.11	0.90			0.81	0.428
30	0.17	8.82	40	0.40	0.42	3.54	40	0.35	0.84	7.13	40	1.01	0.11	0.96			0.81	0.428
29	0.21	8.82	40	0.45	0.48	3.94	40	0.35	0.84	7.13	40	1.05	0.12	0.99			0.81	0.428
28	0.25	8.82	40	0.49	0.51	4.35	40	0.35	0.84	7.13	40	1.08	0.12	1.02			0.81	0.428
27	0.31	8.82	40	0.54	0.58	4.78	40	0.35	0.84	7.13	40	1.11	0.12	1.05	14.00		0.81	0.428
26	0.36	8.82	40	0.59	0.61	5.23	40	0.35	0.84	7.13	40	1.14	0.13	1.08			0.81	0.428
25	0.43	8.82	40	0.64	0.67	5.68	40	0.35	0.84	7.13	40	1.17	0.13	1.11			0.81	0.428
24	0.50	8.82	40	0.70	0.72	6.14	40	0.35	0.84	7.13	40	1.20	0.13	1.14			0.81	0.428
23	0.58	8.82	40	0.75	0.78	6.62	40	0.35	0.84	7.13	40	1.22	0.14	1.16			0.81	0.428
22	0.67	8.82	40	0.80	0.83	7.10	40	0.35	0.84	7.13	40	1.25	0.14	1.19			0.81	0.428
21	0.77	8.82	40	0.86	0.89	7.58	40	0.35	0.84	7.13	40	1.27	0.14	1.21			0.81	0.428
20	0.81	8.12	120	0.80	0.76	6.51	40	0.78	1.86	15.81	20.00	1.28	0.14	1.19			1.13	0.596
19	0.70	8.12	120	0.85	0.81	6.93	40	0.78	1.86	15.81	20.00	1.28	0.14	1.19			1.13	0.596
18	0.78	8.12	120	0.91	0.86	7.38	40	0.78	1.86	15.81	20.00	1.28	0.14	1.19			1.13	0.596
17	0.88	8.12	120	0.96	0.92	7.79	40	0.78	1.86	15.81	20.00	1.28	0.14	1.19			1.13	0.596
16	0.98	8.12	120	1.01	0.97	8.22	40	0.78	1.86	15.81	20.00	1.28	0.14	1.19			1.13	0.596
15	1.09	8.12	120	1.07	1.02	8.66	40	0.78	1.86	15.81	20.00	1.28	0.14	1.19			1.13	0.596
14	1.20	8.12	120	1.12	1.07	9.11	40	0.78	1.86	15.81	20.00	1.28	0.14	1.19			1.13	0.596
13	1.32	8.12	120	1.18	1.12	9.55	40	0.78	1.86	15.81	20.00	1.28	0.14	1.19			1.13	0.596
12	1.45	8.12	120	1.23	1.17	9.99	40	0.78	1.86	15.81	20.00	1.28	0.14	1.19			1.13	0.596
11	1.58	8.12	120	1.28	1.23	10.43	40	0.78	1.86	15.81	20.00	1.28	0.14	1.19			1.13	0.596
10	1.32	10.56	120	1.03	1.28	10.89	40	0.99	2.82	23.02	7.00	1.77	0.13	1.08			1.00	0.524
9	1.43	10.56	120	1.08	1.33	11.35	40	0.99	2.82	23.02	7.00	1.77	0.13	1.08			1.00	0.524
8	1.55	10.56	120	1.12	1.39	11.81	40	0.99	2.82	23.02	7.00	1.77	0.13	1.08			1.00	0.524
7	1.67	10.56	120	1.16	1.44	12.26	40	0.99	2.82	23.02	7.00	1.77	0.13	1.08			1.00	0.524
6	1.79	10.56	120	1.20	1.49	12.70	40	0.99	2.82	23.02	7.00	1.77	0.13	1.08			1.00	0.524
5	1.92	10.56	120	1.24	1.54	13.12	40	0.99	2.82	23.02	7.00	1.77	0.13	1.08			1.00	0.524
4	2.04	10.56	120	1.28	1.59	13.53	40	0.99	2.82	23.02	7.00	1.77	0.13	1.08			1.00	0.524
3	2.16	10.56	120	1.32	1.64	13.92	40	0.99	2.82	23.02	7.00	1.77	0.13	1.08			1.00	0.524
2	2.27	10.56	120	1.35	1.68	14.27	40	0.99	2.82	23.02	7.00	1.77	0.13	1.08			1.00	0.524
1	2.38	10.56	120	1.38	1.71	14.58	40	0.99	2.82	23.02	7.00	1.77	0.13	1.08			1.00	0.524
Sub-total	34.23	325.45				33.59	285.65			70.86	602.95			4.32	38.74		286	2617

←		PANEL - FLANGE (VALUES X 4)				PANEL - WEB (VALUES X 2)				COUPLING BEAM (VALUES X 2)				→				
Level	DPF	V	f'c	Alpha	DPF	V	f'c	Alpha	DPF	V	f'c	Alpha	DPF	V	M	DPFn	Vn	Thick
40	0.01	11.52	40	0.09	0.12	1.04	40	0.09	0.12	1.04	40	0.34	0.04	0.32			0.81	0.428
39	0.02	11.52	40	0.13	0.17	1.49	40	0.13	0.17	1.49	40	0.44	0.05	0.42			0.81	0.428
38	0.03	11.52	40	0.13	0.17	1.49	40	0.13	0.17	1.49	40	0.52	0.06	0.49			0.81	0.428
37	0.06	11.52	40	0.13	0.17	1.49	40	0.13	0.17	1.49	40	0.60	0.07	0.57			0.81	0.428
36	0.09	11.52	40	0.25	0.34	2.90	40	0.13	0.17	1.49	40	0.67	0.08	0.64			0.81	0.428
35	0.12	11.52	40	0.30	0.41	3.48	40	0.13	0.17	1.49	40	0.74	0.08	0.70			0.81	0.428
34	0.17	11.52	40	0.36	0.48	4.11	40	0.13	0.17	1.49	40	0.79	0.09	0.76			0.81	0.428
33	0.23	11.52	40	0.42	0.56	4.79	40	0.13	0.17	1.49	40	0.85	0.10	0.81			0.81	0.428
32	0.31	11.52	40	0.48	0.65	5.53	40	0.13	0.17	1.49	40	0.90	0.10	0.86			0.81	0.428
31	0.41	11.52	40	0.55	0.74	6.33	40	0.13	0.17	1.49	40	0.94	0.11	0.90			0.81	0.428
30	0.30	20.16	40	0.35	0.84	7.13	40	0.35	0.84	7.13	40	1.01	0.11	0.96			0.81	0.428
29	0.37	20.16	40	0.39	0.93	7.93	40	0.35	0.84	7.13	40	1.05	0.12	0.99			0.81	0.428
28	0.45	20.16	40	0.44	1.03	8.80	40	0.35	0.84	7.13	40	1.08	0.12	1.02			0.81	0.428
27	0.55	20.16	40	0.48	1.14	9.70	40	0.35	0.84	7.13	40	1.11	0.12	1.05	14.00		0.81	0.428
26	0.66	20.16	40	0.53	1.25	10.65	40	0.35	0.84	7.13	40	1.14	0.13	1.08			0.81	0.428
25	0.79	20.16	40	0.58	1.37	11.62	40	0.35	0.84	7.13	40	1.17	0.13	1.11			0.81	0.428
24	0.93	20.16	40	0.63	1.48	12.63	40	0.35	0.84	7.13	40	1.20	0.13	1.14			0.81	0.428
23	1.09	20.16	40	0.68	1.60	13.68	40	0.35	0.84	7.13	40	1.22	0.14	1.16			0.81	0.428
22	1.26	20.16	40	0.73	1.73	14.71	40	0.35	0.84	7.13	40	1.25	0.14	1.19			0.81	0.428
21	1.48	20.16	40	0.78	1.86	15.81	40	0.35	0.84	7.13	40	1.27	0.14	1.21			0.81	0.428
20	1.17	18.57	120	0.73	1.59	13.57	40	0.78	1.86	15.81	20.00	1.28	0.14	1.19			1.13	0.596
19	1.32	18.57	120	0.78	1.70	14.43	40	0.78	1.86	15.81	20.00	1.28	0.14	1.19			1.13	0.596
18	1.49	18.57	120	0.82	1.80	15.32	40	0.78	1.86	15.81	20.00	1.28	0.14	1.19			1.13	0.596
17	1.67	18.57	120	0.87	1.91	16.23	40	0.78	1.86	15.81	20.00	1.28	0.14	1.19			1.13	0.596
16	1.86	18.57	120	0.92	2.02	17.18	40	0.78	1.86	15.81	20.00	1.28	0.14	1.19			1.13	0.596
15	2.07	18.57	120	0.97	2.13	18.10	40	0.78	1.86	15.81	20.00	1.28	0.14	1.19			1.13	0.596
14	2.30	18.57	120	1.03	2.24	19.06	40	0.78	1.86	15.81	20.00	1.28	0.14	1.19			1.13	0.596
13	2.54	18.57	120	1.08	2.35	20.03	40	0.78	1.86	15.81	20.00	1.28	0.14	1.19			1.13	0.596
12	2.79	18.57	120	1.13	2.47	21.01	40	0.78	1.86	15.81	20.00	1.28	0.14	1.19			1.13	0.596
11	3.07	18.57	120	1.19	2.59	22.02	40	0.78	1.86	15.81	20.00	1.28	0.14	1.19			1.13	0.596
10	2.58	24.14	120	0.95	2.70	23.02	40	0.99	2.82	23.02	7.00	1.77	0.13	1.08			1.00	0.524
9	2.81																	

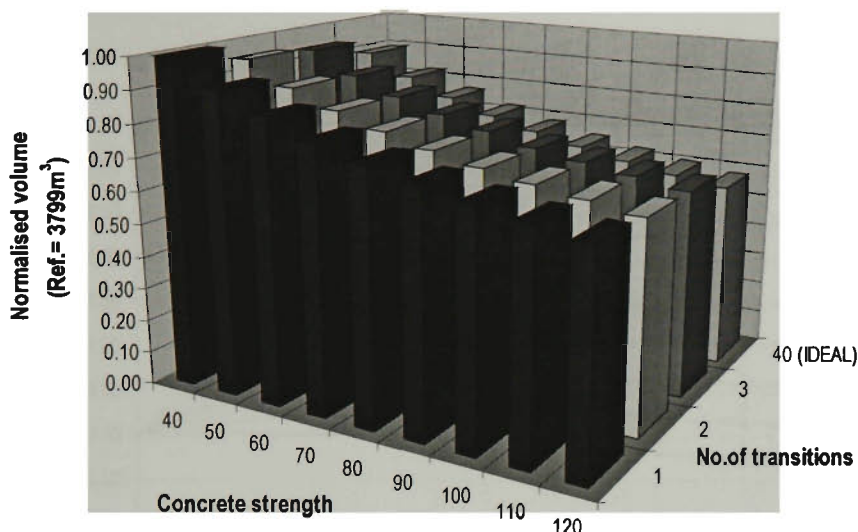


Fig. 7.3 Optimum volumes with uniform concrete strengths

Based on the optimum concrete volumes, the benefits associated with the gains in lettable space area, corresponding to different concrete strengths, may be calculated. In the case of a "C" shape core wall, the extra floor area gain shall be calculated according to the following formula

$$A_x = \frac{O(V_2 - V_1)}{H} \quad (7.4)$$

where  $O$  is total length of the walls,  $V_1$  and  $V_2$  are the wall volumes, with the reference concrete strength, 40 MPa, and the higher concrete strength, respectively, and  $H$  is the overall height of the wall.

Based on the optimum designs for core wall with two thickness transitions, a cost analysis is carried out using the parameters given in Section 5.8. The cost benefits are given by capitalising the floor space gains resulting from the thinner walls and by the structural cost differences associated with higher strength concrete. The results, for the varying capitalisation values, are illustrated in Fig. 7.4.

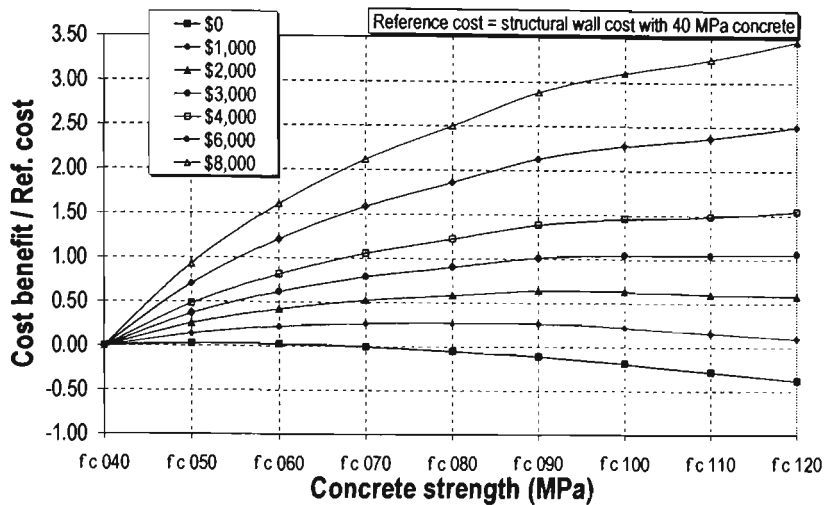


Fig. 7.4 Cost benefits with uniform concrete strengths

It indicates that for a building with capitalisation value of  $\$6000/\text{m}^2$ , increasing the concrete strength by 40 MPa will gain a cost benefit corresponding to 1.9 times the cost of the 40 MPa wall, a significant amount.

#### 7.4 VARIABLE CONCRETE STRENGTHS

The previous section shows the concrete volume reductions with increasing concrete strength throughout the wall height. Chapter 6 illustrates that utilising HSC beyond the middle of the building height does not gain significant concrete volume reductions, with maximum further reduction of less than 20%. For the structural core wall case, the reductions corresponding to the use of higher strength concrete up to various levels are illustrated in Fig. 7.5. The trends observed for rectangular walls are also repeated for the "C" shape core walls. A minimum of 80% of possible cost benefit is achieved by allocating HSC up to the mid-height of the core walls.

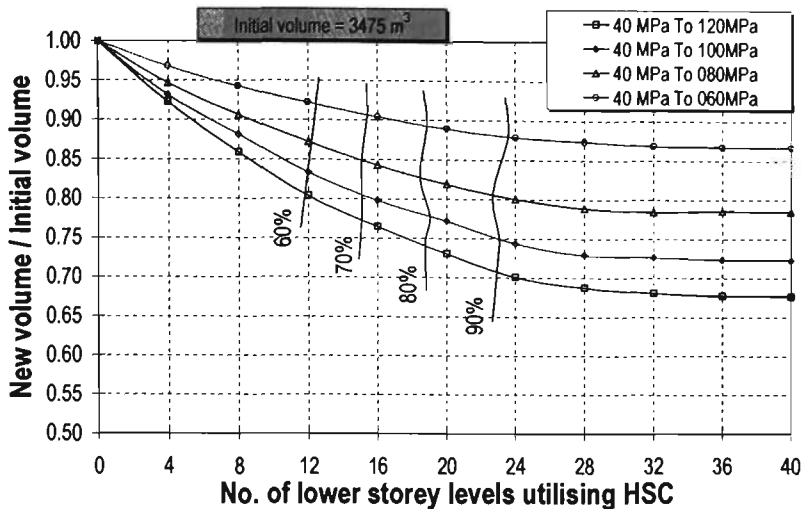


Fig. 7.5 Volume reductions with variable concrete strengths

The results of the cost benefits analysis for replacing 40 MPa concrete with 120 MPa concrete are shown in Fig. 7.6. The cost-benefits gained for the “C” shape core walls are found to be slightly less than the gains for the rectangular walls in Chapter 6. For example, with concrete strength of 120 MPa in the lower half storeys and 40 MPa in the upper half, the cost-benefits gained, for a building with capitalisation yield rate of \$6,000/m<sup>2</sup>, for the coupled “C” wall are in the order of 2.19 of a 40 MPa wall cost. Whereas, for the rectangular walls in Chapter 6, the cost-benefits amount to 2.43 and 2.30 of the 40 MPa wall cost for the cantilever and coupled wall case, respectively. For other concrete strengths, the results are given in Appendix B.

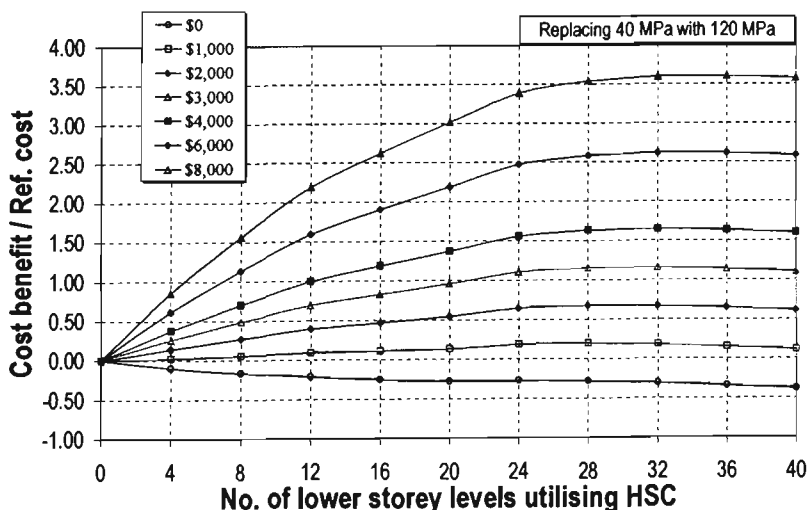


Fig. 7.6 Cost-benefits with variable concrete strengths

The relationships between the cost benefits and the capitalisation values are shown in Fig. 7.7. The linear relationships between the capitalisation yield rates and cost-benefits are also observed in the coupled "C" shape walls, irrespective to the number of storeys using the HSC. The corresponding figures for the other concrete grades are also given in Appendix B.

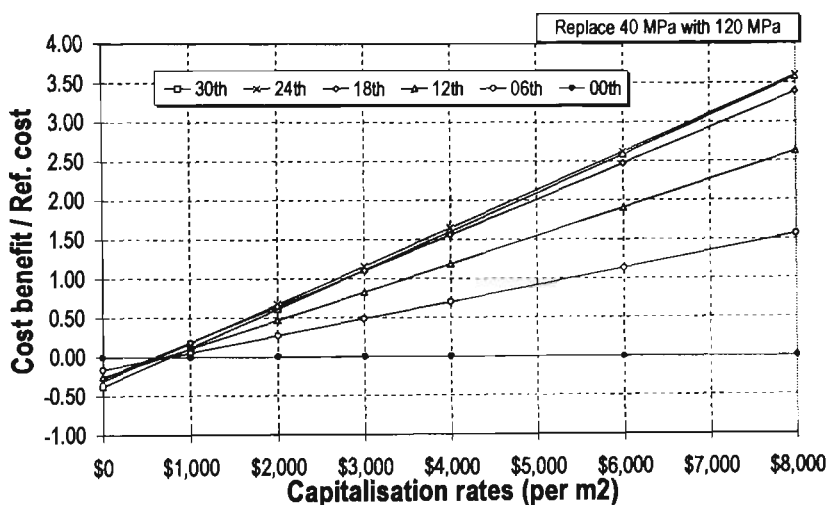


Fig. 7.7 Cost-benefits versus capitalisation yield rates

The positions of the concrete grade transition to achieve an 80% of the maximum benefit are plotted in Fig. 7.8. It can be seen that the transition position is consistently located near the mid-height. The only exception is where only the material cost is considered and capitalisation value of additional floor space benefits is ignored.

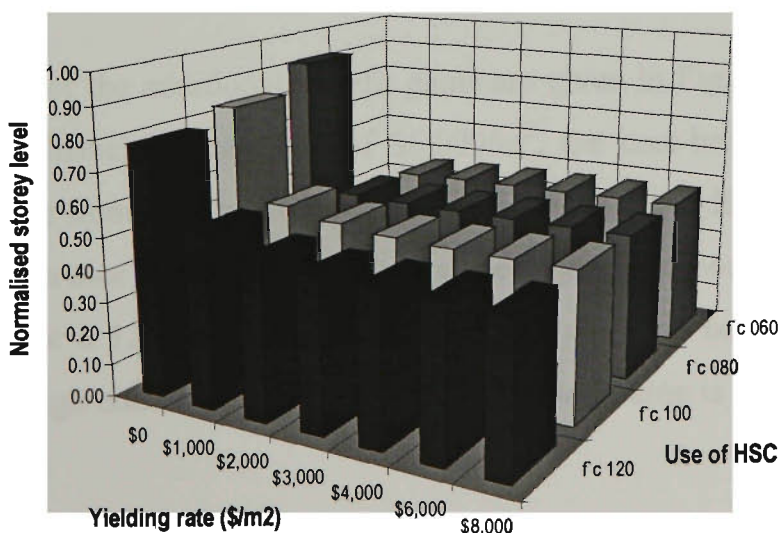
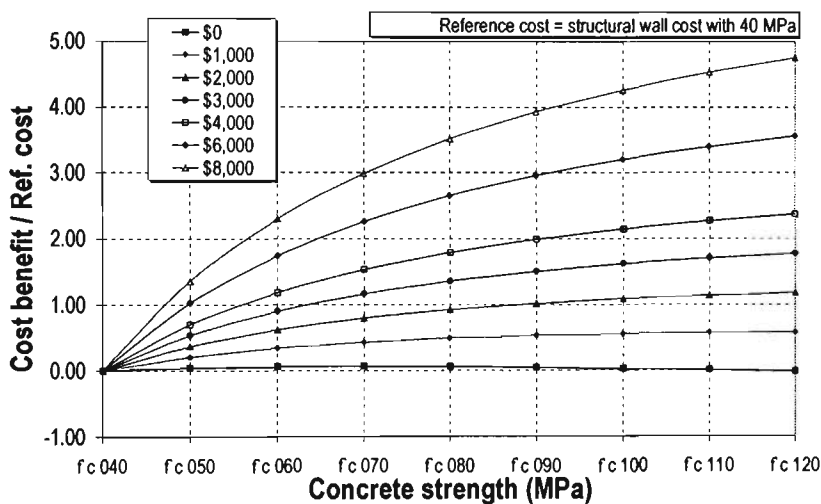


Fig. 7.8 Concrete strength transitions at 80% maximum benefit

## 7.5 IMPLICATION OF WALL THICKNESS OPTIMISATION TO DESIGN SEISMIC LOAD

The additional cost-benefits in buildings designed for seismic loading, associated with a reduced seismic loading, are illustrated in Fig. 7.9. The cost-benefits presented in the figure are computed for a two-thickness-transition wall with HSC used up to the mid-height of the building. Due to the domination of maintaining minimum thickness in most of the upper storey levels, the calculation process of optimum volumes, in according to the diagram in Fig 6.11(b), is limited to two iterations.



**Fig. 7.9** cost benefits due to reduced seismic loads

The magnitudes of the additional benefit gains are given in Fig. 7.10. In the case of buildings with financial return rate of \$6,000/m<sup>2</sup>, the cost-benefits, with 80 MPa concrete, increase from 1.86 to 2.65 of the reference cost, an additional cost-benefit of 0.79 of the reference cost. This additional cost-benefit amounts to 1.06 of the reference cost for a 120 MPa concrete strength. It can also be seen the additional benefit at very high concrete strength and capitalisation value is as high as 1.3 of the reference cost.

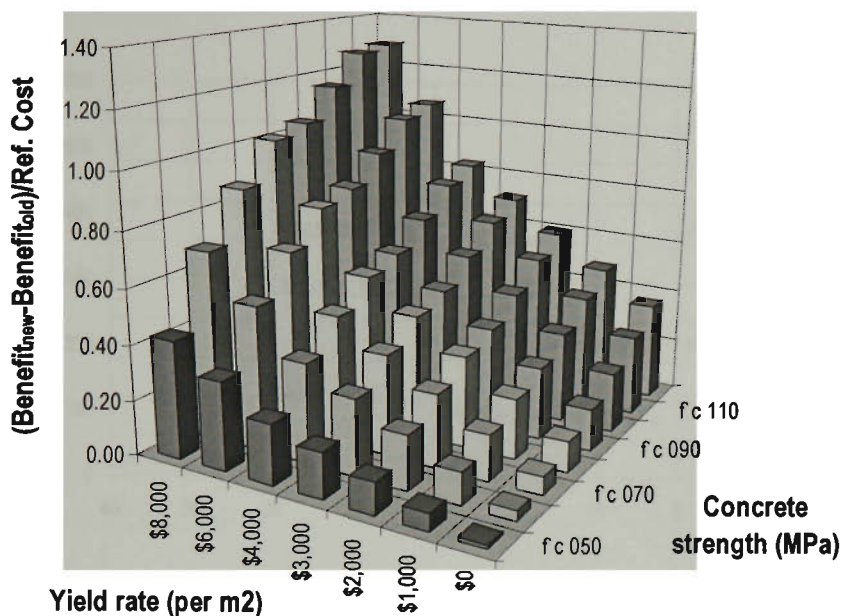


Fig. 7.10 Additional cost-benefits due to reduced seismic loads

## 7.6 STRENGTH AND DUCTILITY

The strength design for the coupled "C" shape core walls are carried out using 120 MPa concrete strength. The sectional dimensions and the corresponding supported floors are given in Table 7.1. For comparison purposes, dimensions of 40 MPa concrete sections are also given.

Table 7.1 Dimensions of designed cross sections

Supported floors	40 MPa concrete		Supported floors	120 MPa concrete	
	Flange thickness	Web thickness		Flange thickness	Web thickness
23rd - 40th	0.156	0.159	21st - 40th	0.153	0.156
16th - 22nd	0.384	0.396	14th - 20th	0.311	0.295
08th - 15th	0.590	0.581	07th - 13th	0.433	0.417
01st - 07th	0.799	0.781	01st - 06th	0.557	0.547

The design forces in the direction of coupling action are illustrated in Fig. 7.11. Also shown in the figure are the elastic response moments, which are taken as  $\mu/K$  times the inelastic response moments. Fig. 7.12 illustrates the design forces and the section capacity diagrams for the four cross sections. The section capacities in Fig. 7.12 are calculated using a minimum reinforcement steel content of 0.4%. It can be seen from the figure that all design forces are within the section capacity envelopes.

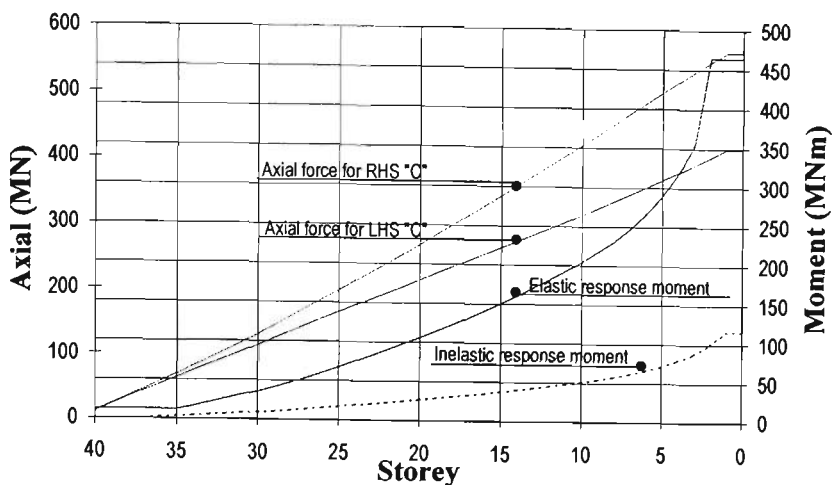
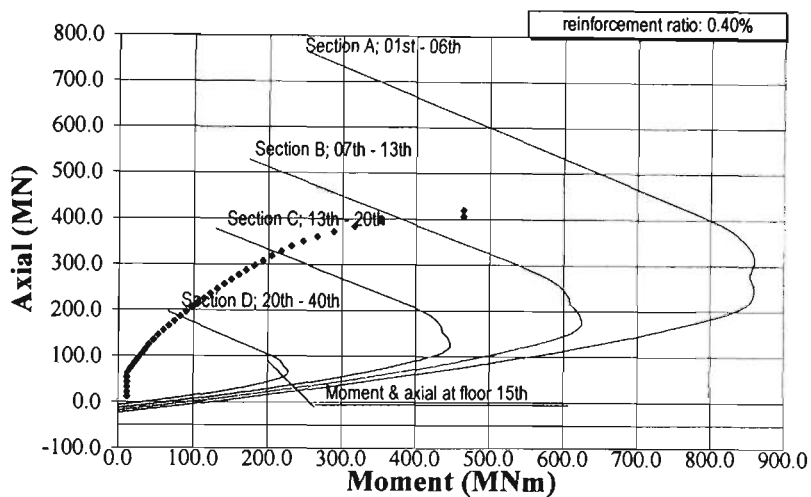
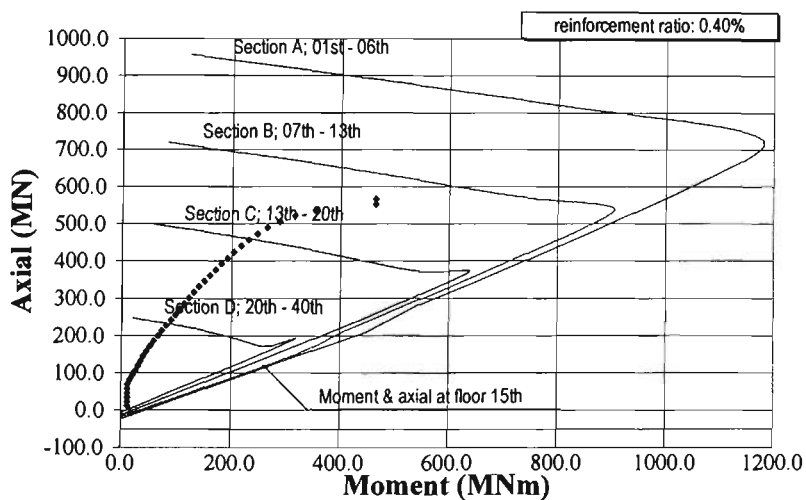


Fig. 7.11 Design forces



(a)



(b)

Fig. 7.12 Flexural-axial strength design in coupling action direction

(a) Left-hand-side (LHS) wall; (b) Right-hand-side (RHS) wall

In the direction where both walls act as cantilevers, the flexural-axial capacities of the wall sections also exceed the elastic response forces as shown in Fig. 7.13. It is concluded that the flexural-axial strength does not govern the design of these coupled "C" shape core walls.

Shear strength is assumed to be provided by the walls parallel to the loading only. Four critical sections are checked for the shear strength, each above the foundation level and the three transition levels, and are summarised in Table 7.2. It is observed that in the regions outside the plastic hinge, the shear contribution of the concrete alone exceeds the design shear forces. At the plastic hinge, the shear reinforcement is 0.4% which is greater than the minimum requirement.

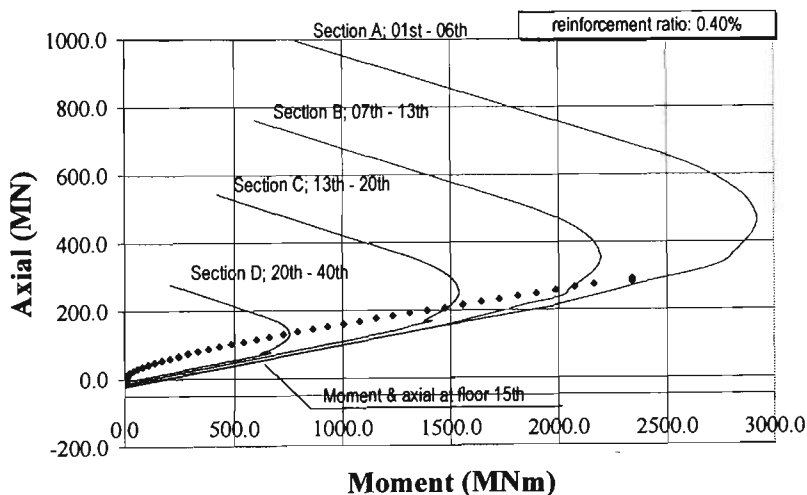


Fig. 7.13 Flexural-axial strength design in cantilever action direction

Table 7.2 Design for shear strength

Floor	$V, w$ (MN)	$\phi \cdot V_c$ (MN)	$\phi \cdot V_s$ (MN) with reinforcement ratio	
Level 21, above 3rd transition	17	17	1	0.20%
Level 14, above 2nd transition	21	27	2	0.20%
Level 07, above 1st transition	23	36	3	0.20%
Plastic hinge at level 1	23	15	8	0.40%

Since the walls are capable of sustaining the elastic response moments, they are expected to respond in the elastic range, and hence no special consideration with regard to the ductility of the wall is required.

## 7.7 CONCLUDING REMARKS

In this chapter, the volumetric optimisation and the cost analysis for the coupled "C" shape core wall are carried out. As for the rectangular shape walls discussed in Chapter 6, significant cost-benefits are also observed for the coupled "C" shape walls. Similar conclusions can also be drawn when two concrete strengths are used in the walls, in which 80% of the maximum benefit is achieved by using HSC up to the mid-height of the wall.

The strength checks conclude that the "C" walls with the minimum requirement for both longitudinal and transversal reinforcements perform satisfactorily in resisting the design forces from the elastic response. Consequently, the walls do not need to be designed for ductility performance.

In the next chapter, a case study for a model building will be presented. This study shall demonstrate the efficiency of the developed procedures and the cost-benefits resulting from the use of HSC.

## CHAPTER EIGHT

---

### A CASE STUDY

Chapters 6 and 7 presented the economic benefit of utilising high-strength concrete (HSC) in two and three-dimensional walls, respectively. The benefits associated with extra floor space gain are significant, particularly for buildings attracting high rental income. Based on the developed procedures outlined in Chapter 5, a cost study of a model building similar to a building in Jakarta, Indonesia, is carried out in this chapter.

#### 8.1 MODEL BUILDING

A 30-storey high concrete building structure with an inter-storey height of 3.2 m, consisting of a pair of coupled 'C' shape central core walls and 8 'L' shape wing walls is analysed. The plan is illustrated in Fig. 8.1 The structural model comprises 660 wall elements and 60 beam elements representing the header beams connecting the two "C" shape walls. The walls are designed to resist the total lateral loads, hence the 20 columns are not incorporated in the structural analysis. The three-dimensional computer model of the structure is shown in Fig. 8.2. A uniform concrete strength of 40 MPa is used for all elements. The wall thickness is 400, 350, and 300 mm with the corresponding transitions occurring at 11<sup>th</sup> and 21<sup>st</sup> and the beam is 400 mm wide by 900 mm deep.

The seismic loads are based on the contribution of wall mass and floor mass over an area of 1200 m<sup>2</sup>. The seismic coefficient is taken as 0.025, resulting in a total base shear of 8833 kN. The distribution of the base shear over the height of the building following Eq. (3.4) results in a triangular shape loading. From the structural analysis,

the total drifts in X-direction and Y-direction, respectively, are 258 mm and 267 mm; and the maximum inter-storey drift ratios are found to be 0.356% and 0.375% for X-direction and Y-direction respectively.

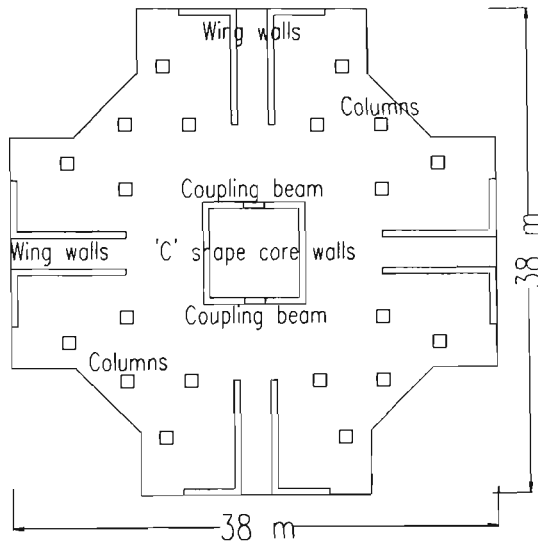


Fig. 8.1 30-storey model building

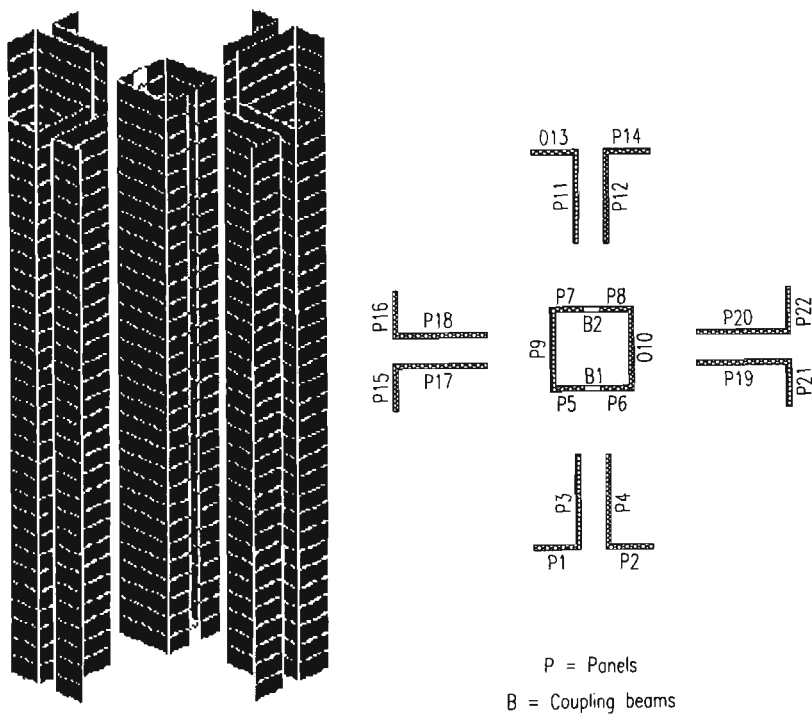


Fig. 8.2 Computer model

## 8.2 COST ANALYSIS

Chapters 6 and 7 concluded that the additional cost-benefits from increasing the number of transitions and / or using HSC beyond the mid-height of the building are minimal. Based on this observation, this cost analysis adopts two transitions in wall thickness and limited the use of HSC to the lower half of the building.

### 8.2.1 CONCRETE VOLUMES AT VARIOUS CONCRETE STRENGTHS

The optimum concrete volumes for the cost comparison study are calculated with two iterations. Fig 8.3 shows the resulting thicknesses and transition positions for all the elements using 40 MPa concrete strength. By adopting a minimum wall thickness of 150 mm for fire rating purposes, the concrete volume reduces by 21% compared to the initial model, demonstrating the significance of the optimisation technique. Reanalysing with the optimum thicknesses using ETABS results in total drifts of 261 mm and 260 mm in the X and Y-direction, respectively.

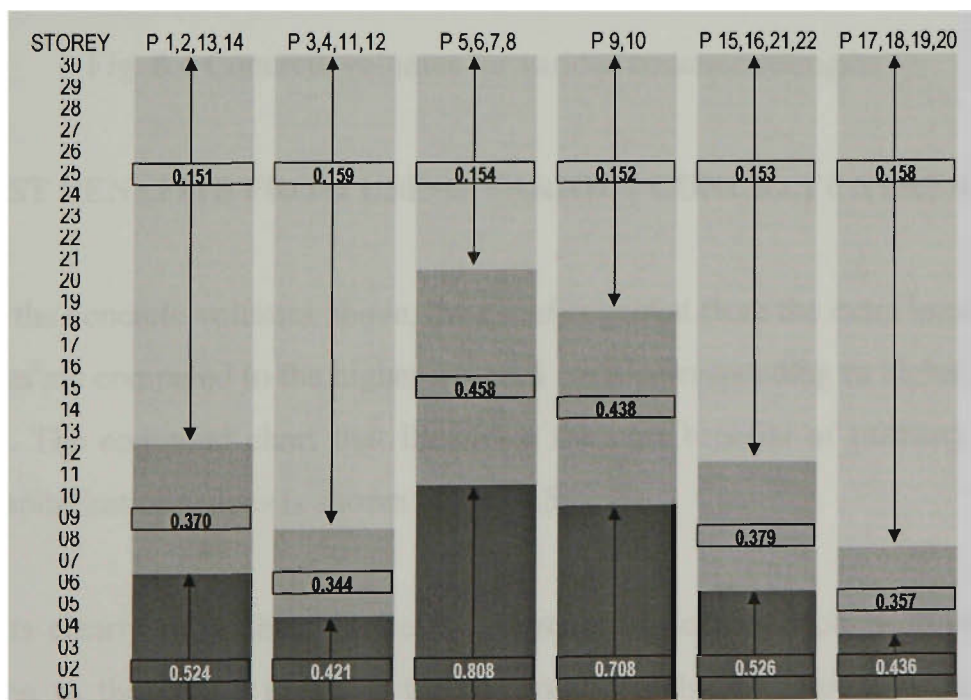


**Fig. 8.3** Optimum thicknesses and transition positions

The resulting concrete volumes for other concrete strengths are illustrated in Fig. 8.4. It is observed that the amount of concrete volume reduction is less than that for the model wall presented in the previous two chapters. The amount of volume reduction with a 120 MPa concrete is 25%, while the reduction for the “C” shape core wall outlined in Chapter 7 is in the order of 33%. The primary reason for the less effectiveness of utilising HSC in this building is the presence of a large number of lateral load resisting walls. As a consequence, a significant portion of the wall elements is governed by the minimum wall thickness criteria.

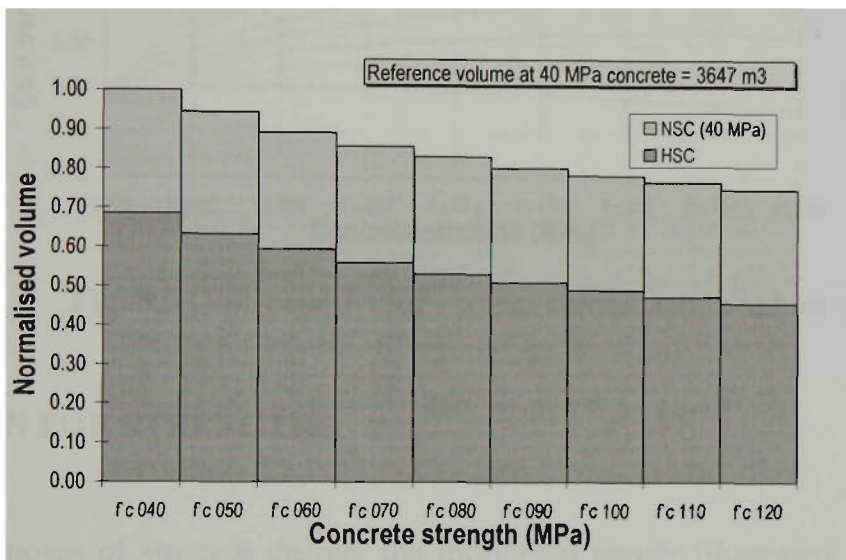


**Fig. 8.4** Concrete volumes for various concrete strengths

### 8.2.2 COST BENEFITS FROM USING VARIOUS CONCRETE STRENGTHS

Based on the concrete volumes above, the benefits gained from the extra lettable floor space areas are compared to the higher material costs corresponding to higher strength concretes. The compiled chart that illustrates the cost benefits of utilising HSC at various capitalisation values is shown in Fig. 8.5.

The results clearly show that despite the decrease of concrete volume reduction in comparison to the values given in the previous models in Chapters 6 and 7, the benefits gained from the use of HSC at high capitalisation values are still quite significant. For example, taking the capitalisation value as \$6,000 per square meter, utilising an 80 MPa concrete in the coupled “C” walls in Chapter 7 results in a cost-

benefit of 1.6 (Appendix B) of the reference cost, which is taken as the material cost of wall with 40 MPa concrete. In the case study building, cost-benefit is in the order of 1.7 of the reference cost.

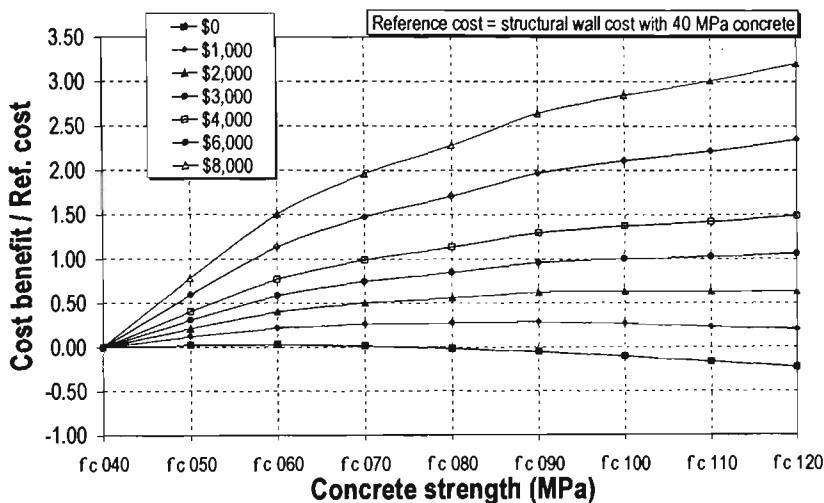


Fig. 8.5 Cost-benefits for various capitalisation values

### 8.3 DESIGN FOR STRENGTHS

For the purposes of strength design, the individual panels illustrated in Fig. 8.2 are assembled to form “L” and “C” shape walls. The identification of the walls is shown in Fig. 8.6.

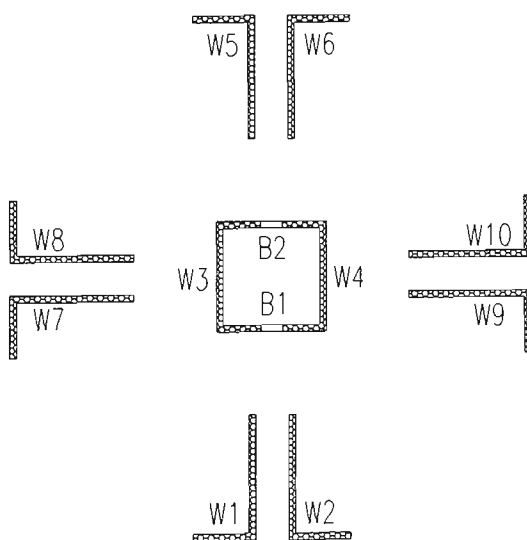
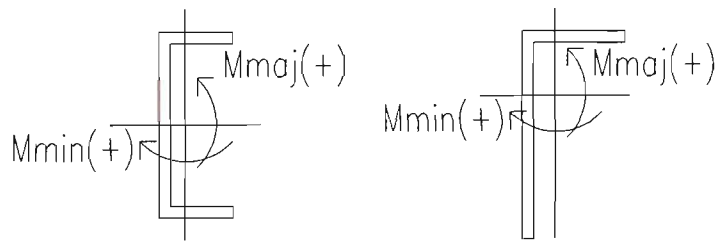


Fig. 8.6 Wall identifications

It is understood that a structure shall be designed for the lateral loading in both orthogonal and the opposite directions. Recognising this issue, symmetrical walls shall also have identical reinforcements, i.e. the reinforcement of W1, W2, W5 and W6 shall be the same. As a consequence, a representative wall shall be designed for the maximum forces and moments from both orthogonal and the opposite directions. Considering the building symmetry, the number of walls to designed are reduced to three, in which walls W7, W8, W9 and W10 are also identical as well as walls W3 and W4.

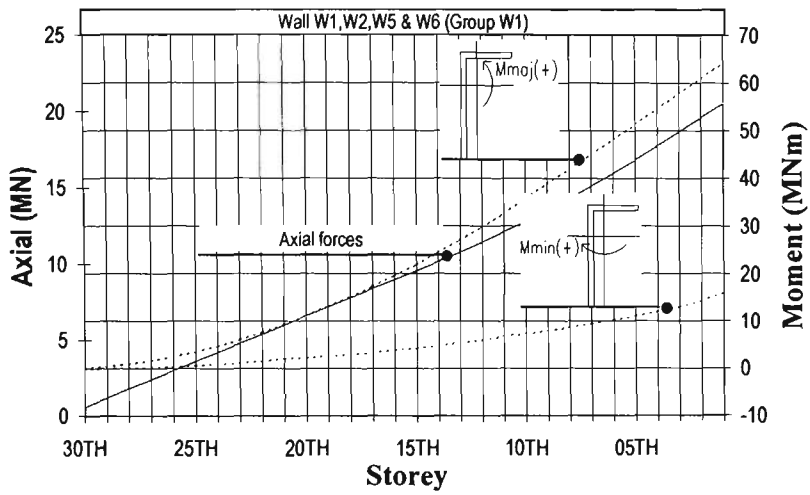
To identify the acting moments, a convention is made in regard to the signs and directions moments as shown in Fig. 8.7. The moment is positive if at a particular direction it causes compression in the flange.



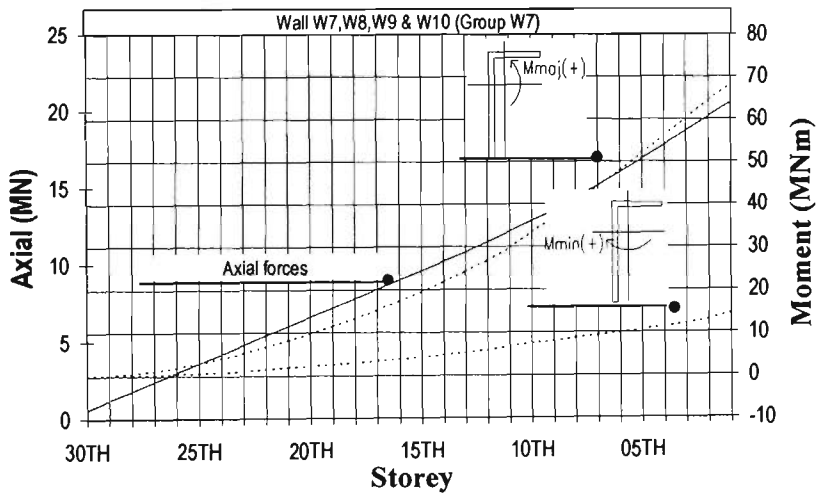
**Fig. 8.7** Sign conventions for positive moments

The design moments for the representative walls, W1, W3 and W9, are summarised in Fig. 8.8. Due to the building symmetry, the positive and the negative moments for all the representative walls are equal in magnitude. In Fig. 8.8, only the positive moments are shown.

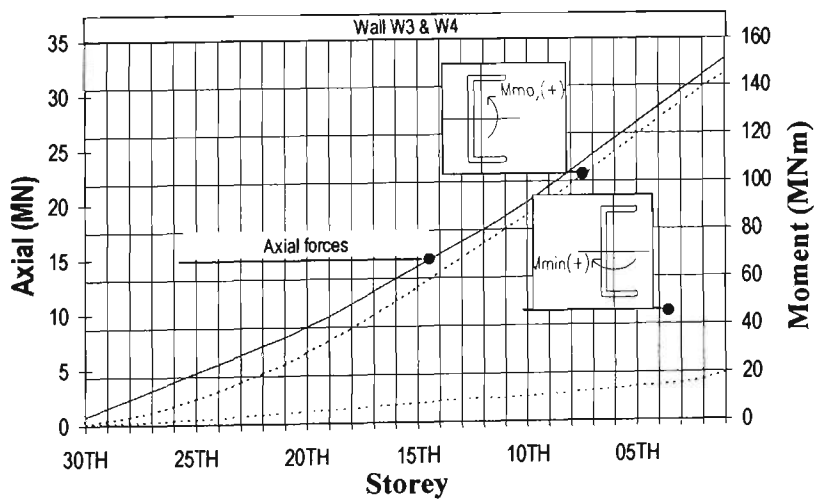
For practical reasons, strength design is checked at critical sections, which are taken at levels above either the thickness transitions or the concrete strength transitions. These sections, for the three wall types, are summarised in Fig. 8.9. The numbers of critical sections to be designed for strength for the wall type W1 and W3 are six and for W9 is four.



(a)



(b)



(c)

Fig. 8.8 Elastic moments.

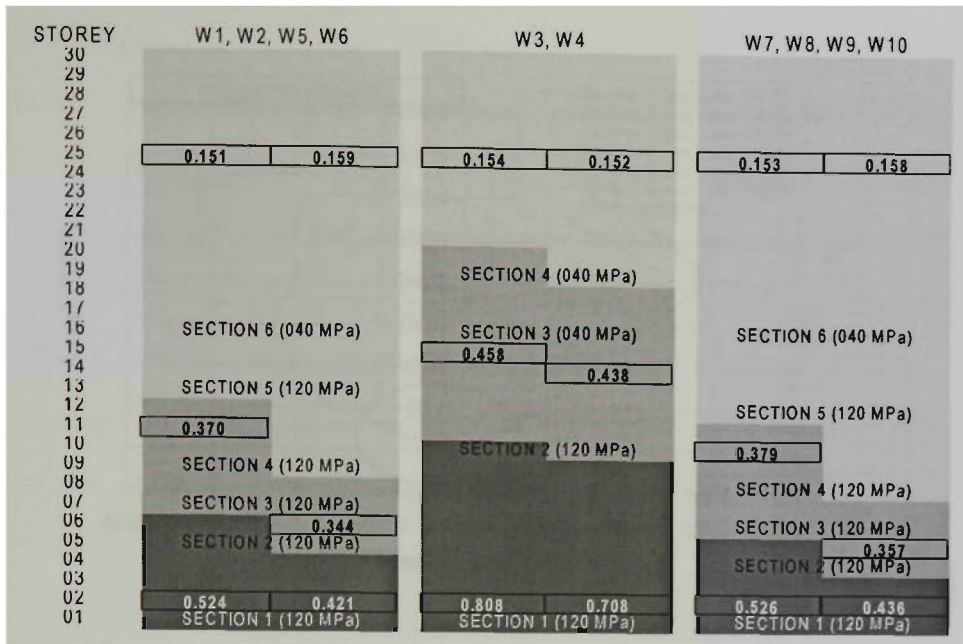


**Fig. 8.9** Critical sections for strength design

Due to the similarity in the design forces and cross sectional geometry between the identical walls W1, W2, W5, W6 and walls W7, W8, W9, W10, the strength design for the walls W7, W8, W9 and W10 are not carried out.

The flexural-axial capacities of the wall W1 in the major direction are shown in Fig. 8.10. Also shown are the design forces associated with the moment envelop developed according to the procedures described in Section 3.2.3. Fig. 8.10(b) shows that the section capacities of the wall are notably larger than the design forces obtained from the elastic analysis. However, in the seismic design it is expected that the critical section at the base develops its overstrength moment, hence the wall sections should be designed for the envelop moments instead.

Fig. 8.10(b) shows that the modified moments, corresponding the moment envelop, become larger than the section capacities. Hence, the reinforcement ratio for the sections above the plastic hinge shall be increased. Fig. 8.10(c) shows the increased section capacities and the corresponding reinforcement ratios. It should be noticed that the reinforcement ratio at upper storeys might be as high as 1.35%.

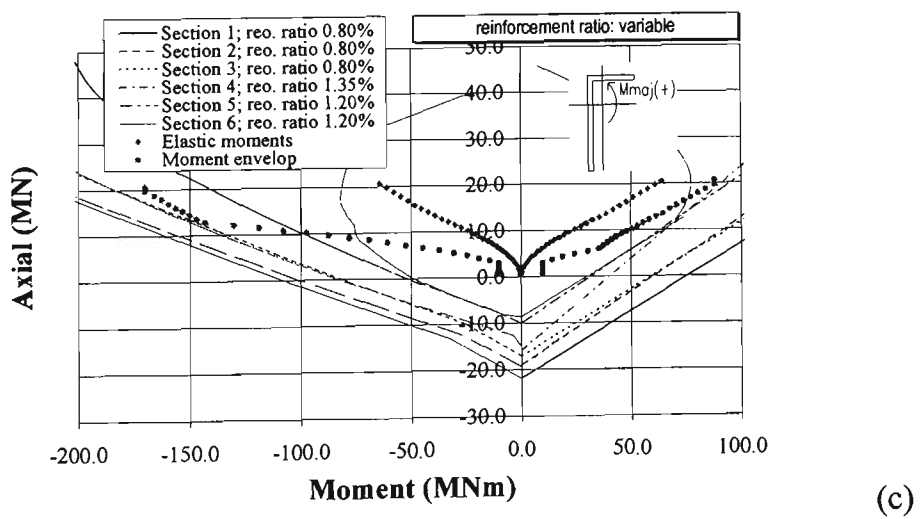
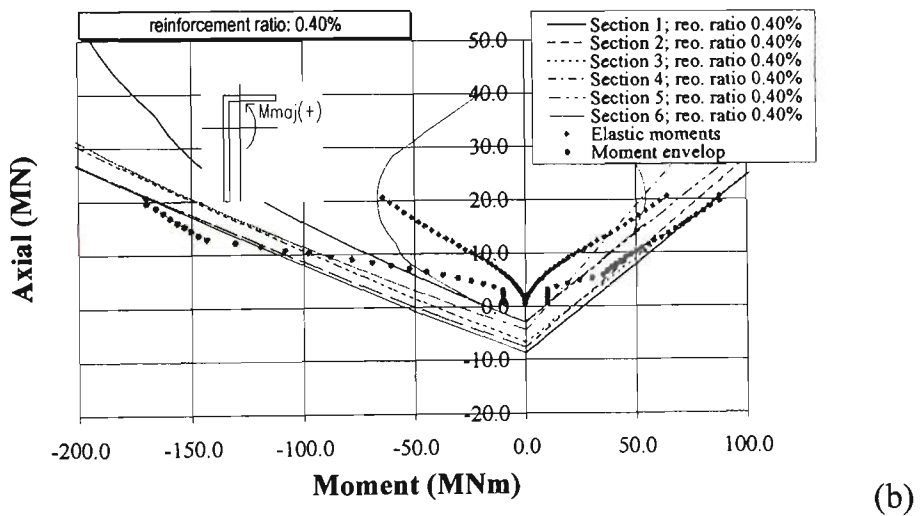
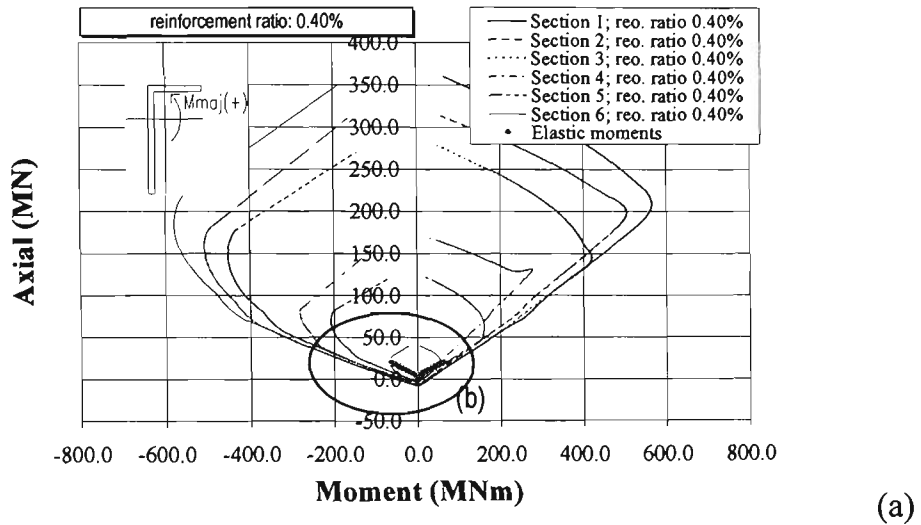
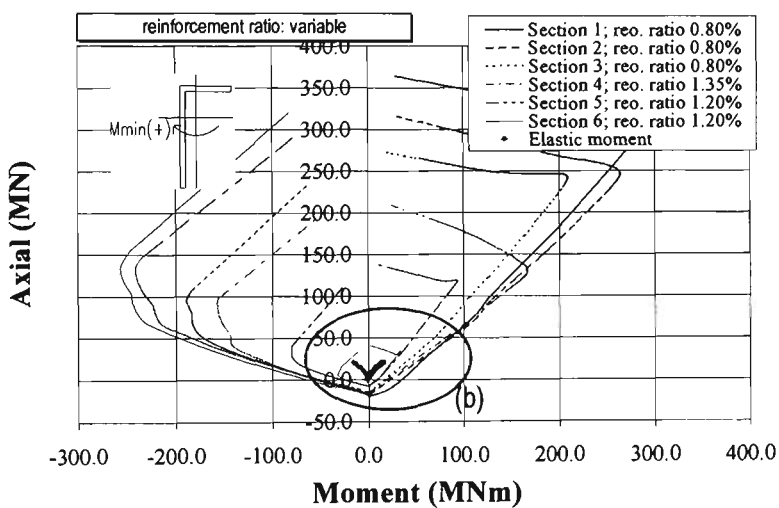
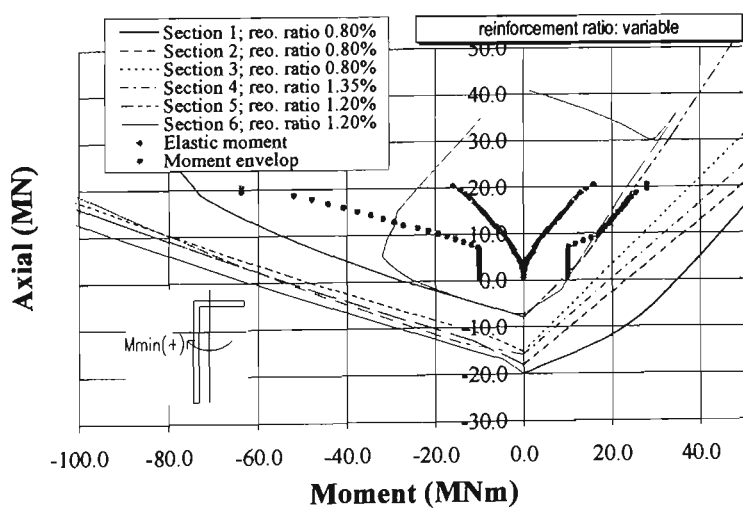


Fig. 8.10 Strength design for wall W1major direction

The design strength in the minor direction is carried out using the reinforcement contents given in Fig. 8.10(c). The moment at the base from the elastic analysis is 16 MNm. However, with the reinforcement ratio of 0.4%, the overstrength moments are +30 and -92 MNm. It should be noticed that overstrength of negative moment (-92 MNm) exceeds the moment due to the elastic response loading ( $\mu/Kx16 = 64$  MNm); therefore this elastic response moment should be used instead in developing the moment envelop. It is shown in Fig. 8.11 that the available section capacities exceed the magnified moments corresponding to the moment envelops.



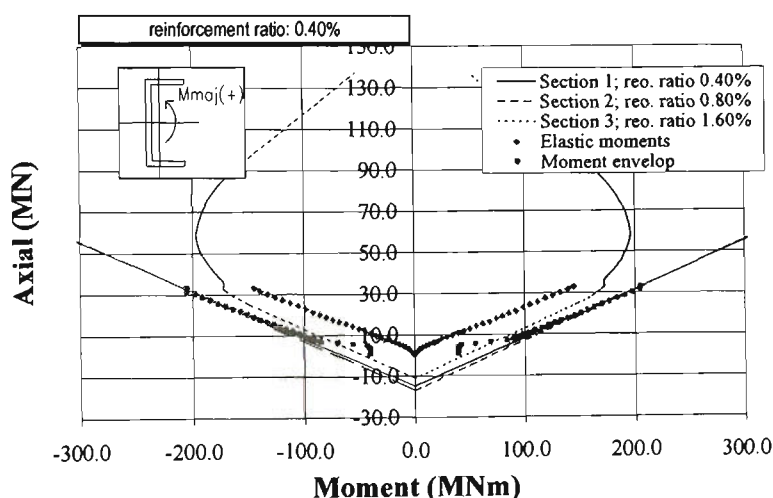
(a)



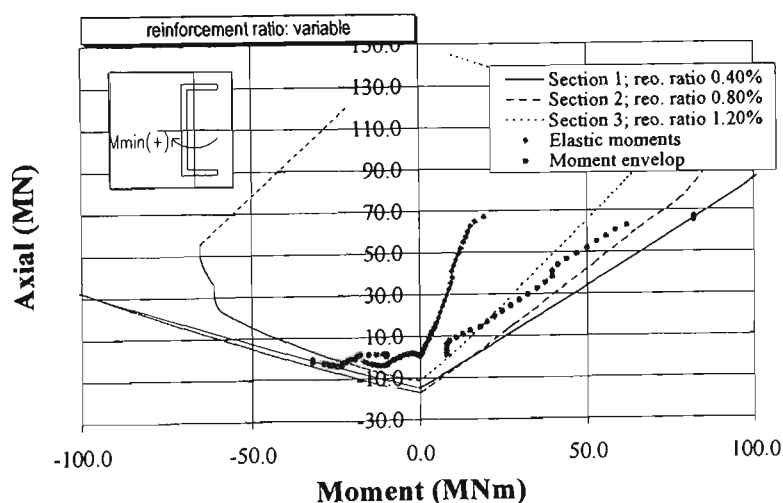
(b)

**Fig. 8.11** Strength design for wall W1 in minor direction

The design of the coupled “C” shape walls is carried similarly. The results are shown in Fig. 8.12(a) and Fig. 8.12(b) for wall bending in major and minor direction, respectively. The design forces for these walls are shown in Fig. 8.8(c). The required reinforcement ratios carry the design loads are found to be 0.4%, 0.8% and 1.60% for the section 1, 2 and 3, respectively.



(a)



(b)

**Fig. 8.12** Strength design for walls W3 and W4

The design for the shear strength is tabulated in Table 8.1. It is concluded that the shear strength contributed by the minimum reinforcing steel (0.5% of longitudinal steel) and/or concrete exceeds the design shear, either calculated according to the shear envelop or the elastic response shear.

**Table 8.1** Design for shear strength

Walls W1, W2, W5 & W6 - Major direction						Walls W1, W2, W5 & W6 - Minor direction					
Floors	$V_w$ (MN)	Thickness	$\phi \cdot V_c$ (MN)	reo. ratio	$\phi \cdot V_s$ (MN)	Floors	$V_w$ (MN)	Thickness	$\phi \cdot V_c$ (MN)	reo. ratio	$\phi \cdot V_s$ (MN)
16 - 30	2.82	159	3.19	0.40%	1.56	16 - 30	0.57	151	2.31	0.40%	0.72
09 - 15	3.87	159	5.17	0.40%	1.56	13 - 15	0.68	151	3.20	0.40%	0.72
05 - 08	3.94	344	9.09	0.40%	3.37	07 - 12	0.94	370	5.91	0.40%	1.77
01 - 04	3.92	421	3.60	0.40%	4.12	01 - 06	2.11	524	2.84	0.40%	2.51

Walls W3 & W4 - Major direction						Walls W3 & W4 - Minor direction					
Floors	$V_w$ (MN)	Thickness	$\phi \cdot V_c$ (MN)	reo. ratio	$\phi \cdot V_s$ (MN)	Floors	$V_w$ (MN)	Thickness	$\phi \cdot V_c$ (MN)	reo. ratio	$\phi \cdot V_s$ (MN)
19 - 30	1.90	152	3.63	0.80%	2.65	21 - 30	4.37	154	2.41	0.80%	2.01
16 - 18	1.90	152	3.63	0.40%	1.32	16 - 20	4.37	154	3.29	0.50%	1.26
09 - 15	2.33	428	10.52	0.40%	3.73	10 - 15	5.34	458	9.16	0.40%	2.99
01 - 08	5.71	708	5.58	0.20%	3.08	01 - 09	5.40	808	5.17	0.20%	2.64

## 8.4 CONCLUDING REMARKS

This chapter presents a cost analysis for a model building similar to a building built in Jakarta. The initial structural model with a 40 MPa concrete strength is optimised using the techniques outlined in Chapters 3 and 5, resulting in a significant concrete volume reduction. A cost comparison is made for various concrete strengths and the results showed a cost saving for using higher strength concretes. It was also shown in the design for the strength that the required strengths could be provided without any special concern in regard to the longitudinal and transverse steel reinforcements.

Concluding the thesis, the results of these research investigations are summarised in next chapter. The limitations of this research project and recommendations for further research are given.

## **CHAPTER NINE**

---

### **CONCLUSIONS AND RECOMMENDATIONS**

This thesis examines the use of high-strength concrete (HSC) in structural walls of tall buildings. The primary concern of the investigation is the cost-benefits resulting from the HSC applications. The findings of the research are concluded in this chapter. It is understood that due to the complexity of the problems, assumptions would need to be made. These assumptions in one or the other way might not produce the best solutions for all design problems. These limitations and the further recommendations for research are given.

#### **9.1 CONCLUSIONS**

Until recently, the primary material for the structural system of tall buildings has been the structural steel. The commercial availability of concrete of an increasing strength has facilitated the evolution of concrete into a viable structural material for tall buildings. Since the research of HSC began in 1970s, a substantial amount of research work has been reported. HSC, like most other state-of-the-art materials, commands a premium price. However, in some cases, the benefits are well worth the additional costs of the raw materials.

A lower cost per strength or stiffness and a greater strength per unit weight make HSC applications more attractive. The most tenable advantage of HSC is the reduction in the vertical member sizes that it creates, providing more rental floor space, which is a significant factor in commercial buildings.

A significant number of reports, as early as 1975 (Schmidt and Hoffman), have been presented. Among the significant ones are the works of Martin (1989). He presented the economic evaluations for a 55-storey core walls building in Melbourne. Increasing the concrete strength from 40 MPa to 60 MPa results in a cost-benefit of about \$100,000 per floor for the client.

This research study investigated the economic aspects of HSC application in structural walls, in the form of cantilever and coupled walls. The primary design loadings are the material dead loads, the functional live loads and the horizontal earthquake loads. Structures are designed for the serviceability limit states in terms of inter-storey drift, the strength limit states and the ductility requirement corresponding to the inelastic seismic response loading.

At the early stage of design process, the engineers are required to determine the member cross sectional sizes. An optimisation technique, which is based on the unit load method, provides an efficient and systematic method for finding the optimum sizing of the structural members for a single displacement constraint problem. It is concluded that, for a given structure, the structural material or volume is minimum if the material in the structure is distributed such that each member has the same strain energy density.

The above optimisation technique results in continuous changes in member sizing and causes unwarranted construction complexity. Therefore, an optimisation method that links several members of the same length to a single representative design variable was developed. This developed method provides simple mathematical formulations for the calculation of optimum member sizes for a given number of sectional transitions. This method allows the material strength to be modified without any additional expense. It was shown that the calculation process could be easily carried out with a spreadsheet program.

The member-linking method requires that the locations of the sectional size transition be known. Often, inadequate information in the optimisation formulas causes difficulty in selecting suitable transition locations. An approximate numerical method for finding the optimum member sizing for a structure with non-predetermined transition locations was proposed. Although this method has successfully calculated the optimum member sizes as well as the optimum transition locations, its numerical complexity increases significantly for each additional transition. With the current mathematical computer software, this method has failed to calculate a structure with two sectional geometry transitions.

For the purpose of the study, a rectangular shape cantilever and coupled wall (Chapter 6), and a three-dimensional core wall comprising two “C” shape walls and header beams coupling the two walls (Chapter 7) were selected for the investigations. The cost-benefits of using HSC in a model building are demonstrated in a case study in Chapter 8. Similar trends in the concrete volume reduction and the cost-benefit gains associated with the use of HSC are observed and concluded as follows.

The results of the concrete volume comparisons for various concrete strengths with differing number of wall thickness transitions shows that significant volume reduction can be obtained by increasing the concrete strength. However, the amount of material saving for introducing each additional thickness transition is insignificant. Moreover, the additional cost associated with the construction delay for each transition introduced may well exceed the material cost savings. Therefore, increasing concrete strength is an effective means of minimising the concrete volume.

A cost analysis study carried using the above concrete volumes showed that on the basis of the construction cost only, ignoring the capitalisation values, the cost-benefits of using low concrete strengths diminishes. Despite the reduction in the concrete volume, the construction cost of wall with HSC increases. The benefit of using HSC only becomes apparent if the capitalisation value of lettable floor space is taken into consideration.

With the increasing cost of quality control corresponding to higher concrete strength and the minimum wall thickness governing criteria at the upper storeys, the use of lower concrete strengths at higher storey levels has an attractive objective of providing a more cost efficient alternative. The results of the investigations showed that, without taking into account the additional cost of quality control, up to 80% cost-benefit could be attained by extending the use of HSC only up to the mid-height of the wall.

Furthermore, the thinner sections of HSC walls attract smaller inertial loads, which is an advantage for seismic resistant structures. Results show that the lower seismic loading increases the cost-benefits with increasing concrete strength and capitalisation yield rate.

The strength design carried out concluded that the optimum wall sections that satisfy the serviceability limit states in terms of deflection criteria possess adequate strength and ductility with reinforcement content within the acceptable values. In the cases of coupled walls, it was found that, due to the efficiency of the coupled wall systems, they are capable to respond elastically when subjected to the design seismic loads. It was also found that the plastic hinges that are expected to develop at the base sections possess adequate ductility capacity and require no additional confining steel.

In conclusion, the use of HSC in structural wall of tall buildings provides significant cost-benefits to the building owners. The benefits become substantial in the cases of buildings attracting high financial returns. Moreover, it is not necessary to use HSC throughout the wall height. The use of HSC at the third of the upper storeys shows no additional cost-benefits. Furthermore, the demand for the use of HSC from building owners could serve as a catalyst for HSC developments and would eventually benefit many areas in the construction industries.

## 9.2 LIMITATIONS OF THIS RESEARCH

It is realised that the subjects of this research investigation are complex. In order to reduce the complexity of the research problems, assumptions were made and design criteria were simplified. As a consequence, this research implies limitations, which need to be understood in order to successfully use the proposed methodology and the design recommendations. Significant efforts have been taken to minimise the design limitations or to maximise the generality of the proposed methods and techniques, subsequently the research results.

The optimisation techniques and the developed member-link method were derived for single-displacement constraint problems. In tall building design, the inter-storey drifts more likely control the governing serviceability criteria. Although this study has made an effort to convert a maximum inter-storey drift into a maximum deflection at the top, the number of design criteria being considered are still limited to one single inter-storey drift. To achieve a more optimum solution, the differences among the storey drift should be also minimised.

The member-linking method requires the locations of wall thickness transition to be determined. The lack of information in the optimisation formulas for selecting the most optimum thickness transitions reduces the capability of the developed method. An approximate numerical method was then derived, however this method has only successfully solved a single transition problem. A better optimisation technique will need to be sought if more optimal solutions are required.

Cost analysis involves a large number of factors. Examination of all these factors in a single cost analysis can be very complex. Normally, an economical design of a building requires an optimisation with regard to material cost, construction time and maximisation of rentable floor space. A typical construction cost of a structural wall comprises concrete, reinforcing steel and formwork operation costs. In the cost-analysis carried out, a single value was adopted for each concrete strength, steel and

formwork cost. This therefore limits the findings to a single market condition. The cost-benefit associated with construction time was not included in the analysis.

### **9.3 RECOMMENDATIONS FOR FURTHER RESEARCH**

In addition to the work carried out in this study, recommendations for further research include the following.

1. The member-linking method was derived for a single displacement constraint problem. Moreover, this method required the locations of sectional size transition to be specified. An area for future research should include a study of finding the optimum transition locations for the wall thickness and concrete strength for multi-constraint problem in term of inter-storey drifts.
2. The cost analysis carried out assumed that the component cost of reinforcing steel is invariable with regard to concrete strength. Future research should incorporate both longitudinal and transversal reinforcement cost as design parameters.
3. Only single values were adopted for the material costs in the cost analysis and the costs associated with construction time were also not included. Future research should include costs associated with construction time and cover various values of material costs.
4. The lateral load resisting systems considered were the structural walls. The use of HSC in other structural systems, such as frame structures, wall-frame structures, etc. should also be of particular interests for future research.
5. This study assumed that the structural design was governed by the serviceability criteria. An optimal use of HSC in the strength governing structures can be a good topic for future research.

## REFERENCES

- ACI Committee 318. (1995). (a) *Building code requirements for structural concrete* (ACI 318-95); (b) *Commentary on Building code requirements for structural concrete* (ACI 318R-95). Farmington Hills, MI: American Concrete Institute.
- ACI Committee 363. (1992). *State-of-the-art report on high-strength concrete*. Detroit: American Concrete Institute.
- ATC 3-06. (1978). *Tentative provisions for the development of seismic regulations for buildings*, NBS Special Publication 510. Washington DC.
- Azizinamini, A., Paultre, P., & Saatcioglu, M. (1994) High-strength concrete columns: State of the knowledge. *Proceedings: Structures Congress 94*. (pp 445-50). New York: American Society of Civil Engineers.
- Baker, W.F. (1990). Sizing techniques for lateral systems in multi-story steel buildings. *Proceedings: Fourth World Congress on Tall Buildings: 2000 and Beyond* (pp.857-68). Hongkong: Council on Tall Buildings and Urban Habitat.
- Beca Carter Hollings & Ferner. (1979). *Indonesian earthquake study*. Wellington.
- Bong, B.G. (1997). *RCDESIGN97 version 1.1*.
- Bong, B.G., Hira, A. & Mendis, P. (1997). Optimal application of high-strength concrete in cantilever structural walls. *Proceeding: Australian Conference on Mechanics and Structures* (pp 123-31). Nederland: Balkema.
- Burnett, I. (1989). High-strength concrete in Melbourne Australia. *Concrete International*, 11, 4, 17-25.
- Carrasquillo, R.L., Nilson, A.H., & Slate, F.O. (1981) Properties of high-strength concrete subject to short-term loads. *ACI Journal*, 78, 3, 171-8.
- Chan, S.Y.N., & Anson, M. (1994). High-strength concrete: the Hongkong experience. *Magazine of Concrete Research*, 46, 169, 235-36.
- CEB. (1993). *CEB-FIP Model Code 1990*. London: Thomas Telford.

- CEB-FIP (1995) *High performance concrete: Recommended extensions to the Model Code 90 - Research needs*. Lausanne: Comite Euro-International du Beton.
- CEN Technical Committee 250/SC8. (1994). *Eurocode 8: Earthquake resistant design of structures* (ENV 1998-1-1). Berlin: CEN.
- Charney, F.A. (1991). The use of displacement participation factor in the optimization of wind drift controlled buildings. *Proceedings: Second Conference on Tall Buildings in Seismic Regions* (pp.91-98). Los Angeles: Council on Tall Buildings and Urban Habitat.
- Charney, F. A. (1994). *DISPAR for ETABS version 5.4* [computer program & users manual]. Colorado: Advanced Structural Concept.
- Council on Tall Buildings and Urban Habitat (CTBUH) Group CB. (1978). *Structural design of tall concrete and masonry buildings*. New York : American Society of Civil Engineers.
- Council on Tall Buildings and Urban Habitat (CTBUH) Committee 3. (1995). *Structural systems for tall buildings: systems and concepts*. New York : McGraw-Hill.
- Departemen Pekerjaan Umum. (1987a). *SNI 1726-1989: Tata cara perencanaan ketahanan gempa untuk rumah and gedung*. Bandung: Yayasan LPMB
- Departemen Pekerjaan Umum. (1987b). *SNI 1727-1989: Tata cara perencanaan pembebanan untuk rumah and gedung*. Bandung: Yayasan LPMB
- Departemen Pekerjaan Umum. (1992). *SNI T-15-1991-03: Tata cara perhitungan struktur beton untuk bangunan gedung*. Bandung: Yayasan LPMB
- De Larrard, F., & Lacroix, R. (Eds.). (1996). *Proceedings: Fourth International Symposium on Utilization of High-Strength/High Performance Concrete*. Paris: Palais des Cong.
- FIP-CEB (1990) *High strength concrete: State-of-the-art report*. London: the Federation Internationale de la Precontrainte.
- Fragomeni, S., Mendis, P., & Grayson, W.R. (1994). Design of high strength concrete walls. *Proceedings: Australasian Structural Engineering Conference* (pp 465-69). Barton: Institution of Engineers Australia.
- Ghosh, S.K., & Saatcioglu, M. (1994). Ductility and seismic behaviour. In Shah, S.P., & Ahmad, S. H. (Eds.), *High performance concretes and applications*. (pp.237-312). Great Britain: Edward Arnold.

- Habibullah, A. (1989). *ETABS version 5.10* [computer program & users manual]. California: Computer & Structures, Inc.
- Hester, W.T. (Ed.). (1990). *Proceedings: Second International Symposium on Utilization of High-Strength Concrete*. Detroit: American Concrete Institute.
- Holand, I. (1987). High-strength concrete - A major research programme. *Proceedings: Utilization of High-Strength Concrete* (pp.135-48). Trondheim: Tapir Publisher.
- Holand, I., Helland, S., Jakobsen, B., & Lenschow, R. (Eds.). (1987). *Proceedings: Utilization of High-Strength Concrete*. Trondheim: Tapir Publisher.
- Holand, I. (1992). High-strength concrete: Main report for phase 1. *Research Report STF70 A92138*, Trondheim: SINTEF Structures & Concrete.
- Holand, I., & Sellevold, E. (Eds.). (1993). *Proceedings: Third International Symposium on Utilization of High-Strength Concrete*. Oslo: Norwegian Concrete Association.
- International Conference of Building Officials (ICBO). (1994). *Uniform Building Code*. California.
- Martin, O. (1989). Economical design of multi-storey concrete buildings. *Reinforced Concrete Digest*, RCD 9.
- Mohammad, H., Choon, T., Azman, T., & Tong, S. (1995). The Petronas Towers: The tallest building in the world. *Proceedings: Fifth World Congress* (pp.321-57). Bethlehem: Council on Tall Building & Urban Habitat.
- Moreno, J., & Zils, J. (1985). Optimization of high-rise concrete buildings. In *Special Publication 97: Analysis and design of high-rise buildings* (pp.25-92). Detroit: American Concrete Institute.
- Morris, A.J. (Ed.). (1982). *Foundations of structural optimisation: A unified approach*. New York: Wiley.
- Muguruma, H., Nishiyama, M., Watanabe, F. & Tanaka, H. (1992). Ductile behaviour of HSC columns confined by high-strength transverse reinforcement. In *Special Publication* (pp 128-54). Detroit: American Concrete Institute.
- Nilson, A.H. (1987). High-strength concrete - An overview of Cornell Research. *Proceedings: Utilization of High-Strength Concrete* (pp.27-38). Trondheim: Tapir Publisher.

- Paks, M., & Hira, A. (1994). Design and construction of cores for tall buildings - Achieving TQM through multi-disciplinary approach. Paper presented at *Politechnika Slaska Construction Chair 40th Anniversary Conference*, Gliwice, Poland.
- Park, H.S. & Park, C.L. (1997). Drift control of high-rise buildings with unit load method. *The Structural Design of Tall Buildings*, 6, 23-35.
- Paulay, T. & Priestley, M.J.N. (1992). *Seismic design of reinforced concrete and masonry buildings*. New York: John Wiley & Sons, Inc.
- Pendyala, R., Kovacic, D., & Mendis, P. (1995). Ductility of high-strength concrete members - beams & columns. *Proceedings: Toward Better Concrete Structures* (pp 465-69). Barton: Institution of Engineers Australia.
- Russell, H.G. (Ed.). (1985). *Special Publication 87: High-strength concrete*. Detroit: American Concrete Institute.
- SANZ. (1992). *Code of practice for general structural design and design loadings for buildings* (NZS 4203). Wellington: Standard Association of New Zealand.
- SANZ. (1995). (a) *Code of practice for the design of concrete structures* (NZS 3101-Part 1); (b) *Commentary on Code of practice for the design of concrete structures* (NZS 3101-Part 2). Wellington: Standard Association of New Zealand.
- Schmidt, W., & Hoffman, E.S. (1975). 9000-psi concrete - Why? Why not? *Civil Engineering-ASCE*, 45, 5, 52-56.
- Shah, S.P. (1981). High-strength concrete: A workshop summary. *Concrete International*, 3, 5, 94-98.
- Shah, S.P., & Ahmad, S. H. (Eds.). (1994). *High performance concretes and applications*. Great Britain: Edward Arnold.
- Smith, G.J., & Rad, F.N. (1989). Economy advantages of high-strength concrete in column. *Concrete International*, 11, 4, 37-43.
- Straub. (1964). A history of civil engineering.
- Velivasakis, E. & DeScenza, R. (1983). Design optimization of lateral load resisting frameworks. *Proceedings: Eighth Conference on Electronic Computation* (pp.130-43). New York: American Society of Civil Engineers.
- Wada, A. (1991). Drift control method for structural design of tall buildings. *Proceedings: Second Conference on Tall Buildings in Seismic Regions* (pp.425-34). Los Angeles: Council on Tall Buildings and Urban Habitat.

Watanabe, F., Muguruma, H., Matzutani, T. & Sanda, D. (1987). Utilization of high strength concrete for reinforced concrete high-rise buildings in seismic area. *Proceedings: Utilization of High Strength Concrete* (pp 655-66). Trondheim: Tapir Publisher.

Xie, Y.M., & Steven, G.P. (1997). *Evolutionary structural optimisation for dynamic problems*. Berlin: Springer-Verlag.

Computer Cuts Column Costs. (1986). *Concrete Construction*, 31, 5, 478-480.

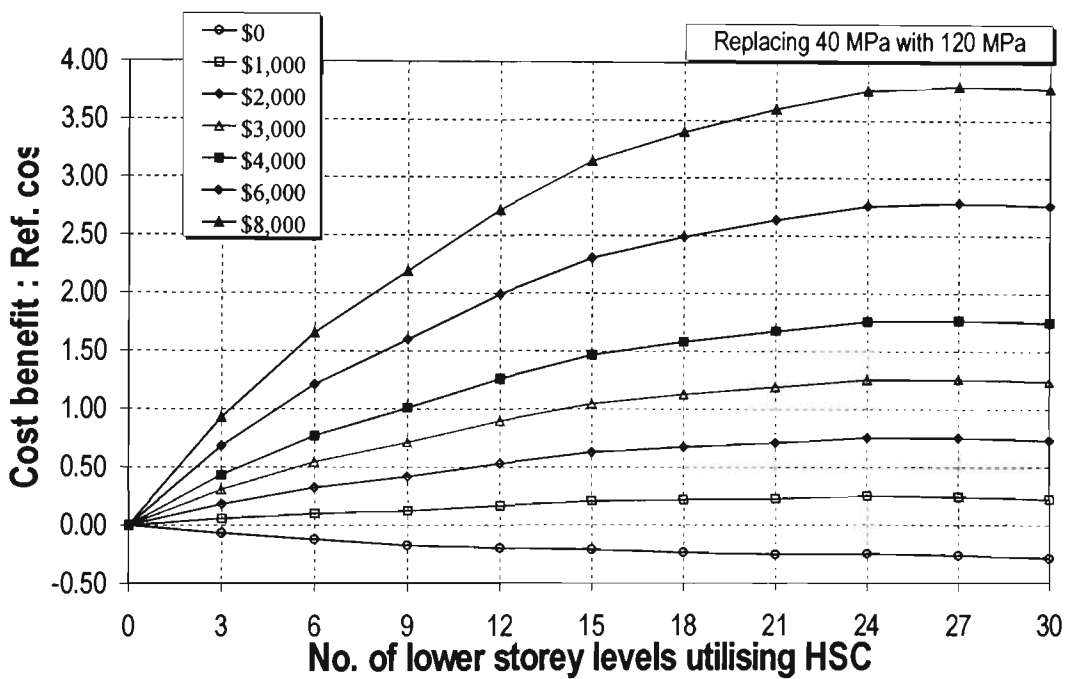
Current construction cost. (1997, June). *The Building Economist: The Journal of the Australian Institute of Quantity Surveyors*, p.36.

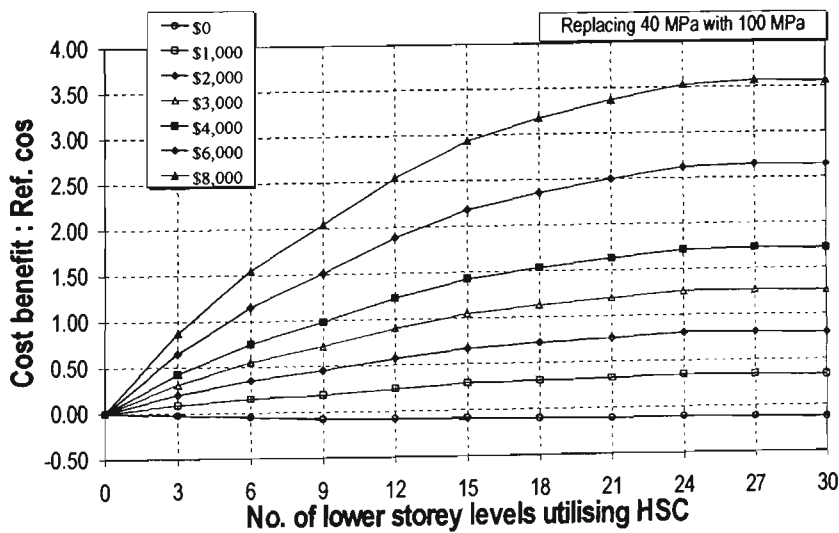
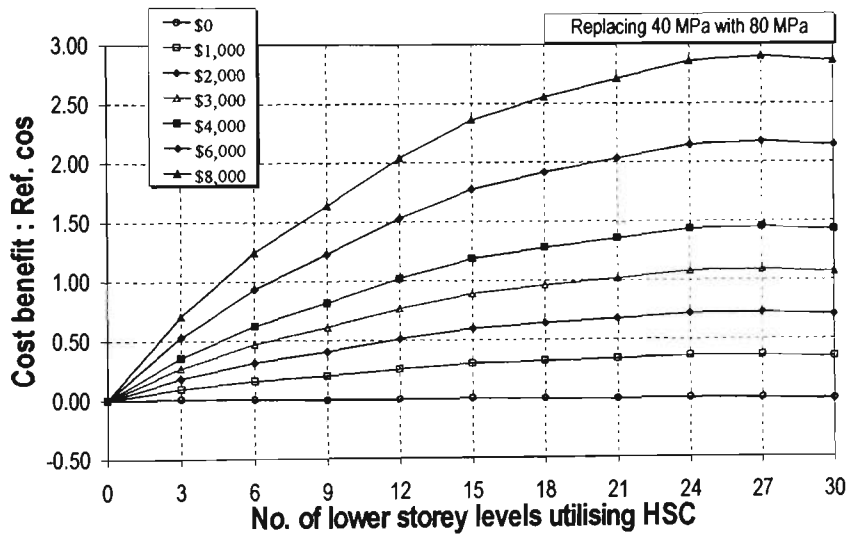
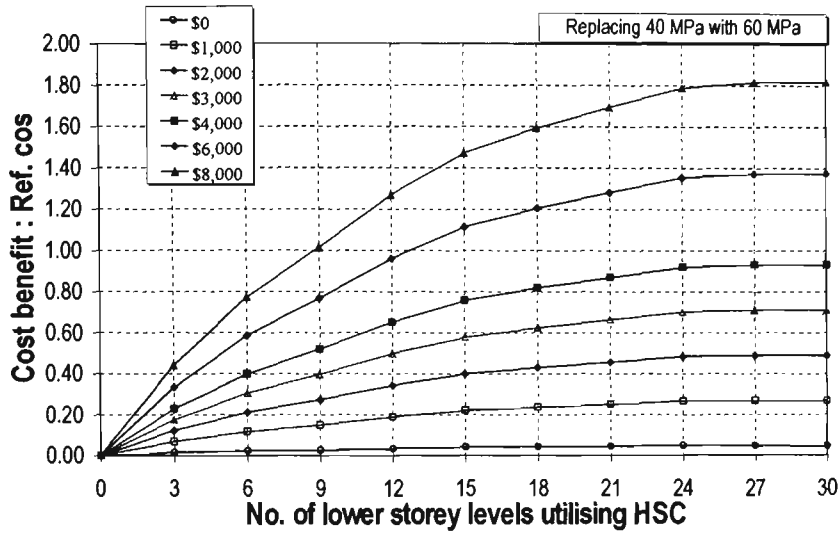
# APPENDIX A

## RESULTS OF COST ANALYSIS FOR CHAPTER 6

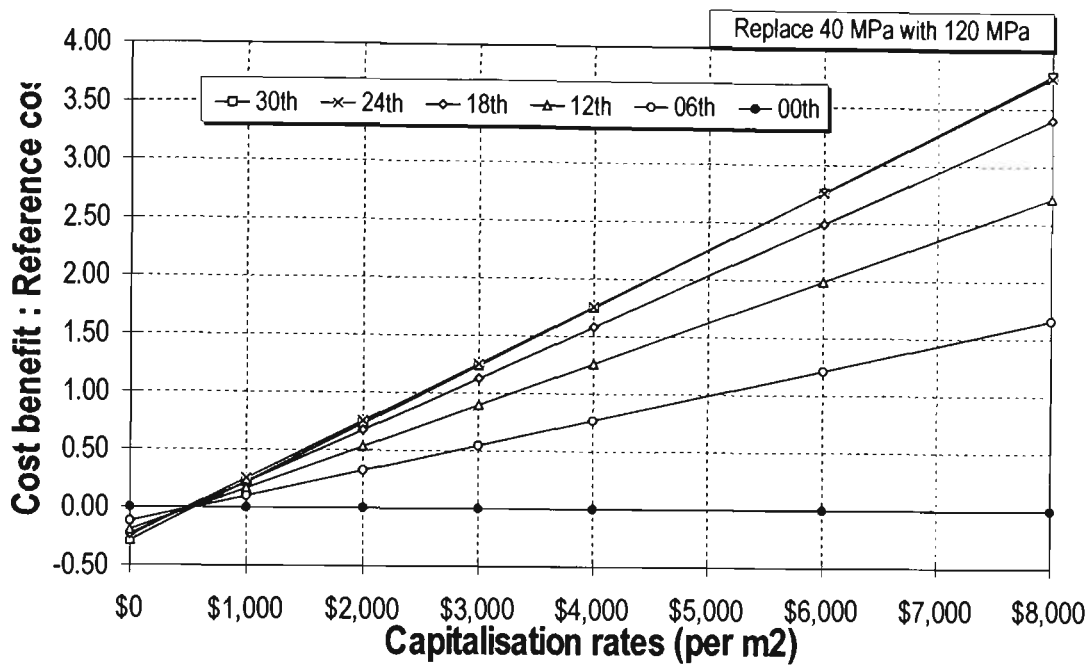
### A.1 COST BENEFITS - CANTILEVER WALL

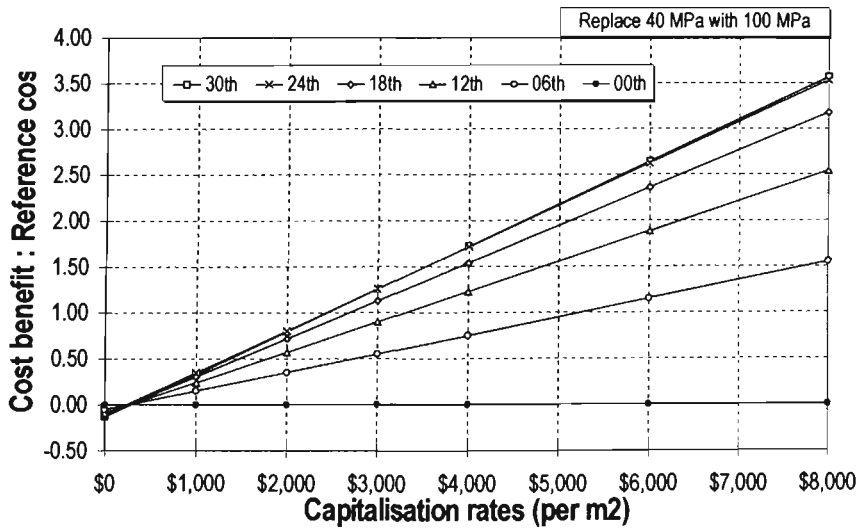
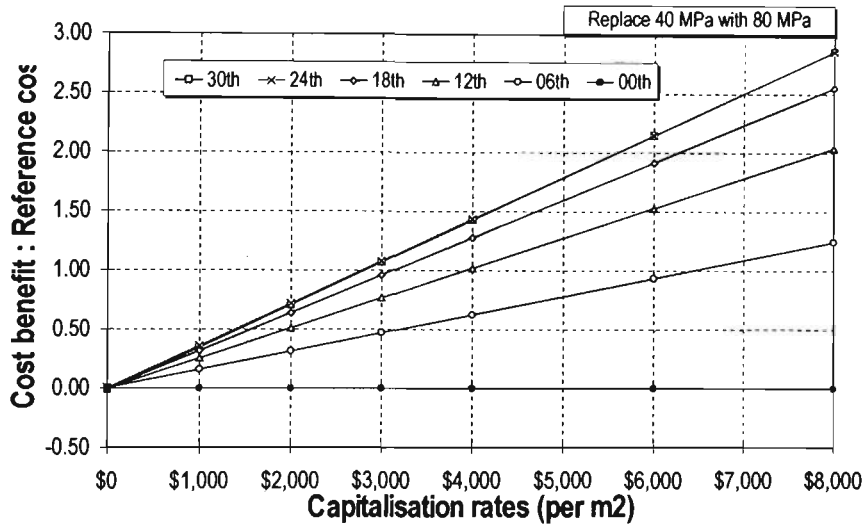
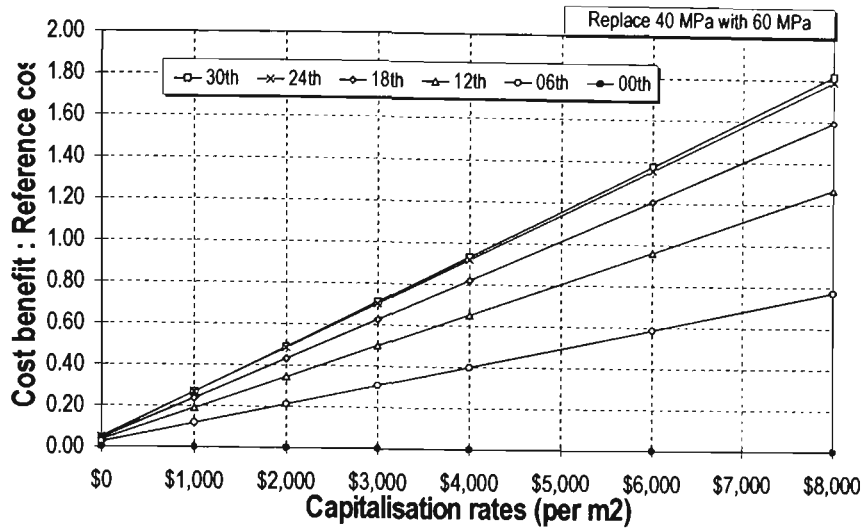
#### COST BENEFITS WITH HSC AT LOWER STOREY LEVELS





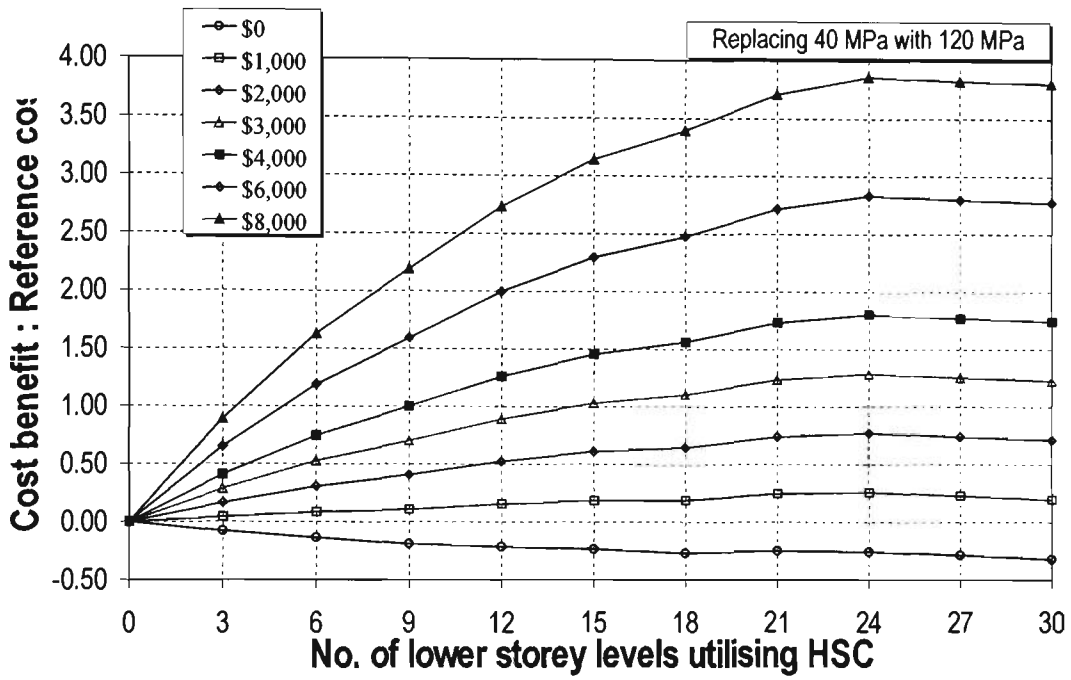
## LINEAR RELATIONSHIP OF COST BENEFITS AND CAPITALISATION VALUES

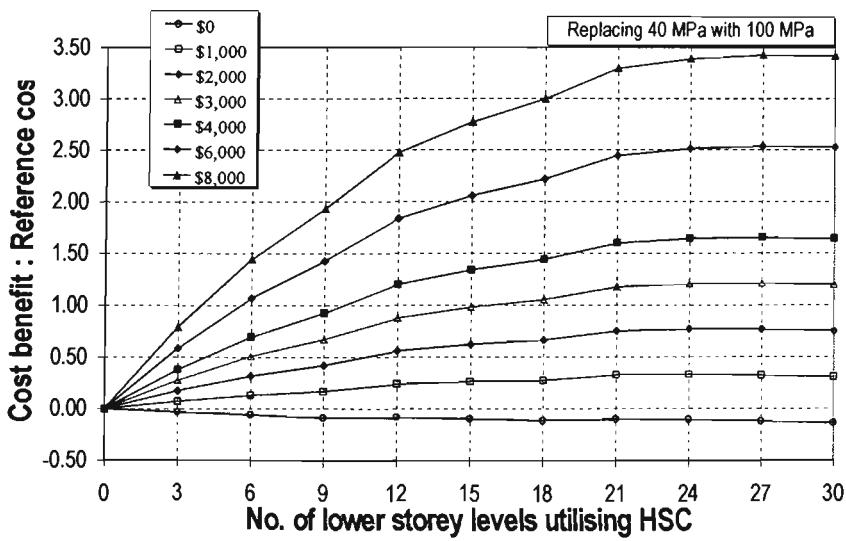
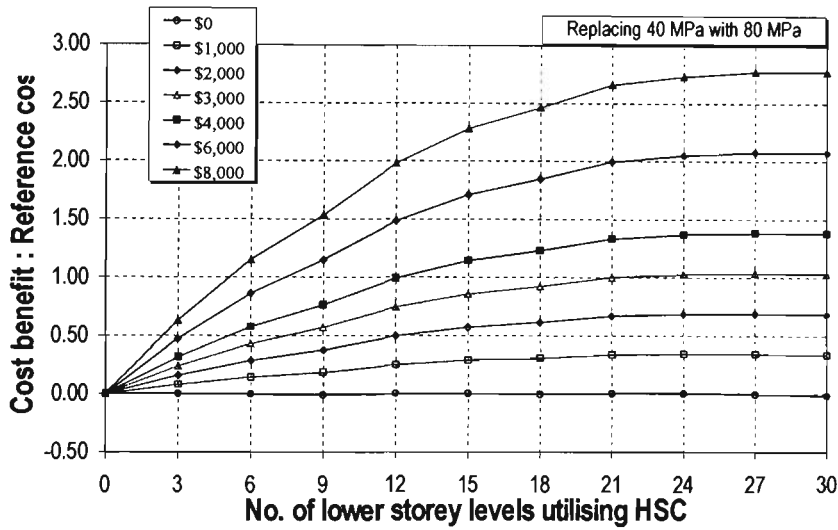
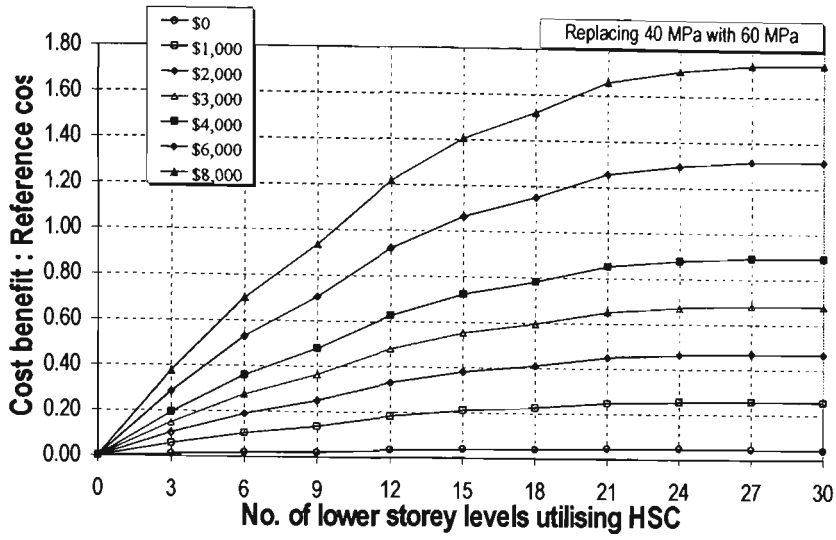




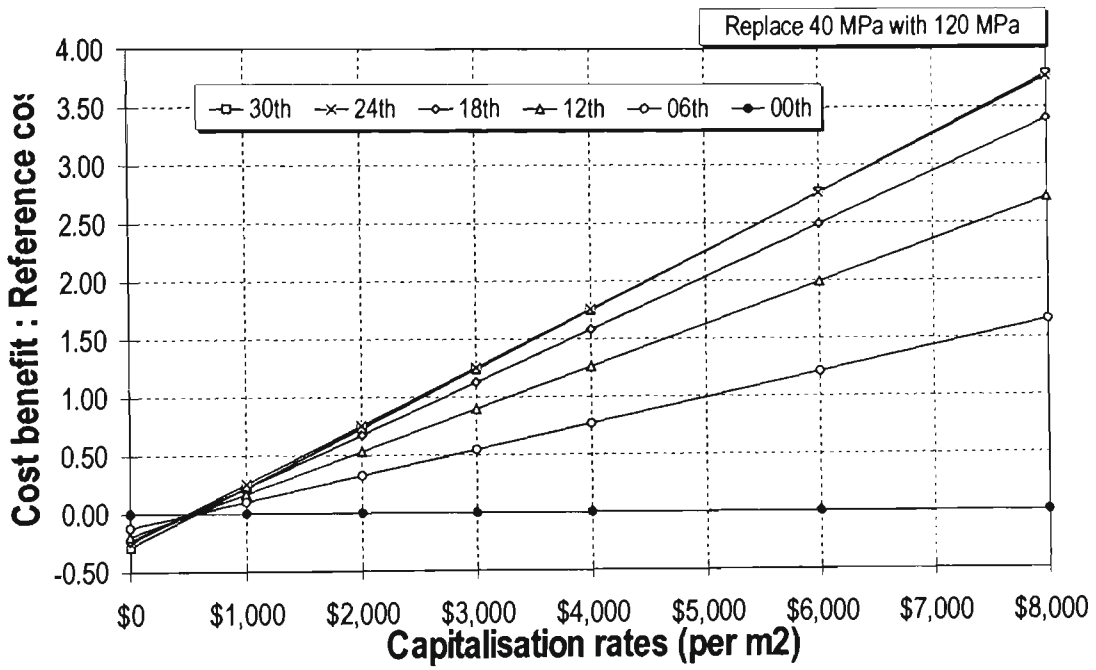
## A.2 COST BENEFITS - COUPLED WALL

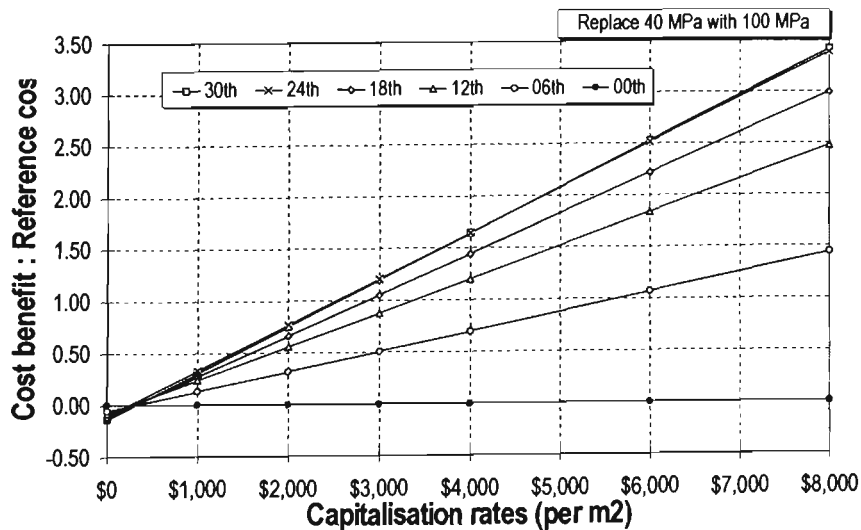
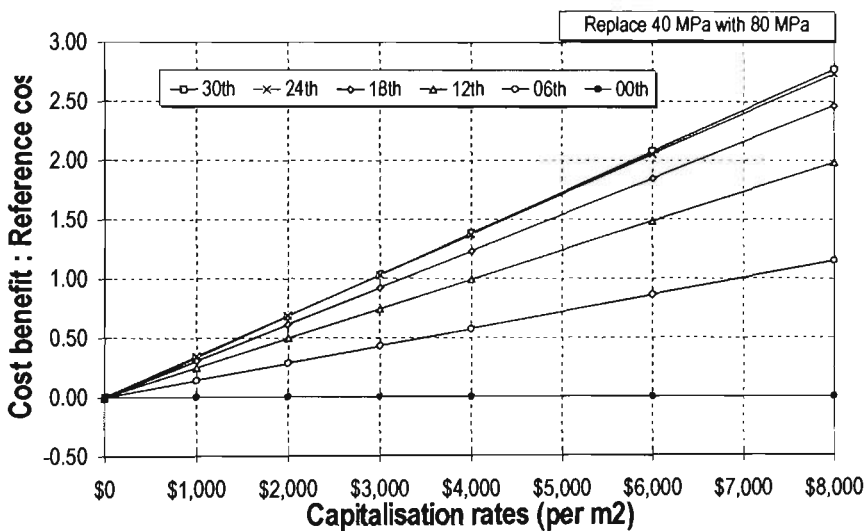
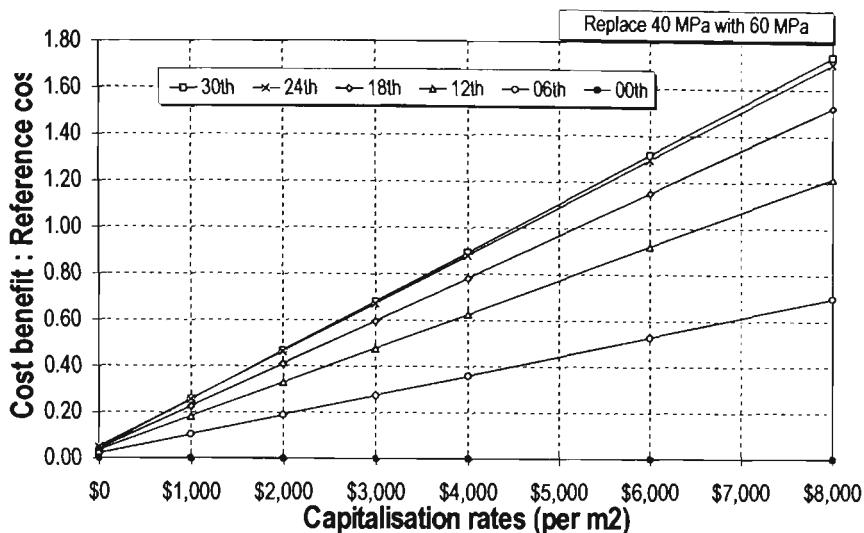
### COST BENEFITS WITH HSC AT LOWER STOREY LEVELS





## LINEAR RELATIONSHIP OF COST BENEFITS AND CAPITALISATION VALUES



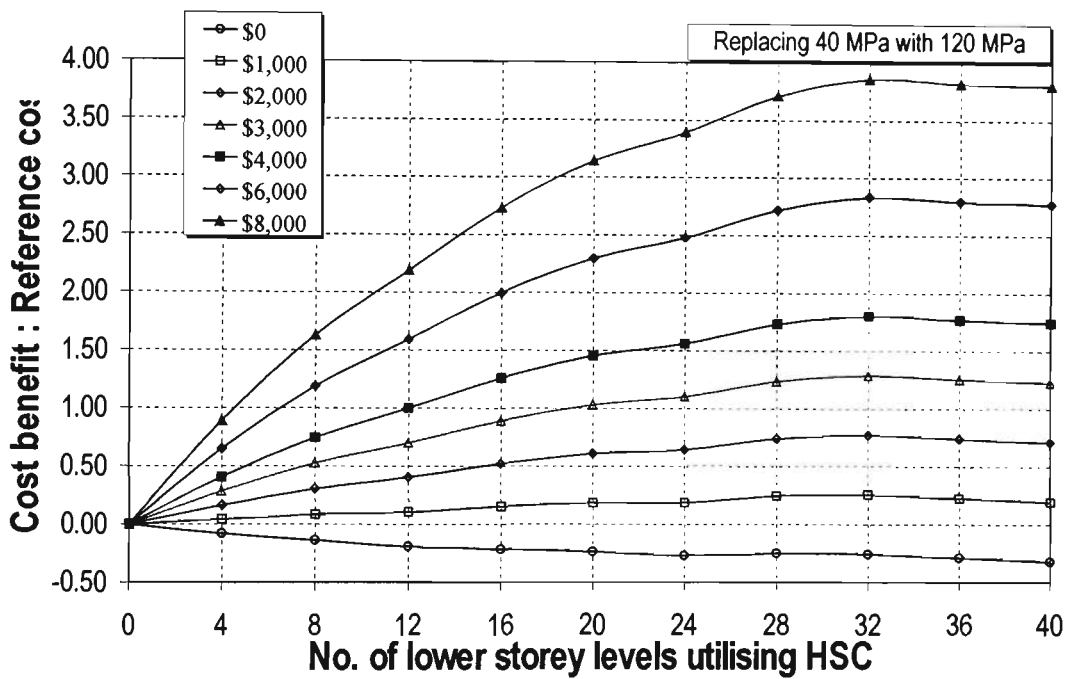


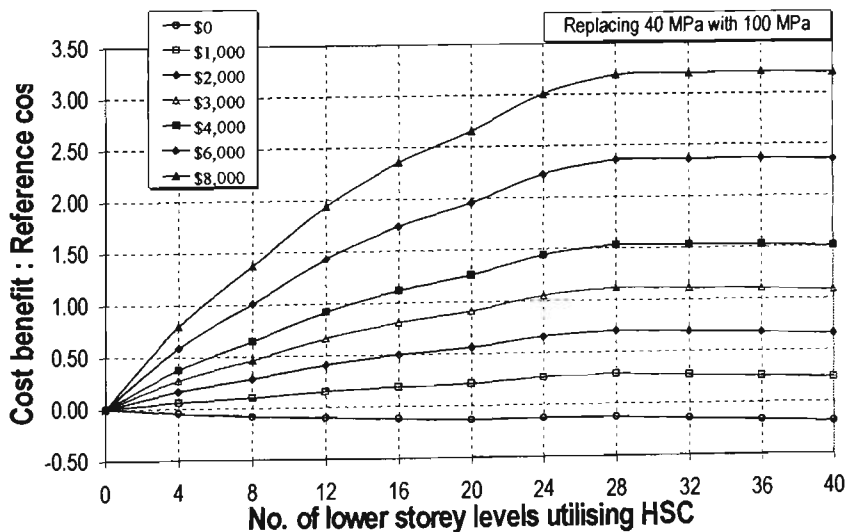
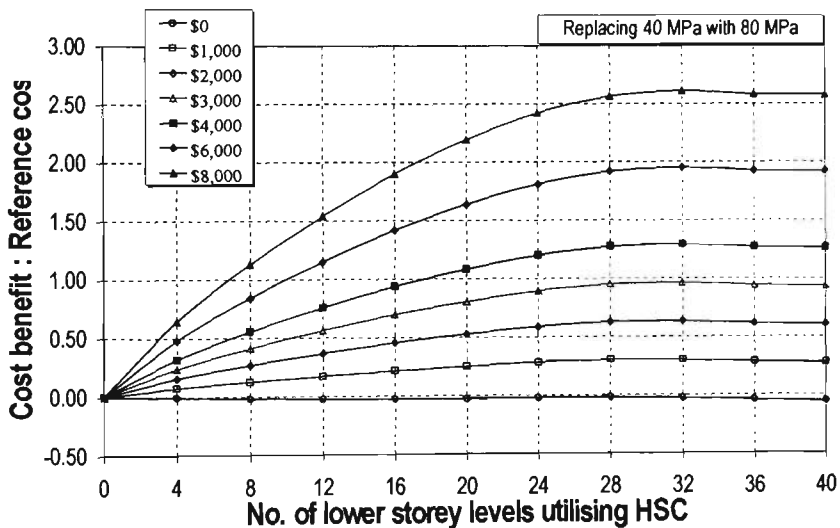
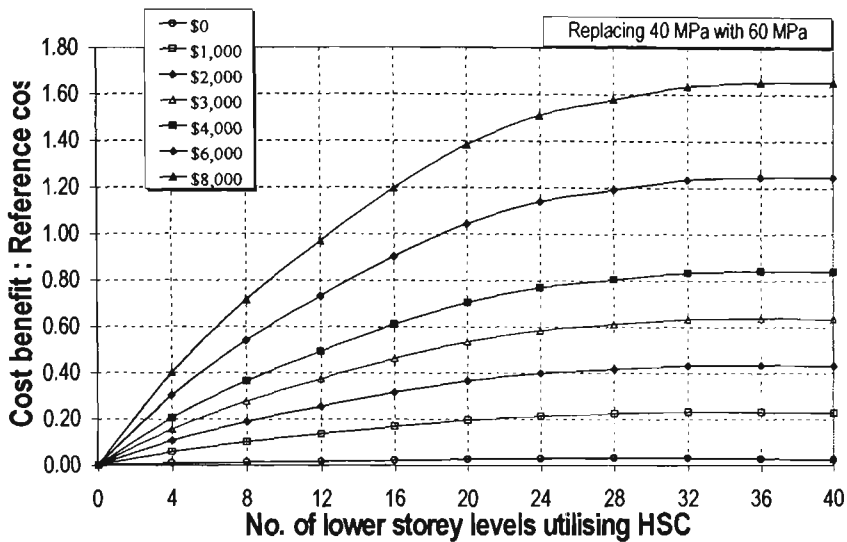
# APPENDIX B

## RESULTS OF COST ANALYSIS FOR CHAPTER 7

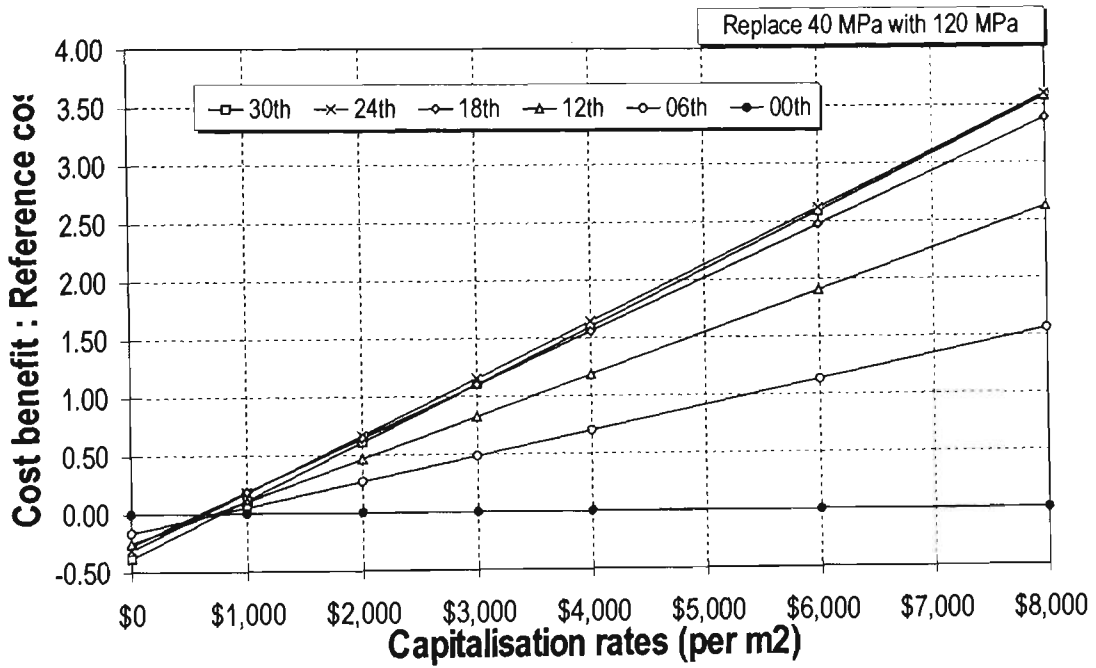
### COST BENEFITS

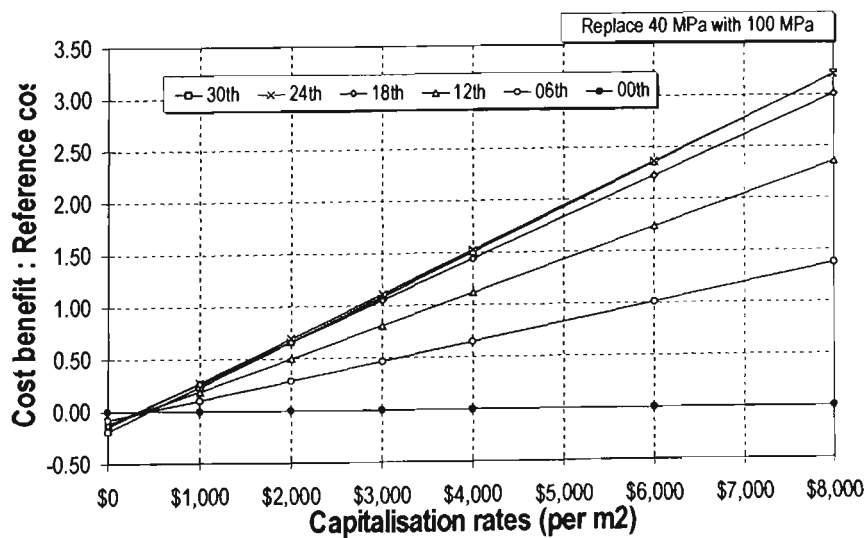
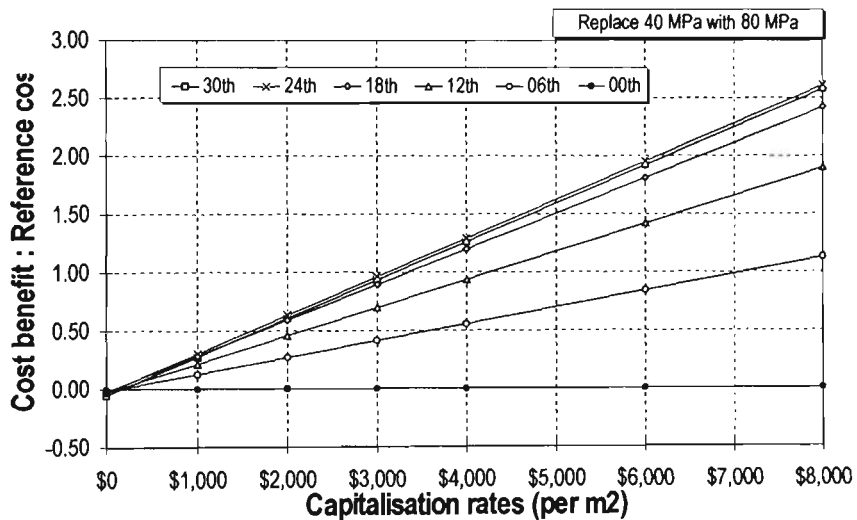
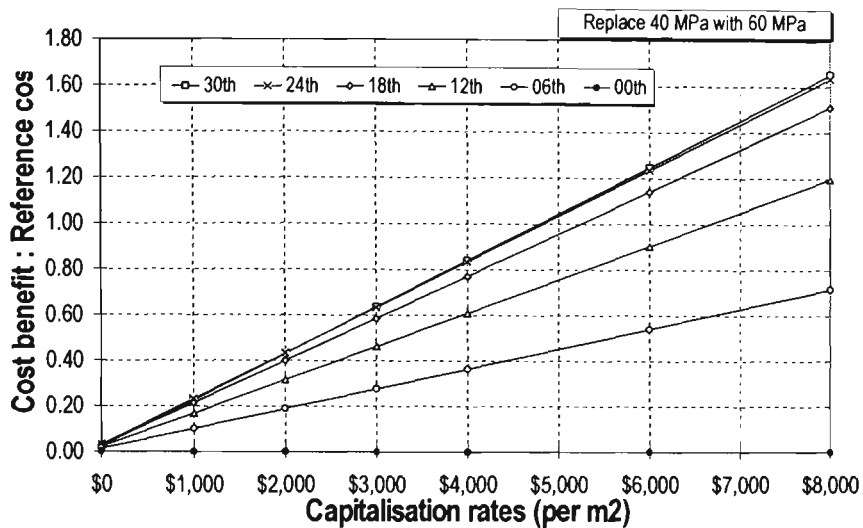
#### COST BENEFITS WITH HSC AT LOWER STOREY LEVELS





## LINEAR RELATIONSHIP OF COST BENEFITS AND CAPITALISATION VALUES





## APPENDIX C

---

### RCDESIGN97 (COMPUTER PROGRAM)

The analytical calculation of RCDESIGN97 program for flexural and axial strength is based on the traditional concepts of equilibrium and strain compatibility, consistent with the normal assumption made below:

- ⇒ Plane sections before bending remain plane after bending.
- ⇒ Stress-strain curves for concrete and reinforcing steel are known.
- ⇒ Concrete carries no tensile stress.
- ⇒ Stress strain curve for reinforcing steel is identical for tension and compression.
- ⇒ Perfect bond exists between concrete and reinforcement.

#### 1 FLEXURAL AND AXIAL STRENGTH RELATIONS

A general methodology for calculating flexural and axial strength ( $M&N$ ) relations of a reinforced concrete section is described here. A section is defined as an assemblage of rectangular elements of width  $b_i$  and depth  $d_i$ , in which the sum of  $d_i$  is equal to the section's depth.

For a given ultimate strain of concrete and for every value of neutral axis depth, it is possible to calculate the axial,  $N$ , and the corresponding moment,  $M$ , of the section. For a given neutral axis depth, a compression area, whose boundaries are defined by compression edges and the axis, is divided into  $m$  horizontal layers (Fig. A.1). The concrete layers, as well as the various reinforcement layers, are referred by their distances from a reference axis which is taken at the location of plastic centroid point. This point is defined as the centroid of resistance of the section when the compressive strains in the concrete and steel are uniform throughout the section.

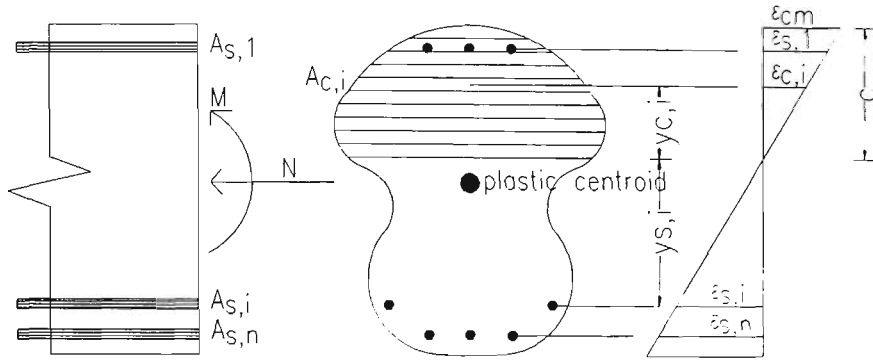


**Fig. A.1** Condition for the calculation of flexural and axial strength.

For each strain  $\varepsilon_{ci}$  at the centre of concrete layer, the corresponding stress  $\sigma_{ci}$  is defined from a stress-strain  $\sigma_{ci}-\varepsilon_{ci}$  diagram, which can be of any shape. Similarly, from the strain  $\varepsilon_{si}$  at the centre of each reinforcement layer the corresponding stress  $\sigma_{si}$  are determined using the (also arbitrary shaped) stress-strain  $\sigma_{si}-\varepsilon_{si}$  diagram. The axial strength for a section of  $n$  reinforcement layers and the subsequent moment may be written as

$$N = \sum_{i=1}^m \sigma_{c,i} \varepsilon_{c,i} + \sum_{i=1}^n \sigma_{s,i} \varepsilon_{s,i} \quad (\text{A.1})$$

and

$$M = \sum_{i=1}^m \sigma_{c,i} \varepsilon_{c,i} y_{c,i} + \sum_{i=1}^n \sigma_{s,i} \varepsilon_{s,i} y_{s,i} \quad (\text{4.2})$$

It is convenient to record in the analysis the neutral axis positions for various combinations of moment and axial strengths, because these give direct indication of curvature ductility involved in developing the appropriate strengths.

An example of a channel-shaped section is shown in Fig. A.2. Similar flexural-axial strength interaction relationships can be constructed for different shapes of cross sections.

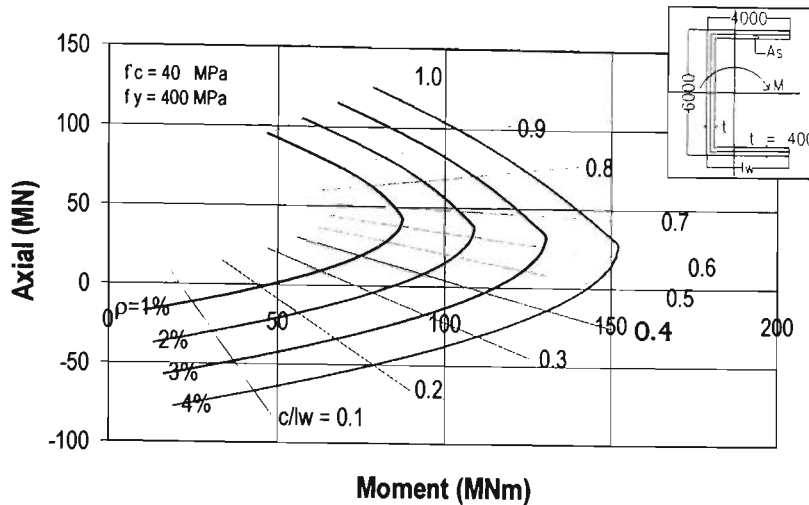


Fig. A.2 Axial-moment interaction for a channel-shaped section (RCDESIGN97).

## 2 FLEXURAL STRENGTH AND CURVATURE RELATIONS

Similar methodology to the calculation of flexural and axial strength relations is used to develop the moment  $M$  and curvature  $\phi$  relations as summarised below. Given an axial load  $N$ , for every compression strain  $\varepsilon_c$  at the extreme fibre, it is possible to calculate the moment and the corresponding curvature of the section. The procedure is to find the neutral axis depth that satisfies the equilibrium equation Eq. A.1. This procedure is usually iterative and requires estimating the initial position of the neutral axis and subsequently correcting it until Eq. A.1 converges within a specified tolerance. The moment of the section can then be calculated from Eq. A.2 while the corresponding curvature, which is defined as the ratio of strain at a certain fibre of the section to the corresponding distance from the neutral axis, is calculated from the relationship (Fig. A.1)

$$\phi = \frac{\varepsilon_{cm}}{c} \quad (\text{A.3})$$

The relationship between flexural strength and curvature has yet to be incorporated in the RCDESIGN97

## APPENDIX D

---

### CONFERENCE PAPERS

Bong, B.G., Hira, A. & Mendis, P. (1997). Optimal application of high-strength concrete in cantilever structural walls. Proceeding: Australasian conference on structural mechanics and materials (pp 243-49). Nederland: Balkema.

Bong, B.G., Hira, A. & Mendis, P. (1998). Optimisation of structural walls in tall buildings. Proceeding: Australasian conference on structural optimisation (pp 123-31). Melbourne: Oxbridge Press.

PROCEEDINGS OF THE FIFTEENTH AUSTRALASIAN CONFERENCE  
ON THE MECHANICS OF STRUCTURES AND MATERIALS  
MELBOURNE/VICTORIA/AUSTRALIA/8-10 DECEMBER 1997

# Mechanics of Structures and Materials

*Edited by*

RAPHAEL H. GRZEBIETA & RIADH AL-MAHAIDI  
*Department of Civil Engineering, Monash University, Clayton, Victoria, Australia*

JOHN L. WILSON  
*Department of Civil and Environmental Engineering, University of Melbourne,  
Victoria, Australia*



A.A. BALKEMA/ROTTERDAM/BROOKFIELD/1997

## Optimal application of high-strength concrete in cantilever structural walls

B.G. Bong

*Victoria University of Technology, Melbourne, Vic., Australia*

A.R. Hira

*Department of Civil and Building Engineering, Victoria University of Technology, Melbourne, Vic., Australia*

P.A. Mendis

*Department of Civil and Environmental Engineering, The University of Melbourne, Vic., Australia*

**ABSTRACT:** The availability of very high-strength concretes in the market place has been a major factor in the development of very tall concrete buildings worldwide. Although concrete strengths of up to 120 MPa is commercially available in Australia and overseas, the costs of production associated with higher strengths and the lack of awareness of the advantages of using this versatile material effectively have discouraged many designers from specifying it for tall building applications. This paper presents the cost benefits associated with optimal use of high-strength concrete in construction of walls in tall buildings. It is shown that the increased lettable space due to thinner walls, makes high strength concrete application extremely cost effective for tall buildings.

### 1 INTRODUCTION

In the last decade, record setting tall concrete buildings are being built around the world. This includes the world's tallest building, the 98-storey twin Petronas Towers in Kuala Lumpur with an overall height of 450 m. The external columns and central core in the lower levels of the towers were constructed with 80 MPa concrete. Another striking example, where high strength concrete has been extensively utilised is the 88 storey Jin Mao Building, currently under construction in Shanghai, which will become the third tallest building in the world. A significantly important factor contributing to the viability of achieving such heights is the development of efficient structural systems and the availability of high strength concrete which was used for the shear core elements and the principal column elements.

The biggest advantages of HSC that makes its use attractive in high-rise buildings are the larger strength/unit cost, strength/unit weight and stiffness/unit cost compared to normal strength concrete and other structural materials. The resulting lower mass reduces inertial load providing a further incentive for its application in tall buildings located in high seismic regions. The benefits of HSC applications in tall building structural systems are explored in a project conducted at Victoria University of Technology. The preliminary results of this project are presented in this paper.

### 2 STRUCTURAL MODEL - CASE STUDY

A 40-storey high single cantilever structural wall with a 4.0 m inter-storey high is considered for this case study (Fig. 1). The dimensions are selected on the basis of satisfying an acceptable lateral drift of 0.002 of the building height when subjected to derived seismic loads based on

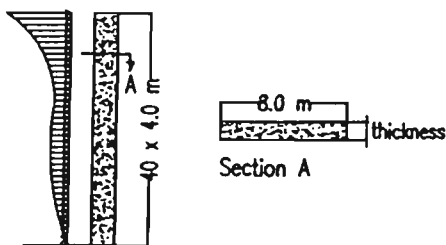
the Indonesian earthquake code (Departemen Pekerjaan Umum, 1983). The seismic mass is based on a vertical floor loading (dead and live) of 5.75 kPa with a tributary area of 160 m<sup>2</sup>. The elastic response spectrum and the resulting dynamic storey inertia load distribution generated by the program ETABS (Habibullah, 1989) is shown in Fig. 2. Using a concrete strength of 40 MPa for the wall section, the calculated first mode period and maximum inter-storey drift ratio is 4.5 seconds and 0.003 respectively.

### 3 WALL OPTIMISATION

An optimisation process by use of Displacement Participation Factors and Sensitivity Index based on the principle of virtual work (Charney, 1991) is utilised. The objective of the process is to obtain the optimum solution corresponding to the use of minimum volume of material while attaining a target stiffness in terms of the lateral displacement at the top of the structure.

The resulting optimised section properties and the equivalent thicknesses are shown in Fig. 3a and 3b respectively.  $V$  is the concrete volume and  $EI$  the flexural rigidity of the section. As expected the wall thickness profile up the height of the structure closely follows a parabolic profile. However in practice the number of transitions in wall thickness are kept to a minimum on both practical and economical grounds with regards to constructability.

The computer program 'OPTIC' is developed to calculate the optimum solutions for cantilever structural walls with different concrete strengths and designated number of wall thickness transitions. For a given deflection limit and a minimum wall thickness the objective of the program is to locate the positions of the transitions and to determine the optimal wall thicknesses that produce minimum overall volume. The procedure involves a systematic sizing-analysing and resizing process within the given limits for the parameters. The process is continued until the minimum volume criterion is reached.



Cantilever Wall Model

Fig. 1 Elevation and plan of wall model

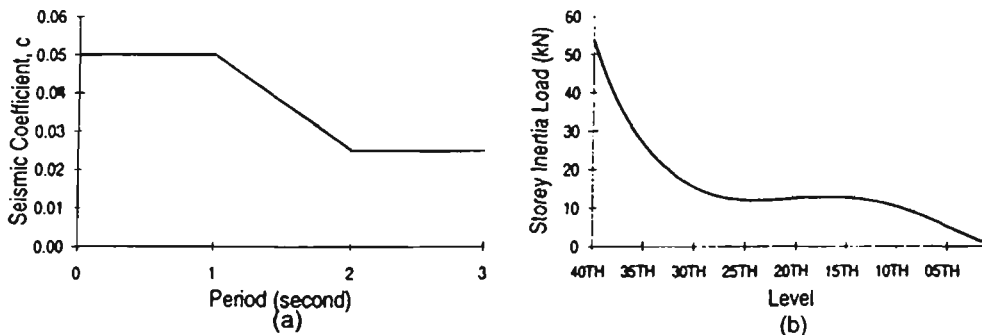


Fig. 2 (a) Elastic response spectrum (b) Dynamic storey inertia load distribution

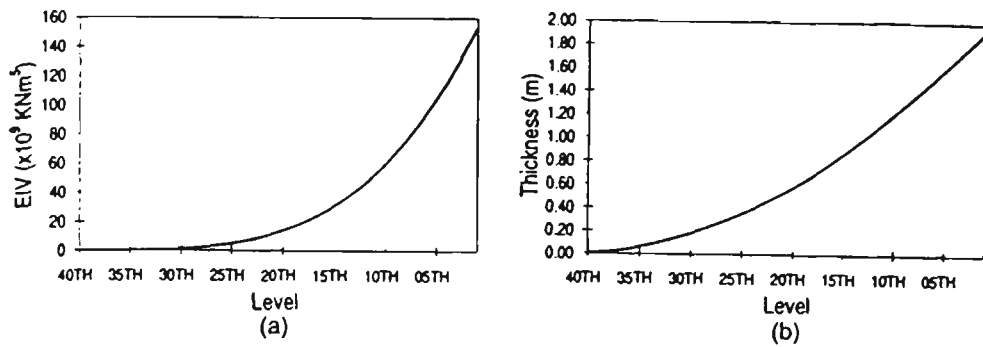


Fig. 3 (a) Optimum section property distribution, EIV (b) Optimum theoretical wall thickness distribution

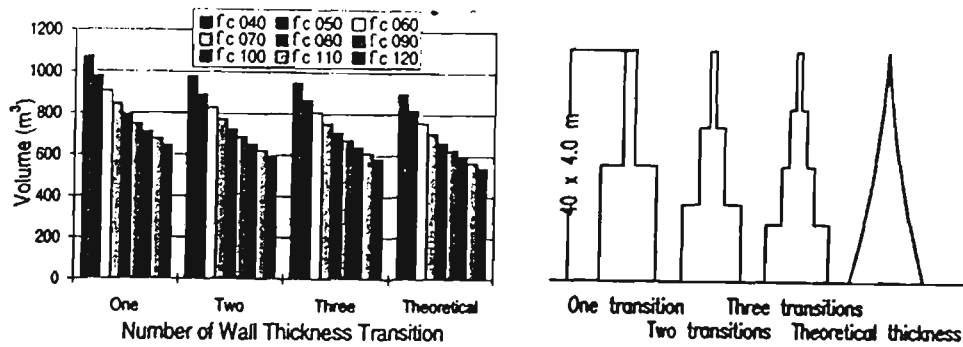


Fig. 4 Optimum volumes with different number of transitions and different concrete strengths

Table 1 Concrete cost

Concrete strength (MPa)	40	50	60	70	80	90	100	110	120
Cost (\$/m <sup>3</sup> )	138	149	163	180	200	230	260	290	320

#### 4 BENEFITS OF USING HIGH-STRENGTH CONCRETE

*Uniform concrete grade for full height.* Fig. 4 illustrates the optimal concrete volumes for the case of a cantilever wall using the program OPTIC, for different concrete grades with differing number of wall thickness transitions. For comparison purposes, results for a cantilever wall with a parabolic wall thickness profile giving an ideal optimal solution are also presented. The principal observation is the significance of the volume reduction that can be obtained by increasing the concrete strength and the insignificance of the effect of number of transitions on the total volume. When one considers the substantial cost increase for introducing each wall thickness transition in terms of construction delay it is clear that use of higher strength concrete is an effective means of minimising concrete volume.

A cost benefit analysis is also carried out. The analysis explores the effect of concrete cost and the additional financial return due to the extra lettable floor space made available by reduction in wall thickness. The cost of concrete used for the cost analysis is given in Table 1.

Fig. 5 summarises the results of the cost benefit analysis at different capitalised rates for the extra lettable area gained by the use of higher concrete strengths resulting in thinner walls. The zero rate considers concrete costs only. The cost of 40 MPa wall is used as the base for cost comparison purposes.

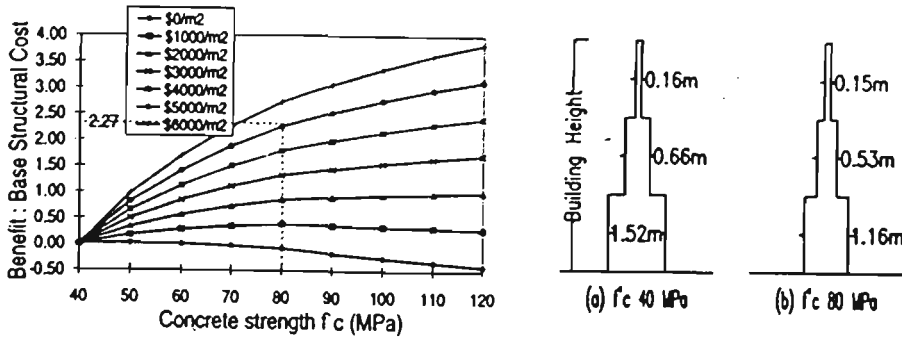


Fig. 5 Cost benefits of using higher strength concretes

(a) Vol.=978 m<sup>3</sup>; Concrete cost =\$134964

(b) Vol.=726 m<sup>3</sup>; Concrete cost =\$145200; Area saving =63.25m<sup>2</sup>; Cost Saving =\$316250; Benefit : Initial cost =2.27

The results clearly illustrate that despite the reduction in concrete volume the cost increases with concrete strength on the basis of material cost only. The benefit of using high-strength concrete only becomes apparent if the capitalised value of the extra lettable space gained from the use of higher strength concrete is taken into consideration. Fig. 5 also indicates that the cost benefit of using very high-strength concrete for buildings attracting low financial returns, diminishes. For example for buildings yielding less than \$2000/m<sup>2</sup>, there is no benefit using concrete strengths exceeding 80 MPa. However for the higher yielding buildings, corresponding to prestigious buildings located in central business districts of most cities, there is a tremendous financial benefit in using very high concrete strength, with benefits increasing with increasing concrete strengths. For example, for a building yielding \$5000/m<sup>2</sup>, utilising 80 MPa concrete for the wall will gain a cost benefit corresponding to 3.27 times the structural cost of the 40 MPa wall, a significant amount.

Locations of wall thickness transitions for optimum solutions are shown in Fig. 6. The results show that to achieve optimum solution for a one transition wall the transition point is approximately at mid height of the building and is independent of the concrete grade. A similar trend is also observed in optimum solution for walls with two transitions where the three zones are approximately equal in height.

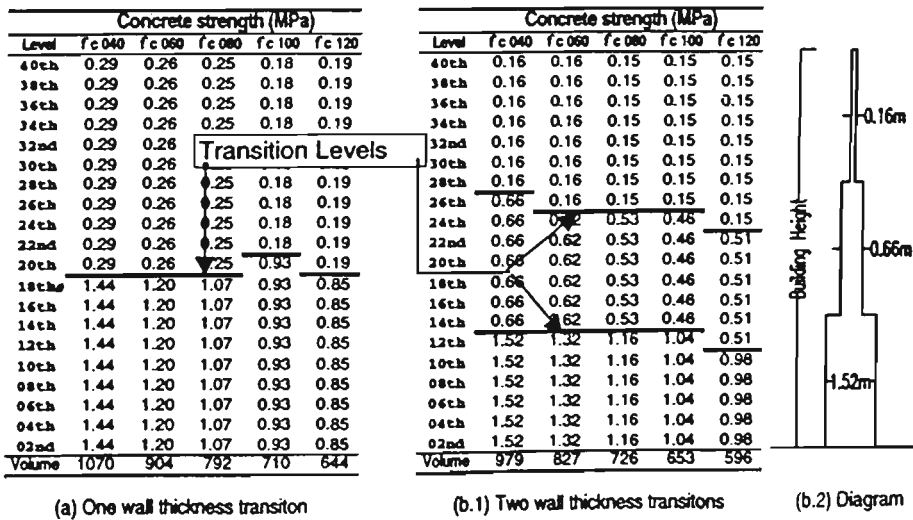


Fig. 6 Locations of wall thickness transitions at optimum solutions

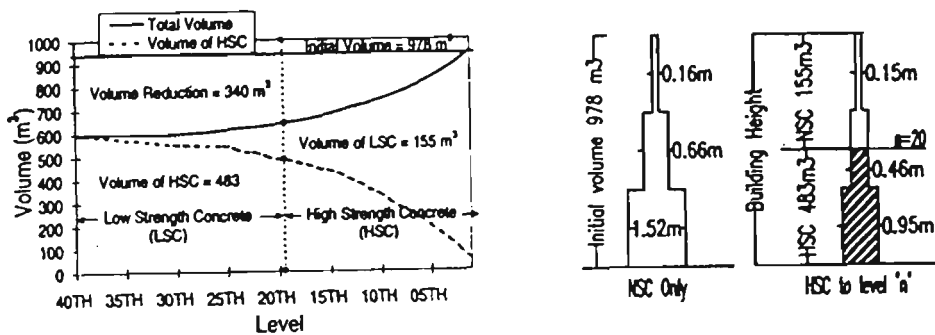


Fig.7 Application of high-strength concrete and the associated reduction of concrete volume

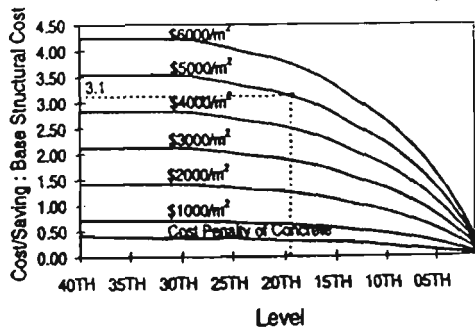


Fig.8 Cost penalty and cost saving of using higher strength concrete.

Base structural volume	= 978m <sup>3</sup>
Base structural cost	= 978m <sup>3</sup> x \$138/m <sup>3</sup> = \$134964
Cost penalty	= (483m <sup>3</sup> x \$320/m <sup>3</sup> + 155m <sup>3</sup> x \$138/m <sup>3</sup> ) - \$134964 = \$40986
Cost saving	= 340m <sup>3</sup> : 4m <sup>1</sup> x \$5000/m <sup>2</sup> = \$425000
Cost Penalty : Base cost	= 0.30; Cost saving : Base cost = 3.15

*Varying concrete grade with height.* The study is repeated to assess the cost benefit of using higher concrete strengths for a more realistic case where concrete strength varies with height. For the purposes of this study the cantilever wall with two concrete strengths is considered, a higher strength concrete for the lower levels of the wall and lower strength concrete for the upper levels for a one and two transition walls. Fig. 7 shows the resulting volume reductions achieved by introducing 120 MPa high-strength concrete up to a particular floor with the remainder of the wall being 40MPa. in a two transition wall. A wall with concrete strength of 40 MPa throughout is used as the base for volume and cost comparisons. As an example Fig 7 shows a volume reduction of 340 m<sup>3</sup> when 120 MPa concrete is used for the first 20 floors.

The total cost benefit analysis of the above wall, taking into account the effects of capitalising the gain in net lettable area and the concrete cost, is carried out with the results shown in Fig. 8. As expected there is a penalty in concrete cost associated with replacing the 40MPa. concrete in the lower levels of the wall with 120MPa. strength concrete, however the benefits from the extra lettable area far exceed the cost penalty of the material. An interesting feature of results reveal that there is no significant gain in cost benefits by extending the higher strength concrete much beyond the mid-level (20<sup>th</sup> level) particularly for buildings yielding low rentals. The main gain in cost benefits is achieved by introducing higher strength concrete in the lower 30% to 40% of the wall height.

Capitalised value																
Level	\$0/m <sup>2</sup>				\$2000/m <sup>2</sup>				\$4000/m <sup>2</sup>				\$6000/m <sup>2</sup>			
	f <sub>c</sub> 060	f <sub>c</sub> 080	f <sub>c</sub> 100	f <sub>c</sub> 120	f <sub>c</sub> 060	f <sub>c</sub> 080	f <sub>c</sub> 100	f <sub>c</sub> 120	f <sub>c</sub> 060	f <sub>c</sub> 080	f <sub>c</sub> 100	f <sub>c</sub> 120	f <sub>c</sub> 060	f <sub>c</sub> 080	f <sub>c</sub> 100	f <sub>c</sub> 120
40th	0	-10	-35	-56	76	116	128	135	152	243	291	326	228	369	454	517
35th	1	-9	-32	-51	77	118	131	140	153	244	294	331	228	371	457	522
30th	1	-8	-30	-48	76	117	131	141	151	241	292	331	226	366	454	520
25th	0	-9	-31	-49	71	109	122	133	141	227	276	314	211	346	429	495
24th	1	-8	-29	-47	71	109	122	132	140	226	274	311	210	342	425	490
23rd	1	-7	-27	-45	70	108	122	132	140	224	272	309	209	339	422	487
22nd	1	-7	-28	-45	70	108	120	131	139	222	268	306	207	337	416	482
21st	1	-6	-27	-43	69	107	119	131	137	220	265	304	204	333	412	477
20th	2	-6	-26	-41	68	105	118	129	135	216	261	300	202	327	405	470
19th	2	-6	-25	-41	67	103	117	126	132	212	259	293	198	321	400	460
18th	2	-5	-25	-40	65	101	113	124	129	208	251	287	193	314	389	451
17th	2	-6	-25	-39	64	97	109	120	126	200	243	280	188	303	378	439
16th	2	-6	-25	-38	61	95	105	117	121	195	235	271	181	295	366	426
15th	1	-5	-22	-38	59	91	104	111	117	188	229	260	174	284	355	409
10th	2	-3	-16	-27	46	73	84	91	91	150	183	209	135	226	283	328
05th	2	0	-8	-15	30	47	53	58	57	94	114	130	85	141	175	203

Notes: Concrete strengths in MPa, Benefit in \$x1000

Fig. 9 Cut off levels for 90% of maximum cost benefit

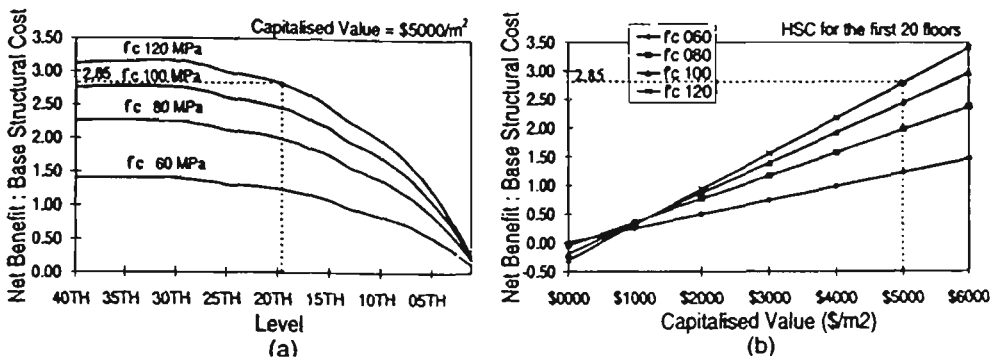


Fig. 10 Cost benefit of using high-strength concrete (a) at capitalised value of \$5000/m<sup>2</sup> (b) level n = 20

Figure 9 provides tabulated values of cost benefits for varying concrete grades and varying capitalisation rates. The table also identifies the level designated as 90% cost benefit. Extending of the use of high-strength concrete above this level will reap a maximum increase in the cost benefit of less than 10%. It can be seen that the line is consistently located at the mid-height of the wall. This suggests that a convenient transition for concrete grade is approximately mid-height of the wall as there is no significant cost benefit in using higher strength concrete in top half of the wall.

Fig. 10a shows the benefit of using different concrete strengths compared with the structural cost of 40 MPa wall. The benefit is calculated for the value of lettable area capitalised to \$5000/m<sup>2</sup>. Fig. 10b indicates that a linear relationship can be assumed between the net benefits and the values of lettable area.

## 5 CONCLUSIONS

This paper presents some of the early results of assessing the benefits of using high-strength concrete in tall buildings. Results reveal that the capitalisation value of the additional lettable area gained through thinner structural walls by use of higher strength concrete provides significant cost savings for the building owners.

## REFERENCES

Chamey, F.A. 1991. The use of displacement participation factors in the optimization of wind drift controlled buildings. Proceeding of the second conference on tall buildings in seismic regions. Los Angeles: Council on Tall Buildings and Urban Habitat

Chamey, F.A. 1994. DISPAR for ETABS ver. 5.4, users manual. Colorado: Advance Structural Concept.

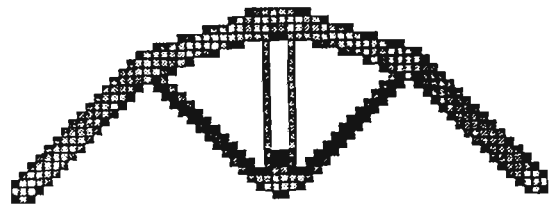
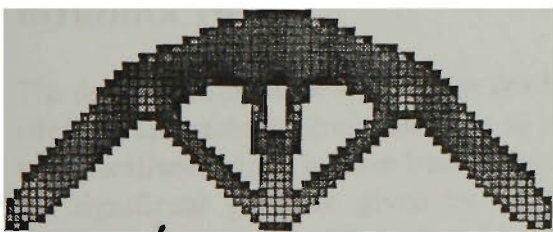
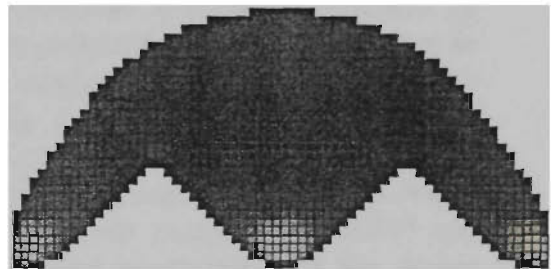
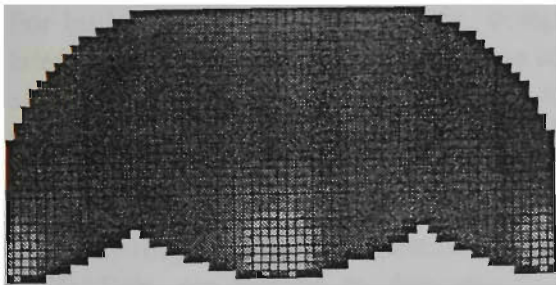
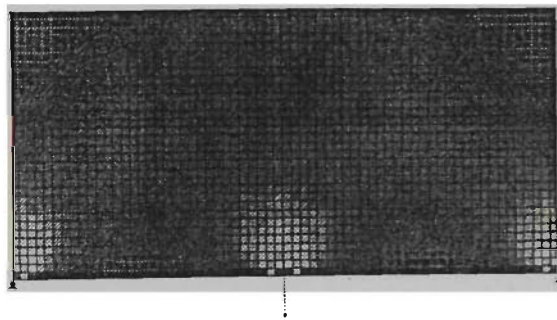
Departemen Pekerjaan Umum. 1983. Buku Pedoman Perencanaan untuk Struktur Beton Bertulang Biasa dan Struktur Tembok Bertulang untuk Gedung. Bandung: Pusat Penelitian dan Pengembangan Pemukiman.

Habibullah, A. 1989. ETABS ver. 5.10, users manual. California: Computers & Structures, Inc.

# STRUCTURAL OPTIMISATION

Proceedings of Australasian Conference on  
Structural Optimisation

February 11-13, 1998  
Sydney, Australia



*Editors:*

**G.P. Steven, O.M. Querin, H. Guan and Y.M. Xie**

## Optimisation of Structural Walls in Tall Buildings

B.G. Bong<sup>1)</sup>, A. Hira<sup>1)</sup> and P. Mendis<sup>2)</sup>

<sup>1)</sup> *Department of Civil and Building Engineering, Victoria University of Technology, Vic., Australia*

<sup>2)</sup> *Department of Civil and Environmental Engineering, The University of Melbourne, Vic., Australia*

### ABSTRACT

For buildings of increasing height, design of structural elements is primarily governed by lateral drift criteria. The use of principle of virtual work in structural optimisation provides an effective method to evolve an efficient structure whilst maintaining the drift to acceptable limits. Frequent changes in member sizes undesirably cause unwarranted construction complexity. A technique of member-linking is proposed to overcome this difficulty. In this paper, this method is applied to design of structural walls, which acts as the principle lateral load-resisting system. Commercially available structural analysis packages, ETABS<sup>TM</sup> and DISPAR<sup>TM</sup>, are applied to demonstrate the applicability and practicability of the design method. Since the method can only be applied to structure of predetermined topology, an approximate method is derived and applied to a cantilever wall system for verification.

### INTRODUCTION

The design of structural systems for tall buildings typically needs to satisfy the serviceability, strength, and stability limit states. At an early stage of the design process, member sizes need to be finalised, which is often based on satisfying the serviceability limit state criteria. Despite the significant guidance given by codes and design aids on initial sizing of horizontal members (beams and slabs), there is very little information on sizing of vertical elements (columns and walls) that participate in the lateral load-resisting system for tall buildings. This is primarily due to the highly indeterminant nature of the problem. This leads to a need to develop an efficient method for selecting sizes for the vertical elements, based on application of structural optimisation techniques.

It is well understood in the building industry the undesirability of frequently changing member sizes. It normally lengthens the construction time as well as increases the formwork operation costs. Slow construction increases the holding costs in terms of interest and delays the time for financial return from rental income. Recognising this issue, an optimisation process that links several members of the same length to a single representative is derived.

This so-called member-linking method provides simple formulation to find the optimum volume for a confined problem, in terms of a number of cross sectional sizes.

This paper outlines the development of a basic technique of structural optimization for a lateral load-resisting structural system subjected to a displacement constraint. The method employs the well known principles of virtual work to obtain one essential parameter for use in the optimisation process. This parameter, the Displacement Participation Factor (DPF), is the deformation of a member that contributes to the total displacement at the point and direction of an applied unit load. The DPFs are computed by use of a commercially available structural analysis package DISPAR™ (Charney, 1994), which is a third party licensed software for the three dimensional structural analysis program, ETABS™ (Habibullah, 1989).

To illustrate the optimization method, a typical example of a core wall structure is presented. The example demonstrates the use of spreadsheets as an efficient computational tool.

Since the method can only be applied to a structure with fixed transition locations, an approximate method of a numerical analysis is derived and applied to a cantilever wall example for verification. This method defines a DPF function and employs partial differentiation to solve the design variables that defines the locations of the transitions and member sizes.

## BASIC STRUCTURAL OPTIMISATION TECHNIQUE

The problem of finding the minimum volume (weight) design,  $V$ , of a lateral load-resisting framework having  $m$  members to satisfy lateral drift constraint,  $D$ , can generally be written as:

minimise

$$V = \sum_{i=1}^m v_i \quad (1)$$

subject to

$$D = \sum_{i=1}^m \delta_i \quad (2)$$

where  $v_i$  and  $\delta_i$  are, respectively, the volume and DPF of member  $i$ .

On the assumption that materials are elastic and changes in cross sectional area and moment of inertia are proportional to volume change of members, Eqs. (1) and (2) can be rewritten as: (Wada, 1991)

$$V' = \sum_{i=1}^m \alpha_i v_i \quad (3)$$

and

$$D' = \sum_{i=1}^m \frac{\delta_i}{\alpha_i} \quad (4)$$

One of the most effective techniques for solving constrained problems are to solve sequences of related unconstrained problems. The transformation of the above constrained optimisation

problem of Eqs. (3) and (4) into an unconstrained problem is accomplished by introducing the Lagrange multiplier,  $\lambda$ . Therefore:

$$V' = \sum_{i=1}^m \alpha_i v_i + \lambda \left( \sum_{i=1}^m \frac{\delta_i}{\alpha_i} - D' \right) \quad (5)$$

Differentiate Eq. (5) with respect to the coefficient  $\alpha$  and  $\lambda$ , and set the derivatives to zero to obtain the local extremes.

$$\frac{\partial V'}{\partial \alpha} = v_i - \lambda \frac{\delta_i}{\alpha_i^2} = 0 \quad (6)$$

and

$$\frac{\partial V'}{\partial \lambda} = \sum_{i=1}^m \frac{\delta_i}{\alpha_i} - D' = 0 \quad (7)$$

Rearranging Eq. (6) gives

$$\lambda^{-1} = \left( \frac{\delta_i}{\alpha_i} \right)^{\div} (\alpha_i v_i) \quad (8)$$

where  $\lambda^{-1}$  is the sensitivity index of element  $i$ . Thus, for the optimisation problem above, the minimum volume is achieved when the sensitivity index for each member of the structure is equal. (Morris, 1982)

For a complete solution, the optimising values for the design variables need to be identified. By substituting  $\alpha_i$  from Eq. (8) into Eq. (7), the Lagrange multiplier can be extracted.

$$\lambda^{0.5} = \frac{\sum_{i=1}^m (\delta_i v_i)^{0.5}}{D'} \quad (9)$$

Hence, the optimising values  $\alpha_i$  are found by substituting  $\lambda$  of Eq. (9) into Eq. (8) and the optimum displacement and volume are given by Eqs. (3) and (4). The value  $\alpha_i$  is:

$$\alpha_i = \frac{\left( \frac{\delta_i}{v_i} \right)^{0.5} \sum_{i=1}^m (\delta_i v_i)^{0.5}}{D'} \quad (10)$$

### MEMBER-LINKING METHOD

The optimisation technique presented above produces continuous changes in the cross sectional dimension for the structural members, which is impractical and costly to achieve. An optimisation technique that links several members into a single representative element has an

attractive objective of producing a desirable solution in the context of practical design. This method is as follows.

Based on the assumption that the change of stiffness is proportional to the change of volume, the relationship of individual optimum and initial values of the design variables can be written as:

$$v'_i = \alpha_i v_i \quad \text{and} \quad \delta'_i = \alpha_i \delta_i \quad (11)$$

or

$$v'_i \delta'_i = v_i \delta_i \quad (12)$$

In the member-linking method, members of equal length are linked into a group having the same cross sectional properties. For a group  $n$  of  $m$  members, rewrite Eq. (12) as:

$$v'_{m,n} [\delta']_{m,n} = [v]_{m,n} [\delta]_{m,n} \quad (13)$$

in which the group values are given in brackets.

As mentioned earlier, the volume of the material will be minimum when the material is distributed such that each group has the same sensitivity index. Therefore

$$\frac{[\delta']_{m,n}}{[v']_{m,n}} = \lambda^{-1} \quad (14)$$

Substituting the group volume  $[v']_{m,n}$  of Eq. (14) into Eq. (13) and solving for the group DPF,  $[\delta']_{m,n}$ , yields

$$[\delta']_{m,n} = \left( \frac{m}{\lambda} [v]_{m,n} [\delta]_{m,n} \right)^{0.5} \quad (15)$$

While it appears that the target displacement (the sum of all group DPFs) may be calculated from Eq. (15) by substituting the sensitivity index from Eq. (9), it is intuitively obvious that such is not the case, because the sensitivity index for each member in each group will no longer be equal. This deficiency, which results in a larger displacement, needs to be justified.

To obtain the desired target displacement, the sensitivity index is adjusted such that

$$D_{\text{target}} = \sum \left( \frac{m}{\lambda'} [v]_{m,n} [\delta]_{m,n} \right)^{0.5} \quad (16)$$

Dividing Eq. (16) by the sum of Eq. (15) gives

$$\lambda' = \left( \frac{D'}{D_{\text{target}}} \right)^2 \cdot \lambda \quad (17)$$

Thus, the optimum volume for each member is given by

$$v'_{m,n} = \left( \frac{\lambda'}{m} [v]_{m,n} [\delta]_{m,n} \right)^{0.5} \tag{18}$$

This above technique is applied to structures with uniform material properties. However, if the design is to optimise the volume for a target displacement, increasing the stiffness properties of the material will decrease the volume of the structural members. Generally, a member DPF for constant cross sectional properties can be expressed as:

$$\delta_i = \frac{1}{E_i V_i} \int_0^L \left( \frac{m_i M_i}{r_i^2} + (2 + 2\mu_i) q_i Q_i + n_i N_i \right) L_i dx \tag{19}$$

where the integral part is a constant for a particular member and loading condition. Eq. (19) asserts that the multiplication of  $\delta_i$ ,  $V_i$ , and  $E_i$  should stay the same in spite of the changes made to either of those individual values. Therefore, the relationship between the optimum and initial values are expressed as:

$$\delta'_i \cdot V'_i = \frac{\delta_i \cdot V_i}{E'_i \cdot E_i} \tag{20}$$

Eq. (20) indicates that if either the initial  $\delta_i$  or  $V_i$  is replaced with its value divided by  $E'_i \cdot E_i$  prior to the optimisation process, not only do the resulting optimum values,  $\delta'_i$  and  $V'_i$  maintain the value of  $\delta_i \cdot V_i \cdot E_i$ , but also they satisfy the optimality theorem of equal sensitivity index.

**Example A**

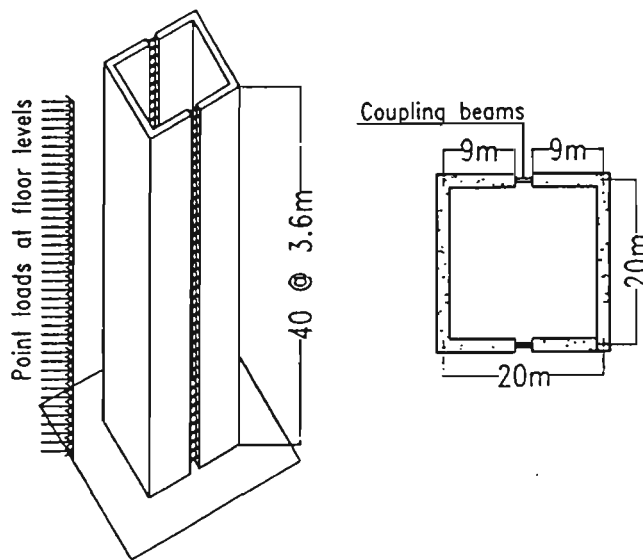


Fig. 1 Coupled-wall

STOREY	Flange of C-wall (values x 4)				Web of C-wall (values x 2)				Coupling beam (values x 2)				M DPF <sub>ni</sub>	V <sub>ni</sub>					
	DPF <sub>i</sub>	DPF <sub>1</sub>	DPF <sub>2</sub>	DPF <sub>3</sub>	DPF <sub>1</sub>	DPF <sub>2</sub>	DPF <sub>3</sub>	DPF <sub>4</sub>	DPF <sub>1</sub>	DPF <sub>2</sub>	DPF <sub>3</sub>	DPF <sub>4</sub>			V <sub>i</sub>	DPF <sub>i</sub>	V <sub>i</sub>		
40	20000	0.71	19.44	0.18	0.39	0.06	0.13	1.22	0.00	43.20	0.00	0.02	0.20	0.03	1.00	0.57	0.06	0.57	0.99
39	20000	0.02	19.44	0.31	0.58	0.09	0.18	1.72	0.00	43.20	0.00	0.02	0.20	0.05	1.00	0.66	0.07	0.66	0.99
38	20000	0.03	19.44	0.64	0.47	Optimum values	2.11	Linking values	0.00	43.20	0.01	0.07	0.64	0.06	1.00	0.74	0.08	0.74	0.99
37	20000	0.04	19.44	0.82	0.80	0.13	0.26	2.48	0.01	43.20	0.03	0.15	1.44	0.07	1.00	0.82	0.09	0.82	0.99
36	20000	0.05	19.44	1.01	0.90	0.14	0.29	2.79	0.01	43.20	0.05	0.24	2.32	0.09	1.00	0.91	0.09	0.91	0.99
35	20000	0.06	19.44	1.22	1.01	0.16	0.33	3.11	0.03	43.20	0.08	0.35	3.34	0.10	1.00	0.99	0.10	0.99	0.99
34	20000	0.08	19.44	1.48	1.11	0.16	0.36	3.42	0.05	43.20	0.10	0.46	4.36	0.12	1.00	1.07	0.11	1.07	0.99
33	20000	0.09	19.44	1.75	1.22	0.19	0.39	3.76	0.07	43.20	0.13	0.58	5.53	0.14	1.00	1.15	0.12	1.15	0.99
32	20000	0.11	19.44	2.04	1.32	0.21	0.43	4.09	0.11	43.20	0.16	0.70	6.71	0.16	1.00	1.22	0.13	1.22	0.99
31	20000	0.12	19.44	2.37	1.43	0.23	0.48	4.42	0.15	43.20	0.18	0.83	7.97	0.17	1.00	1.29	0.13	1.29	0.99
30	20000	0.14	19.44	2.74	1.54	0.24	0.50	4.76	0.21	43.20	0.22	0.97	9.29	0.19	1.00	1.35	0.14	1.35	1.65
29	20000	0.16	19.44	3.17	1.66	0.26	0.54	5.17	0.28	43.20	0.25	1.12	10.68	0.21	1.00	1.42	0.15	1.42	1.65
28	20000	0.19	19.44	3.62	1.78	0.28	0.58	5.59	0.38	43.20	0.28	1.27	12.12	0.23	1.00	1.48	0.15	1.48	1.65
27	20000	0.21	19.44	4.12	1.90	0.30	0.62	5.98	0.45	43.20	0.32	1.43	13.63	0.25	1.00	1.54	0.16	1.54	1.65
26	20000	0.24	19.44	4.67	2.03	0.32	0.66	6.28	0.56	43.20	0.35	1.59	15.18	0.27	1.00	1.59	0.17	1.59	1.65
25	20000	0.27	19.44	5.27	2.18	0.34	0.70	6.68	0.68	43.20	0.39	1.76	16.78	0.28	1.00	1.64	0.17	1.64	1.65
24	20000	0.31	19.44	5.95	2.30	0.37	0.74	7.10	0.82	43.20	0.43	1.93	18.45	0.30	1.00	1.70	0.18	1.70	1.65
23	20000	0.34	19.44	6.67	2.44	0.39	0.79	7.54	0.98	43.20	0.47	2.11	20.15	0.32	1.00	1.75	0.18	1.75	1.65
22	20000	0.43	12.96	5.55	2.58	0.41	0.84	7.98	1.18	43.20	0.51	2.29	21.90	0.34	1.00	1.80	0.19	1.80	1.65
21	30000	0.48	12.96	6.18	2.36	0.56	0.78	7.28	1.36	43.20	0.55	2.48	23.70	0.38	1.00	1.85	0.19	1.85	1.65
20	30000	0.53	12.96	6.83	2.48	0.59	0.80	7.67	1.58	35.37	0.85	2.42	23.10	0.38	0.82	2.09	0.18	1.71	1.92
19	30000	0.58	12.96	7.54	2.61	0.62	0.85	8.08	1.82	35.37	0.70	2.60	24.81	0.39	0.82	2.14	0.18	1.75	1.92
18	30000	0.64	12.96	8.32	2.75	0.66	0.89	8.49	2.09	35.37	0.75	2.78	26.56	0.41	0.82	2.19	0.19	1.79	1.92
17	30000	0.71	12.96	9.15	2.88	0.69	0.93	8.92	2.38	35.37	0.80	2.97	28.35	0.43	0.82	2.24	0.19	1.83	1.92
16	30000	0.77	12.96	10.03	3.02	0.72	0.96	9.35	2.69	35.37	0.85	3.16	30.17	0.45	0.82	2.28	0.20	1.87	1.92
15	30000	0.85	12.96	10.98	3.17	0.78	1.02	9.79	3.04	35.37	0.91	3.35	32.04	0.46	0.82	2.33	0.20	1.91	1.92
14	30000	0.92	12.96	11.96	3.31	0.79	1.07	10.24	3.41	35.37	0.98	3.55	33.94	0.48	0.82	2.37	0.20	1.94	1.92
13	30000	1.00	12.96	13.00	3.46	0.88	1.17	11.15	3.81	35.37	1.01	3.75	35.87	0.50	0.82	2.41	0.21	1.97	1.92
12	30000	1.09	12.96	14.10	3.78	0.90	1.21	11.61	4.24	35.37	1.07	3.96	37.85	0.51	0.82	2.45	0.21	2.00	1.92
11	30000	1.20	12.96	15.30	4.00	0.97	1.30	12.51	4.70	35.37	1.13	4.17	39.87	0.53	0.82	2.48	0.21	2.03	1.92
10	30000	1.35	12.96	16.66	4.19	1.00	1.35	12.95	5.20	35.37	1.19	4.39	41.93	0.54	0.82	2.51	0.21	2.05	1.86
09	30000	1.44	12.96	18.66	4.32	1.03	1.40	13.36	5.74	35.37	1.25	4.61	44.04	0.55	0.82	2.53	0.22	2.07	1.86
08	30000	1.52	12.96	19.70	4.44	1.06	1.44	13.72	6.32	35.37	1.31	4.83	46.21	0.55	0.82	2.53	0.22	2.07	1.86
07	30000	1.59	12.96	20.58	4.54	1.08	1.47	14.03	6.94	35.37	1.37	5.07	48.44	0.54	0.82	2.52	0.22	2.06	1.86
06	30000	1.64	12.96	21.23	4.61	1.10	1.49	14.24	7.82	35.37	1.44	5.31	50.76	0.53	0.82	2.48	0.21	2.03	1.86
05	30000	1.69	12.96	21.89	4.68	1.11	1.50	14.37	8.37	35.37	1.50	5.57	53.20	0.49	0.82	2.40	0.21	1.96	1.86
04	30000	1.71	12.96	22.12	4.68	1.12	1.51	14.46	9.21	35.37	1.58	5.84	55.79	0.43	0.82	2.25	0.19	1.84	1.86
03	30000	1.81	12.96	21.89	4.68	1.12	1.51	14.46	10.16	35.37	1.66	6.13	58.59	0.34	0.82	2.00	0.17	1.64	1.86
02	30000	1.89	12.96	21.89	4.68	1.12	1.51	14.46	11.27	35.37	1.74	6.46	61.71	0.22	0.82	1.60	0.14	1.31	1.86
01	30000	1.96	12.96	21.89	4.68	1.12	1.51	14.46	12.82	35.37	1.85	6.83	65.30	0.08	0.82	0.97	0.08	0.80	1.86
TOTAL		24	648	332	103	33	319	34	330	120	11671	2108	1033	13	38	7	82	7	84

Fig. 2 Spreadsheet for the computations of optimum values  
 Note: DPF is in mm; V in mm<sup>2</sup>, and f in MPa

Consider a coupled-wall structure illustrated in Fig. 1. The structure is modelled using 240 concrete panel elements and 80 beam elements. The coupling beams have a fix depth of 1000 mm. Initially, both the wall and the beam thicknesses are assumed to be 500 mm thick and the material modulus of elasticity is 20,000 MPa. A uniform horizontal load of 400 kN is assumed to act at each floor level. From a static analysis, the displacement at the top is found to be 360 mm.

The optimisation objective is to optimise the wall and beam thicknesses for the same displacement at the top. To illustrate the use of different material properties in the process of optimisation, the elasticity modulus of the lower half of the wall is increased to 30,000 MPa. A spreadsheet is created to perform the computations. The results of the optimum values without and with member-linking method are shown in Fig. 2.

It was shown that there is a significant reduction in structure material for the optimised structures, even with a small number of wall thickness transitions. These reductions are in the order of 48% for the ideal walls and 46% for the three-thickness transition walls.

### APPROXIMATE METHOD

The optimisation technique presented in the previous section is to optimise structures with predetermined group members. Often, inadequate information in the optimisation formulas causes difficulty in selecting suitable group members. In the absence of an efficient tool, the decision is often made by the structural engineer based on intuition and experience. This section proposes an approximate numerical method for solving an optimisation problem with non-predetermined group members. This method finds the local optimum values for a volume function by solving its partial derivatives.

Considering a cantilever wall in Fig. 3. The displacement at the point of virtual load is the sum of the DPFs. ie.  $\sum \delta_i$ . Given the DPF as defined in Eq. (19), it is possible to obtain a function that defines the parameters  $k/E$ , where  $k$  is the integral part of Eq. (19) and  $E$  is the material modulus of elasticity. Suppose the function is  $f(x)$ , the displacement is written as:

$$D = \int_0^l \frac{1}{v_x} f(x) = \frac{g(x)}{v_x} \tag{21}$$

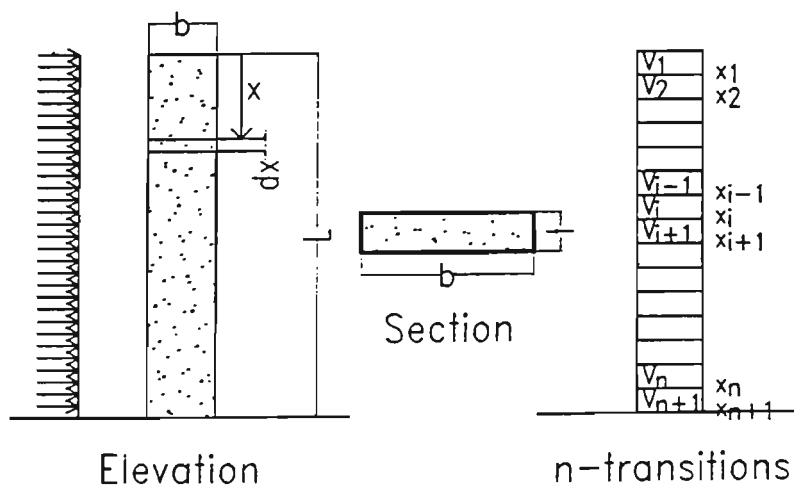


Fig. 3 Cantilever wall

For a cantilever wall with  $n$  transitions or  $n+1$  groups, Eq. (21) is written as:

$$D = \int_0^{x_1} \frac{1}{v_1} f(x) + \dots + \int_{x_n}^{x_{n+1}} \frac{1}{v_{n+1}} f(x) \quad (22)$$

or

$$D = \sum_{i=1}^{n+1} \frac{1}{v_i} (g(x_i) - g(x_{i-1})) \quad (23)$$

Having the displacement function formulated, the optimisation problem is to minimise

$$V = \sum_{i=1}^{n+1} v_i (x_i - x_{i-1}) \quad (24)$$

subject to

$$D = \sum_{i=1}^{n+1} \frac{1}{v_i} (g(x_i) - g(x_{i-1})) \quad (25)$$

where  $v_i$  is the volume per linear length of element  $i$  and  $g(x_i) = \int_0^{x_i} f(x)$

By substituting  $v_{n+1}$  from Eq. (25) into Eq. (24), the volume can be defined as a function of  $x_i$  and  $v_i$ , ie.  $f(x_i, v_i)$ , where  $i=1$  to  $n$ . Differentiating the volume function with respect to  $x_i$  and  $v_i$  gives a set of  $2n$  non-linear equations. Setting these derivative equations to zero and solving the optimising variables, the optimum locations of transition and volumes are given by  $x_i$  and  $v_i$ , respectively.

### Example B

Consider a 30-storey cantilever wall, illustrated in Fig. 3, with a uniform cross section of  $600 \times 9000 \text{ mm}^2$  and a storey height of  $3600 \text{ mm}$  (initial volume =  $583.2 \text{ m}^3$ ). A lateral load of  $40 \text{ kN}$  per storey is applied to the structure. Based on the principle of virtual work, the displacement at the top is calculated to be  $272 \text{ mm}$  [Eq. (19)]. During the redesign cycle the wall is optimised for minimum volume. To simplify the design problem, only one thickness transition is considered. Hence, the optimisation problem is written as:

minimise

$$v(v_i, x_i) = v_1 x_1 + v_2 (x_2 - x_1) \text{ where } x_2 = 30 \quad (26)$$

subject to

$$\frac{1}{v_1} g(x_1) + \frac{1}{v_2} [g(x_2) - g(x_1)] = 270 \text{ mm} \quad (27)$$

By curve-fitting the values of  $k_x / E_x$ , defined in Eq. (19), the function  $f(x)$  is found as:

$$f(x) = 0.03323x^0 - 0.07259x^1 + 0.02488x^2 + 0.02488x^3$$

and the integration is given as:

$$g(x) = 0.03323x^1 - 0.03630x^2 + 0.00829x^3 + 0.00622x^4$$

Solving the  $v_1$  of Eq. (28) and substituting it into Eq. (27), the volume in Eq. (27) becomes a function of  $x_1$  and  $v_2$ . Differentiating this volume function with respect to  $x_1$  and  $v_2$ , then setting the derivatives to zero, results in  $x_1 = 14.59$ ,  $v_1 = 5.90 \text{ m}^3$ ,  $v_2 = 22.79 \text{ m}^3$ . Therefore, the optimum volume is  $437 \text{ m}^3$ , reducing the volume of over  $146 \text{ m}^3$ .

## CONCLUSION REMARK

This paper develops a systematic methodology of optimising structural wall elements acting as the primary lateral load-resisting system for tall building. Application of this method can lead to substantial cost benefits in terms of material cost savings by use of thinner walls. By introducing a member-linking technique, discrete optimised wall thickness and transition levels can be derived.

## REFERENCES

- Charney, F.A. (1994). *DISPAR for ETABS Version. 5.4* (Computer program and the users manual). Colorado: Advanced Structural Concepts.
- Habibullah, A. (1989). *ETABS Version. 5.10* (Computer program and the users manual). California: Computer & Structures, Inc.
- Morris, A.J. (Ed.). (1982). *Foundations of Structural Optimization: A Unified Approach*. New York: John Wiley & Sons.
- Wada, A. (1991). "Drift control method for structural design of tall buildings", *Proceeding: Second Conference on Tall Buildings in Seismic Regions*. Los Angeles: Council on Tall Buildings and Urban Habitat.